Fundamentals of Gas-Liquid-Solid Fluidization

The successful design and operation of a gas-liquid-solid fluidized-bed system depend on the ability to accurately predict the fundamental properties of the system, specifically, the hydrodynamics, the mixing of individual phases, and the heat and mass transfer properties. Identification of the flow regimes under which the system operates is crucial to an understanding of both the variations of these properties and overall system performance. This timely, comprehensive review describes in a systematic manner the status of fundamental gas-liquid-solid fluidization behavior. This review also discusses the areas in which current knowledge is deficient and further research is needed.

KATSUHIKO MUROYAMA and LIANG-SHIH FAN

Department of Chemical Engineering
The Ohio State University
Columbus, OH 43210

SCOPE

Gas-liquid-solid fluidization is defined as an operation in which a bed of solid particles is suspended in gas and liquid media due to the net drag force of the gas and/or liquid flowing opposite to the net gravitational force or buoyancy force on the particles. Such an operation generates considerable, intimate contact among the gas, liquid and solid particles in these systems and provides substantial advantages for applications in physical, chemical or biochemical processing involving gas, liquid and solid phases.

Various modes are possible for gas-liquid-solid fluidized-bed operation. The gas-liquid-solid fluidized bed can be operated with a cocurrent or countercurrent flow of a gas and a liquid with gas as the continuous phase. It can also be operated with a cocurrent or countercurrent flow of a gas and a liquid with liquid as the continuous phase. The states of fluidization are altered when the fluidized bed is tapered, or an upper retaining grid or a draft tube is present in the bed.

This review examines both the experimental and modeling studies of the fundamental characteristics of gas-liquid-solid fluidization. Specifically, a comprehensive review is made on the hydrodynamics, the mixing of individual phases, and the heat and mass transfer behavior of various modes and states of gas-liquid-solid fluidization. Industrial application of the gas-liquid-solid fluidized bed is briefly described.

CONCLUSIONS AND SIGNIFICANCE

Gas-liquid-solid fluidization became a subject for fundamental research only about two decades ago. Considerable progress has been made with respect to an understanding of the phenomena of gas-liquid-solid fluidization since then. This review summarizes and analyzes the available information in the literature on this subject.

Gas-liquid-solid fluidization can be classified mainly into four modes of operation. These modes are: cocurrent three-phase fluidization with liquid as the continuous phase (Mode I-a); cocurrent three-phase fluidization with gas as the continuous phase (Mode I-b); Inverse three-phase fluidization (Mode II-a); and fluidization represented by a turbulent contact absorber (TCA) (Mode II-b). Modes II-a and II-b are achieved with a countercurrent flow of gas and liquid. Due to the complex nature of three-phase fluidization, however, various methods are possible in evaluating the operating and design parameters for each mode of operation.

Among the four modes of fluidization, Mode I-a has been the most widely investigated. The characteristics of Mode I-a fluidization depend to a great extent on bubble flow behavior, which varies strongly with the properties of the solid particles. The generalized wake model, with proper account of the solids holdup in the wake and the volume fraction of the wake, is commonly employed to describe the individual phase holdups for Mode I-a fluidization. Various empirical correlation equations are also available which can be directly utilized to estimate phase holdups. Reliable data on phase holdups, however, are lacking for systems involving organic or non-Newtonian media.

The backmixing of liquid for Mode I-a fluidization can be generally represented by the axial dispersion model. Several correlation equations are available for the liquid-phase dispersion coefficient. Extensive work has been performed on the wall-to-bed heat transfer. The gas-liquid mass transfer coeffi-

K. Muroyama is on leave from the Department of Environmental Chemistry and Technology, Tottori University, Tottori, 680, Japan. The last part of his work was completed upon returning to Japan.

Correspondence concerning this paper should be addressed to L.-S. Fan.

cient and interfacial area vary appreciably with the bubble flow pattern. Little information, however, is available on solids mixing and gas mixing for Mode I-a fluidization.

Extensive investigation has also been conducted with regard to hydrodynamics and mass transfer of Mode II-b fluidization. Numerous correlations have been proposed for estimating the hydrodynamic properties including phase holdups and pressure drop. The bed behavior is often affected by the extent of openings on the supporting grid. Considerable work has been performed on gas-liquid mass transfer. Numerous correlations for the overall mass transfer coefficient and interfacial area are also available.

Relatively little work has been conducted on Modes I-b and II-a fluidization and fluidization involving tapered beds, spouted beds, semifluidized beds, and draft tube fluidized beds. Optimal design and operation of three-phase fluidized-bed reactors for chemical, petrochemical and biochemical reactions should be stressed in future research.

INTRODUCTION

Gas-liquid-solid (or gas-slurry-solid in a broad sense) fluidized beds have emerged in recent years as one of the most promising devices for three-phase operation. Such a device is of considerable industrial importance as evidenced in its wide use for chemical, petrochemical and biochemical processing. Most notably, three-phase fluidized beds have been fully developed and demonstrated in processing technology; as three-phase reactors, they have been employed for the H-Oil process for hydrogenation and hydrodesulfurization of residual oil, the H-Coal process for coal liquefaction, turbulent contacting absorption for flue gas desulfurization, and the biooxidation process for waste water treatment. Other applications involving three-phase fluidized beds are also commonly encountered in physical operations.

Early reviews of gas-liquid-solid fluidization were made by Ostergaard (1969, 1971, 1977), Davidson et al. (1977), Kim and Kim (1980), Wild et al. (1982), and Epstein (1981, 1983). These reviews, however, are mainly concerned with only one mode of gas-liquid-solid fluidization, namely cocurrent upward fluidization with liquid as the continuous phase. Important needs, however, arise in examining operational alternatives involving other modes of gas-liquid-solid fluidization (Muroyama and Fan, 1982). This review provides a more comprehensive coverage of the entire scope of the subject matter, not only on cocurrent upward fluidization with a liquid as the continuous phase, but also on the other modes of fluidization.

This review covers six parts. The first part describes the fundamental distinction among the various modes of gas-liquid-solid fluidization. The second part describes the hydrodynamic behavior. The third part details the backmixing of both the liquid and gas phases, and the solids mixing. The fourth and fifth parts delineate the heat transfer and mass transfer properties, respectively. The sixth part summarizes knowledge gaps and areas in need of future research in the fundamentals and applications of gas-liquid-solid fluidization.

MODES OF GAS-LIQUID-SOLID FLUIDIZATION

Although there are considerable similarities between the gas–sparged slurry column and the gas-liquid-solid fluidized bed, distinct differences in operation exist between them.

In the gas–sparged slurry column, the size of the solid particle is usually less than 100 μm in diameter, the volumetric fraction of the solids is less than 0.1, and the particles are maintained in a suspended state by bubble agitation. In three-phase fluidization, the particle size is relatively large, normally greater than 200 μm, and the volumetric fraction of the solid particles varies from 0.6 (packed state) to 0.2 (close to the dilute transport state). In three-phase fluidized beds, the particles are supported by the liquid phase and/or the gas phase. The bed of particles may expand nonuniformly with elutriation as in gas-solid fluidized beds, or it may expand uniformly without elutriation as in liquid-solid fluidized beds while the bubbles intensify the mixing of the solid particles. The solid particles in both systems can be operated in either a batch or continuous mode. However, in the slurry column, the solid particles are usually carried in and out by the liquid stream. In the fluidized bed, on the other hand, the solid particles are supplied or withdrawn independent of the liquid stream. This review purposely distinguishes the three-phase fluidized-bed reactor from the three-phase slurry reactor because of the inherent differences between these reactors mentioned above. Such a distinction, however, was not clearly made in the book on the gas-liquid-solid reactors by Shah (1979) as indicated by Epstein (1981).

Tables 1 and 2 highlight the fundamental operational differences between gas-liquid-solid fluidized beds and other gas-liquid-solid contactors. To date, there are two types of three-phase fluidized beds which are relatively well established for industrial use. They are fluidized beds with cocurrent flow of gas and liquid, and those with countercurrent flow of gas and liquid. In the former, the bed of particles is supported by the liquid serving as the continuous phase, while, in the latter, the bed of particles is supported by the gas serving as the continuous phase. The former is employed as a major reactor system in the well-known H-Oil process for hydrodesulfurization of residual oils (Schuman et al., 1965; Griswold et al., 1966) and in the H-Coal process for coal liquefaction (Schuman et al., 1967). It is also used for biological processing such as biooxidation of wastewater (Cooper and Atkinson, 1981; Hirata et al., 1982). The latter, which is known as the turbulent contact absorber (TCA), was utilized among others for flue gas scrubbing (Kielback, 1959, 1964), and alcohol fermentation (Moebus and Teuber, 1982).

Based on the differences in flow directions of gas and liquid and in contacting patterns between the particles and the surrounding gas and liquid, several types of operation for gas-liquid-solid fluidization are possible. Recently, Epstein (1981) presented a taxonomy for three-phase fluidization, Figure 1. In this figure, three-phase fluidization is divided into two types according to the relative direction of the gas and liquid flows, namely, cocurrent

TABLE 1. CRITERIA FOR THE CLASSIFICATION OF THE GAS-LIQUID-SOLID REACTORS

Factors	Variation
State of motion of solid particles	• Stationary • Slurry suspension with mechanical agitation • Slurry suspension without mechanical agitation • Fluidization
Type of operation	Gas: Continuous Liquid: Batch or continuous Solid: Batch or continuous
Relative flow direction of phases for continuous operation	Gas, Liquid: Cocurrent upward or downward flow, Countercurrent flow or cross current flow Solid: Upward or downward flow
Situation of phases	Gas: Continuous phase or discrete bubble Liquid: Continuous phase, film or drop Solid: Packed, slurry suspension, fluidization with either liquid or gas as a continuous phase

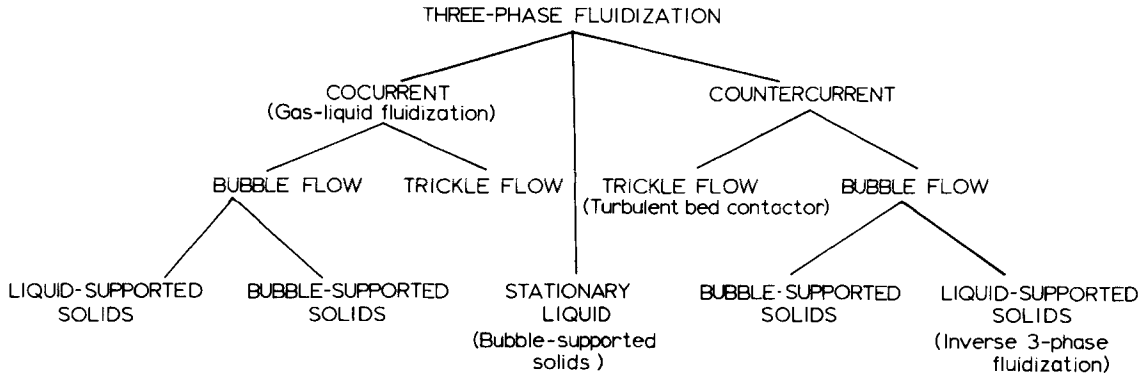

Figure 1. Taxonomy of Three-Phase Fluidized Beds (Epstein, 1981).

three-phase fluidization and countercurrent three-phase fluidization (Bhatia and Epstein, 1974b; Epstein, 1981).

In cocurrent three-phase fluidization, there are two contacting modes characterizing different hydrodynamic conditions between the solid particles and the surrounding gas and liquid. These modes are denoted as Mode I-a and Mode I-b, Figure 2. Mode I-a defines cocurrent three-phase fluidization with the liquid as the continuous phase, while Mode I-b defines cocurrent three-phase fluidization with gas as the continuous phase. In Mode I-a fluidization, the particles are supported by the liquid with the gas-forming discrete bubbles. Mode I-a is generally referred to as gas-liquid fluidization. The term bubble flow, in Epstein's taxonomy (1981), includes two types of flow for Model I-a: namely, liquid-supported solids and bubble-supported solids. According to Epstein (1981, 1983), the liquid-supported solids operation characterizes fluidization with the liquid velocity beyond the minimum fluidization velocity; the bubble-supported solids operation characterizes fluidization with the liquid velocity below the minimum fluidization velocity where the liquid may even be in a stationary state. Three different flow patterns are observed for Mode I-a fluidization: coalesced bubble flow, dispersed bubble flow, and slug flow. A more precise classification of these flow patterns for Mode I-a fluidization (for an air-water system) is given in Figure 3.

An increase of the gas flow rate in the slug flow regime in Mode I-a fluidization increases the slug frequency and decreases the volume fraction of the liquid in the liquid-solid suspension. As the gas flow rate increases further, the liquid-solid mixture forms fragmented agglomerates and eventually the operating state Mode I-b is reached, in which the gas becomes the continuous phase and the liquid becomes the dispersed phase in the form of liquid films or droplets (Mukherjee et al., 1974). It should be noted that the transition from Mode I-a to Mode I-b has not been clearly investigated. Furthermore, the determination of the boundaries among various flow regimes for Modes I-a and I-b, which are commonly made based on visual observation, may be to some extent subjective. However, the macroscopic flow pattern in cocurrent three-phase fluidization is well represented by Figure 3.

Countercurrent three-phase fluidization with liquid as the continuous phase, denoted as Mode II-a in Figure 2, is known as inverse three-phase fluidization. Countercurrent three-phase fluidization with gas as the continuous phase, denoted as Mode II-b in Figure 2, is known as a turbulent contact absorber, fluidized packing absorber, mobile bed, or turbulent bed contactor. In Mode II-a operation the bed of particles with density lower than that of the liquid is fluidized by a downward liquid flow, opposite to the net buoyant force on the particles, while the gas is introduced

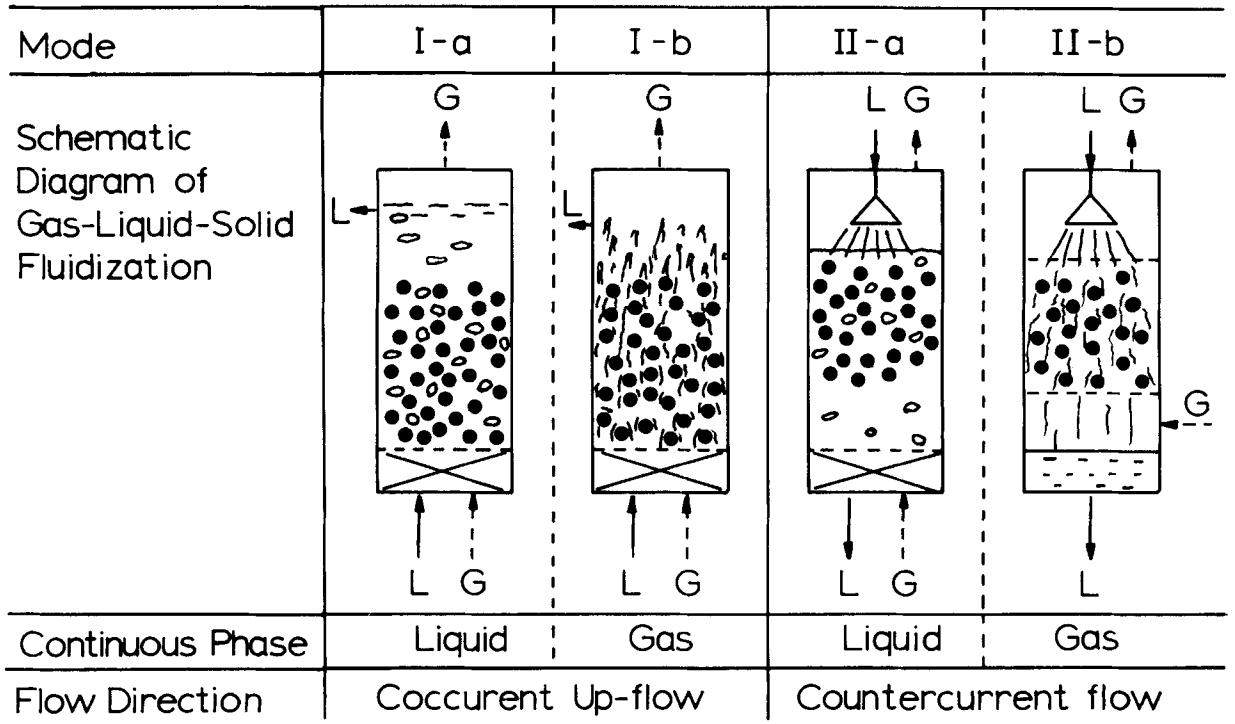

Figure 2. Modes of Gas-Liquid-Solid Fluidization.

TABLE 2. CLASSIFICATION OF GAS-LIQUID-SOLID REACTORS AND CONTACTORS

Operation	Type of Reactor	Operating Conditions: Operation for Gas and Liquid	Operating Conditions: Continuous Phase	Operating Conditions: Operation for Solid	Operating Conditions: Particle Size	Operating Conditions: Force for Solid Suspension	Transport Properties (Water-Like Fluids as Liquid Phase): Gas-Liquid Mass Transfer	Transport Properties (Water-Like Fluids as Liquid Phase): Wall-Bed Heat Transfer	Transport Properties (Water-Like Fluids as Liquid Phase): Fluid Mixing	Process Application
Class I	Packed Bed	•countercurrent •cocurrent upflow •cocurrent downflow	•gas (trickle flow) •liquid (dispersed bubble flow, slug flow)	•batch	$d_p > 1$ mm	•stationary	gas, liquid phase controlling $k_la = 5 \times 10^{-4} \sim 0.1$ (1/s) (counter current) $k_la = 5 \times 10^{-4} \sim 1$ (1/s) (cocurrent)	•poor for trickle flow low •fair for dispersed bubble or slug flow	low	•absorption •desorption •chemical absorption •gas-liquid-solid catalytic reaction •biochemical reaction
	Packed Bubble Column	•countercurrent •cocurrent upflow •internal liquid circulation	•liquid	•batch	$d_p > 10$ mm (high voidage packing)	•stationary	liquid phase controlling $k_la = 0.04 \sim 0.2$ (1/s)	•fair	intermediate	•chemical absorption •biochemical reaction
Class II	Agitated Vessel	•cross current	•liquid	•batch •continuous	$d_p < 0.1$ mm	•mechanical agitation	liquid phase controlling $k_la = 0.005 \sim 0.8$ (1/s)	•good	complete mixing	•gas-liquid-solid catalytic reaction •biochemical reaction
Class III	Gas Sparged Slurry Reactor	•cocurrent •countercurrent •internal liquid circulation •external liquid circulation •jet mixing	•liquid	•continuous	$d_p < 0.2$ mm	•mainly gas	liquid phase controlling $k_la = 0.005 \sim 0.3$ (1/s) (depend on reactor type)	•good	high	•gas-liquid-solid catalytic reaction •chemical absorption •biochemical reaction •absorption-adsorption processing
Class IV	Fluidized Bed Spouted Bed	•cocurrent upflow •countercurrent	•liquid •gas	•batch •continuous	Cocurrent System: $d_p = 0.2 \sim 8$ mm (liquid continuous) TCA system: $d_p = 3 \sim 40$ mm $\rho_s = 90 \sim 1{,}200$ kg/m^3 (gas continuous)	•liquid and gas (liquid continuous) •mainly gas (gas continuous)	liquid phase controlling $k_la = 0.005 \sim 0.2$ (1/s) (liquid continuous) gas, liquid phase controlling (gas continuous)	•very good (liquid continuous)	intermediate (fluidized bed) complete mixing (shallow spouted bed)	Fluidized Bed Cocurrent System: •gas-liquid-solid catalytic reaction •biochemical reaction •chemical absorption Countercurrent System: •biochemical reaction TCA Systems: •physical absorption •chemical absorption •particulate collection •cooling tower Spouted Bed Cocurrent System: •dissolution •gas-liquid-solid reaction •drying, granulation Countercurrent System: •similar to those for TCA

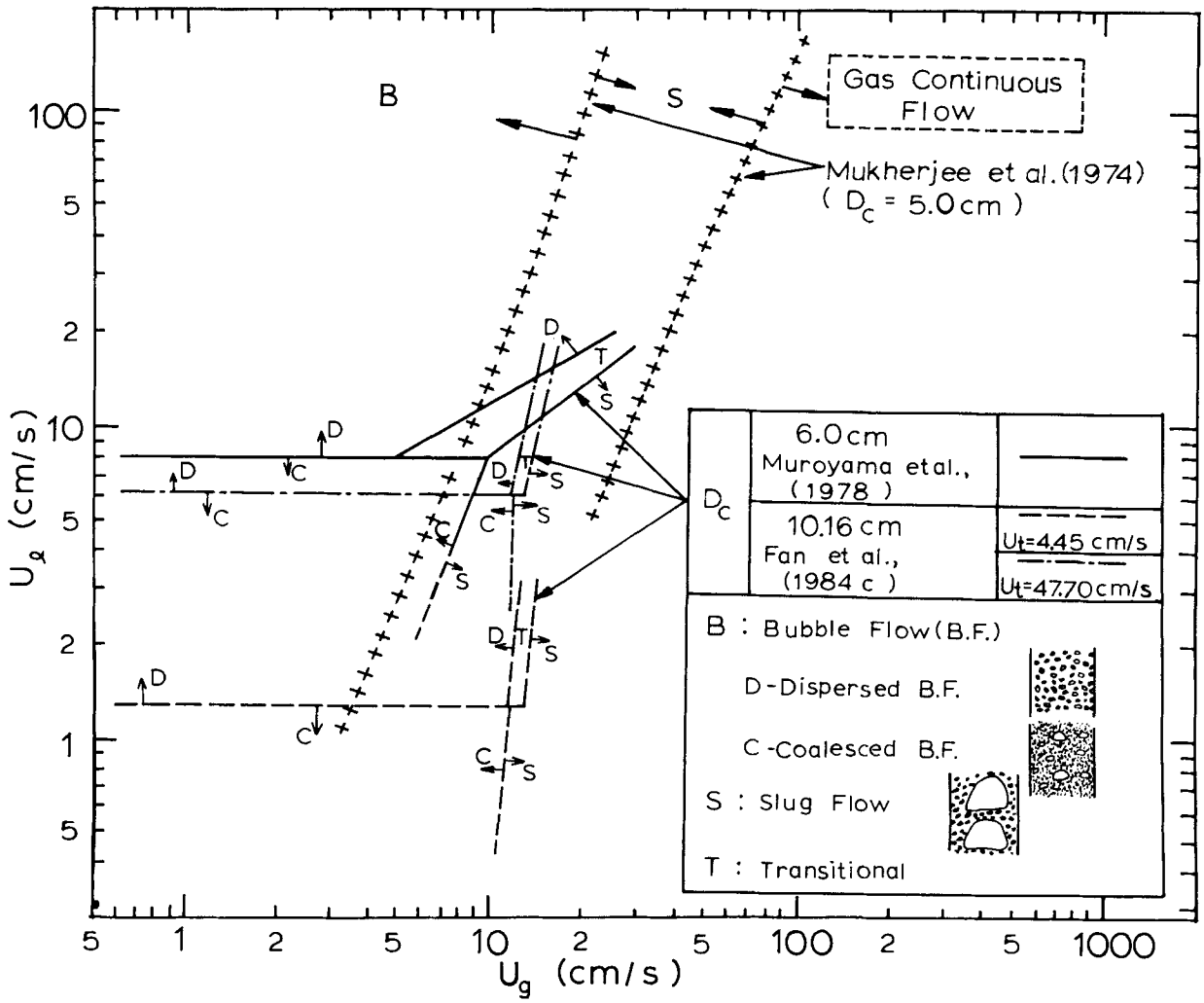

Figure 3. The Flow Regime Diagram for the Cocurrent Gas-Liquid-Solid Fluidized Bed.

countercurrently to the liquid forming discrete bubbles in the bed. As shown in Figure 4, four distinct flow regimes—fixed bed with dispersed bubble regime, bubbling fluidized bed regime, transition regime, and slugging fluidized bed regime—can be distinguished for Mode II-a fluidization (Fan et al., 1982a,b).

In the Mode II-b operation (TCA operation), an irrigated bed of low-density particles is fluidized by the upward flow of gas as a continuous phase. When the bed is in a fully fluidized state, the vigorous movement of wetted particles gives rise to excellent gas-liquid contacting. The gas and liquid flow rates in the TCA are much higher than those possible in conventional countercurrent packed beds, since the bed can easily expand to reduce the hydrodynamic resistances. Flow regimes in a TCA for a specific packing are given in Figure 4.

The state of gas-liquid-solid fluidization is strongly dependent on the geometry of the bed, methods of gas-liquid injection, and the presence of a retaining grid or internals. This is exemplified by the operation of a tapered fluidized bed, spouted bed, semi-fluidized bed, and draft tube spouted bed. The tapered fluidized bed uses a tapered column which diverges at a small angle in the upward direction (Scott et al., 1975, 1976; Holladay et al., 1978a,b). The upper part of the bed is at or near the state of incipient fluidization and behaves similarly to the packed bed part of the semi-fluidized bed. The hydrodynamic characteristics were experimentally studied by Pitt et al. (1978). In a spouted bed, gas and liquid are introduced into the bed through a gas-liquid injector located at the bottom of the bed. The solid particles in the core area are carried by the fountain and separated from the liquid at the surface of the fountain. The solid particles then move downward in the annular area. Like the Mode I-a operation, four different flow regimes can also be observed in three-phase spouted bed operation.

The semifluidized bed is formed when a mass of fluidized particles is compressed against a porous restraining grid resulting in the creation of a fluidized bed and a fixed bed in series within a single vessel. The flow regimes which occur in the countercurrent three-phase semifluidized bed operation resemble those for the Mode II-a operation of three-phase fluidization.

HYDRODYNAMICS OF GAS-LIQUID-SOLID FLUIDIZATION

Cocurrent Gas-Liquid-Solid Fluidization

Pressure Drop and Phase Holdup. A schematic diagram of the cocurrent three-phase fluidized bed reactor or the Mode I-a fluidized bed reactor is shown in Figure 5. The reactor consists of three main sections: the gas-liquid distributor section, the three-phase fluidized bed section, and the disengagement section. The disengagement section serves to settle the particles erupted into the dilute phase by the bubble. In the fluidized bed section, the solid holdup, ϵ_s, can be expressed as

$$\epsilon_s = \frac{W}{\rho_s S H} \tag{1}$$

The following relationship holds among individual holdups:

$$\epsilon_g + \epsilon_l + \epsilon_s = 1 \tag{2}$$

Under the steady-state condition, the total axial pressure gradient (static pressure gradient) at any cross section in the column

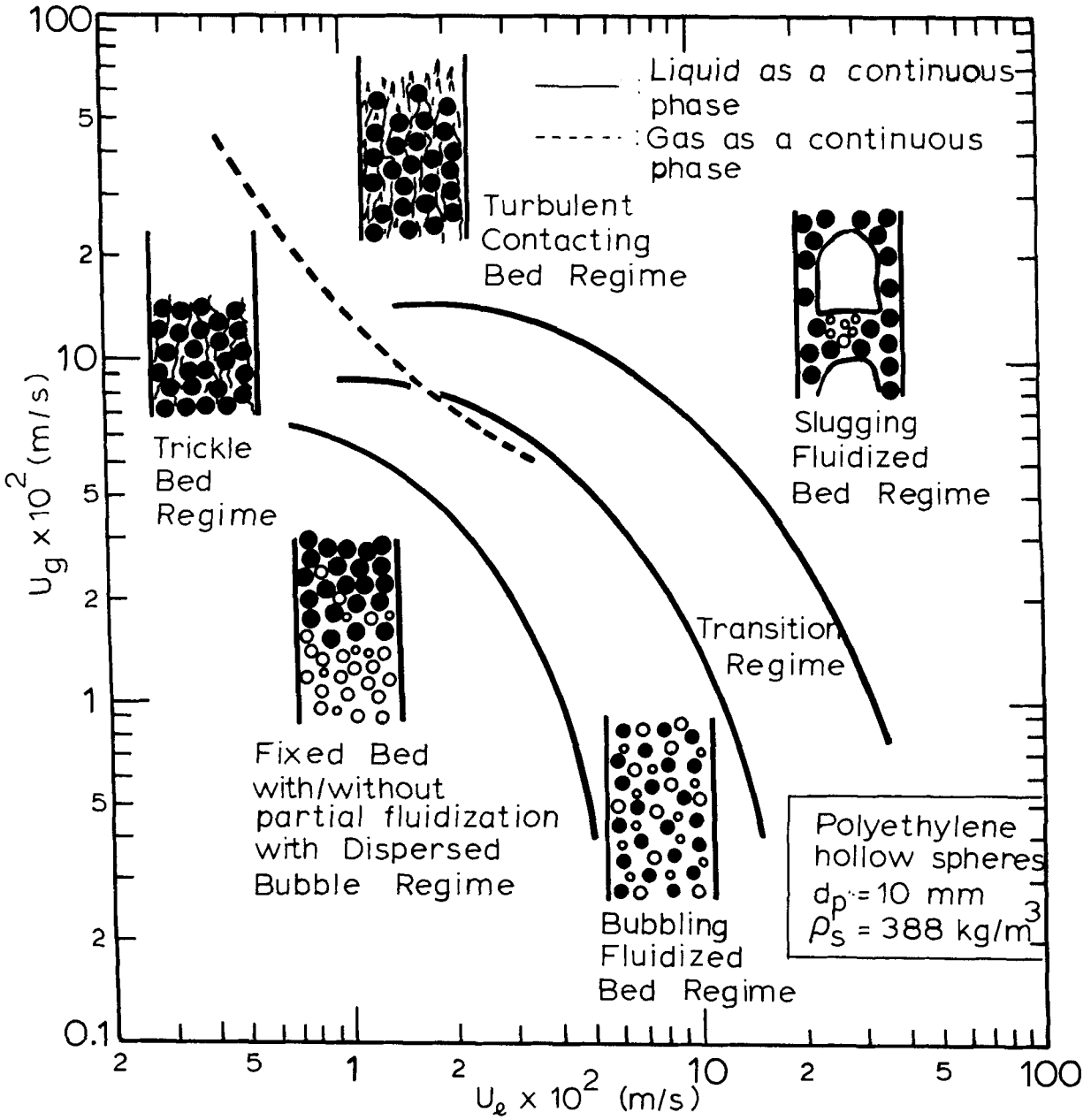

Figure 4. The Flow Regime Diagram for the Countercurrent Gas-Liquid-Solid Fluidized Bed (Fan, et al., 1982a).

represents the total weight of the bed consisting of the three phases per unit volume as given by

$$-\frac{dP}{dz} = (\epsilon_s \rho_s + \epsilon_l \rho_l + \epsilon_g \rho_g)g \qquad (3)$$

Equation 3 can be easily deduced from the one-dimensional multiphase flow model developed by Wallis (1969) who assumes that the frictional drag on the wall of the column and the acceleration of the gas and liquid flows can be neglected. In Eq. 3, the term $\epsilon_g \rho_g$ in the righthand side is usually negligibly small compared to the other terms. The evaluation of individual phase holdups based on the pressure gradient method has been employed by a number of investigators. In this method, ϵ_s can be directly obtained from Eq. 1 with the height of bed expansion measured experimentally while ϵ_l and ϵ_g can be calculated from Eqs. 2 and 3 simultaneously with the experimentally measured static pressure gradient. Preliminary experimental verification of Eq. 3 was provided by Ermakova et al. (1970a). More recently, Dhanuka (1978) compared the experimental values of the pressure drop with those predicted by Eq. 3, using the gas and liquid holdups measured independent of the electroconductivity method, and showed that the prediction is satisfactory. The maximum deviation between the predicted and measured values is only about 5%. Begovich and Watson (1978b) also showed that the holdup values obtained using the pressure gradient method agree with those measured using an electroconductivity technique within 5% deviation. Equation 3 is also valid for the countercurrent turbulent contact absorber system (Barile and Meyer, 1971; Tichy and Douglas, 1972; Kuroda and Tabei, 1979), and for the inverse three-phase fluidized bed system (Fan et al., 1982a). In these systems, the bed is in free and uniform expansion and the accelerations of the fluids and the wall friction are negligible. Similar to that in the gas-solid fluidized bed, the dominant frequency of the pressure fluctuation in the gas-liquid-solid fluidized bed correlates strongly with the flow regime in the bed (Fan et al., 1984c). The definition of dynamic and frictional pressure drops and their interrelationship with experimental measuring methods were elaborated by Epstein (1981).

Measuring Techniques for Phase Holdups. The hydrodynamic models so far presented to assess the holdup behavior can generally be described by the *wake model*, which takes into account the role of the wake behind the bubble. On the other hand, empirical correlations for the individual phase holdups have also been developed by many authors.

The bed height can be determined either from visual observation

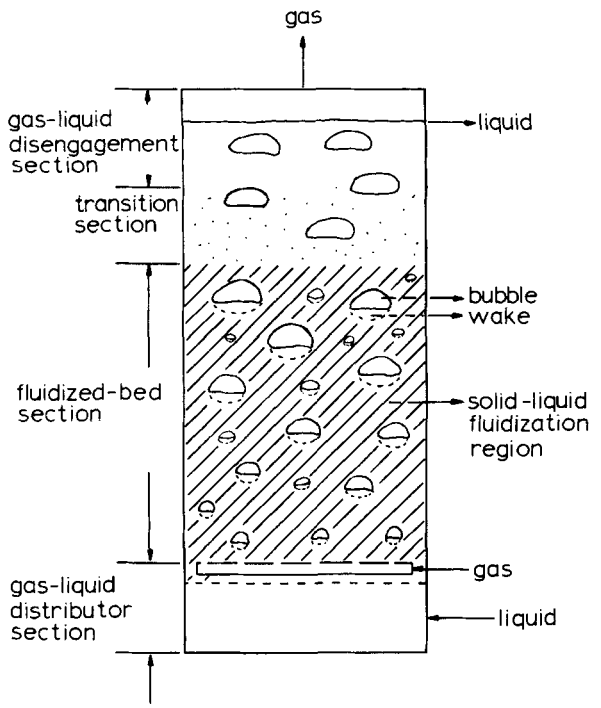

Figure 5. Schematic Representation of the Mode I-a Fluidized Bed Reactor.

or from the measured pressure gradient. The determination of the bed height based on visual observation is reasonably accurate for beds of coarse or dense particles because of a distinct bed surface. The visual observation method, however, becomes quite subjective and unreliable for beds of fine particles because of an indistinct bed surface. Particle entrainment is of particular significance at high gas flow rates. For fine particle fluidization, the bed height can be determined by the intercept of the pressure gradient curves with two distinct slopes representing the pressure gradient in the fluidized bed section and in the disengagement section.

When a deep dilute particle zone above the bed prevails, however, the determination of bed height from the intercept becomes unsatisfactory. In such a case, either the local liquid holdup or solid holdup should be directly measured in conjunction with the measurement of the static pressure gradient. One can then determine the holdups of the other phase from Eqs. 2 and 3. For example, Begovich and Watson (1978a, 1978b) measured the local gas holdups using the electroconductivity probe and the pressure gradient to obtain the local solids concentration. Kafarov et al. (1973) employed induction transducers mounted on the column wall to measure the concentration of fine metal catalysts in a three-phase transport system. The concentration of fine solids in a dilute slurry can be measured by direct sampling (Kafarov et al., 1973) in the same manner as that commonly employed for bubble column slurry reactors.

The local liquid holdup can be directly measured by the electroconductivity techniques employed by Begovich and Watson (1978a, 1978b), Dhanuka (1978), Dhanuka and Stepanek (1978), and Kato et al. (1981). A capacitance probe technique was also employed by Razumov et al. (1973) to measure the solid and liquid holdups. The gas holdup can be measured by the isolation technique, i.e., measurement of gas occupied in an isolated section after simultaneously turning off two quick closing valves located at the inlet and outlet of the fluidized bed section (Bhatia and Epstein, 1974a). A similar method was employed for vertical three-phase flow by Bhaga and Weber (1972a, 1972b). Kim et al. (1972) showed that the holdups can be measured by simultaneously shutting off the liquid and gas flows. The γ-ray absorption technique was employed by Lee and Worthington (1974) to measure the gas holdup just above the surface of a three-phase fluidized bed. The use of an electrical resistance probe which also allows measurement of the local value of the gas holdup was employed by Rigby et al. (1970a), and Darton and Harrison (1974a). Rigby et al. (1970a) reported that the gas holdup is higher in the core region than in the region near the wall in a column containing fine particles. Ostergaard and Michelsen (1968) measured the gas holdup by means of a radioactive tracer technique in which the residence time distribution of the gas was analyzed to obtain information on gas mixing. Vasalos et al. (1977, 1979, 1980) also employed the radioactive tracer technique to measure gas holdup and gas-phase mixing. The measurement of the average bubble velocity by means of a motion analyzer from cine films is an indirect method to evaluate the gas holdup (Baker et al., 1977; Kim et al., 1977). Recently, an optical probe technique utilizing a single quartz fiber was proposed by Ishida and Tanaka (1982) to obtain holdups for both bubbles and particles in a three-phase fluidized bed. They showed that a flat-topped single-fiber probe could yield characteristic signals for both the bubbles and particles in the three-phase system.

Bed Behavior. The flow behavior of the gas bubbles which are in a discrete state in a liquid medium varies depending on the particle size, the degree of bed expansion, the liquid velocity, and the gas velocity. Three gas-liquid flow regimes have received attention: (1) the bubble coalescing regime (Kim et al., 1972) or the churn-turbulent regime (Darton and Harrison, 1975); (2) the bubble breakup regime (Michelsen and Ostergaard, 1970), the bubble disintegration regime (Kim et al., 1972), or the ideal bubbly flow regime (Darton and Harrison, 1975); and (3) the slug flow regime (Michelsen and Ostergaard, 1970; Kim et al., 1972). Kim et al. (1975) reported the existence of a critical particle size which separates the bubble coalescing regime and bubble disintegrating regime. The critical size for particles with a density similar to that of glass was reported to be about 2.5 mm in diameter for an air-water system. The study of flow regimes by Muroyama et al. (1978) and Fan et al. (1982c), however, indicates that in addition to the particle size, flow regimes also strongly depend on the liquid and gas velocities used in the system.

Three-phase fluidization using fine particles displays unique bed expansion characteristics: i.e., upon initial introduction of the gas into the liquid-solid fluidized bed, contraction, instead of expansion, of the bed occurs. An increasing gas flow rate causes further contraction up to a critical gas flow rate beyond which the bed expands. Massimilla et al. (1959), who first reported this contraction phenomenon, observed that the bed contraction is larger when the liquid velocity is greater. Turner (1964) and Ostergaard (1964) also reported this phenomenon and presented some data on bed expansion. A quantitative elucidation of bed contraction was reported by Stewart and Davidson (1964). From the photographs of a single bubble ascending in a two-dimensional column, they distinguished two types of solid-free wake behind the bubble using particles with identical sizes but different densities. These types are: (1) a water bubble stabilized by small gas bubbles collecting on its roof in a bed containing dense particles such as iron shot or lead shot; and (2) a particle-depleted wake behind the gas bubble in a bed containing glass particles. In the latter type, Stewart and Davidson (1964) also observed shedding vortices which are largely free of particles left on the zigzag trail of the bubble, and these vortices moved upward with a velocity somewhat less than that of the bubble itself. They concluded that bed contraction is due to the formation of air/water bubbles which move upward with the same velocity as the bubble, reducing the velocity of the water through the liquid-solid fluidized phase.

The bubble breakup phenomena in a bed of coarse particles were first revealed by Lee (1965). Michelsen and Ostergaard (1970) observed that the bed always expands in the bubble breakup regime. In this regime, the bubble size is comparable to or even much smaller than the size of the solid particles. In addition, bubble size is quite uniform. Ostergaard (1971) reported that bubbles emerging from the surface of the bed of 2 mm lead shot fluidized by the cocurrent upflow of air and water are also uniform and small in size, but they move in clusters in contrast to the rather evenly distributed bubble swarms observed in a bed of 6 mm glass beads. Ostergaard suggested that this phenomenon is probably an effect of the heterogeneous mixture of water in a fluidized bed of lead

TABLE 3. CORRELATIONS OF PHASE HOLDUPS BASED ON THE WAKE MODELS

Investigators	Correlation Equation for k	Assumption for x	Liquid-Solid Interrelation and Gas-Liquid Interrelation	Remarks
Ostergaard (1965)	$k = 0.14\epsilon_g^{-0.5}[U_l - U_{lmf0}]$	$x = 1$ without solid circulation	Richardson and Zaki equation	air/water system
			$\frac{U_g}{\epsilon_g} = 21.7 - 4.6\ ln\ U_g + U_l$	$U_g = 0 \sim 2$ cm/s $U_l = 1 \sim 3$ cm/s
Efremov and Vakhrushev (1970)	$k = 5.1(\epsilon_l)^{4.85}_{U_g=0}\left\{1 - \tanh\left[\frac{40U_g(\epsilon_l)^{10}_{U_g=0}}{U_l} - 3.32(\epsilon_l)^{5.45}_{U_g=0}\right]\right\}$	$x = 0$	Richardson and Zaki equation	air/water system $d_p = 0.32 \sim 2.15$ mm
			$\epsilon_g = (\epsilon_g)_{g-l}\left\{\frac{\rho_l}{(\epsilon_l)_{U_g=0}\rho_l + [1 - (\epsilon_l)_{U_g=0}]\rho_s}\right\}^{1.22}$	$U_g = 0 \sim 7$ cm/s U_l = around 11 cm/s
			$(\epsilon_g)_{g-l}$ = gas holdup in gas-liquid system	
Rigby and Capes (1970b)	Graphical description	$x = 0$ or $x = 1$	Richardson and Zaki equation Bubble velocity was estimated by Rigby, van Blockland, Park and Capes (1970a)	air/water system $d_p = 0.29$, 0.47 and 0.775 mm U_g = around 2.0 cm/s $U_l/U_{lmf0} = 2 \sim 8$
Bhatia and Epstein (1974a)	$k = k_0'(1 - \epsilon_s)^3$ According to El-Temtamy and Epstein (1978) $k_0' = \left(0.61 + \frac{0.037}{\epsilon_g + 0.013}\right)$	$0 \le x \le 1$ adjustable parameter	Richardson and Zaki equation Large columns;	air/water air/aqueous glycerol air/aqueous polyethylene glycol
			$\frac{U_g}{\epsilon_g} - \frac{U_l}{\epsilon_l} = V_{b\infty} + 2(U_g)$	$d_p = 0.25 \sim 3$ mm $\rho_p = 2.5 \sim 11$ g/cm^3
			Smaller columns;	$\mu_l = 1 \sim 63$ cp
			$\frac{U_g}{\epsilon_g} - \frac{U_l}{\epsilon_l} = \frac{V_{b\infty}\sqrt{\tanh(0.25\epsilon_g^{-1/3})}}{\epsilon_l}$ (bubble flows)	$U_g = 0 \sim 20$ cm/s
			$\frac{U_g}{\epsilon_g} - \frac{U_l}{\epsilon_l} = \frac{0.2(U_g + U_l) + 0.35\sqrt{gD_c}}{\epsilon_l}$ (slug flows)	$U_l = 0 \sim 39$ cm/s
Darton and Harrison (1975)	$k = 1.4\left(\frac{U_l}{U_g}\right)^{0.33} - 1$, for $\frac{U_l}{U_g} \ge 0.4$	$x = 0$	Richardson and Zaki equation	air/water
			$U_g(1 - \epsilon_g) - U_l\epsilon_g\frac{(1 - \epsilon_g)}{\epsilon_l} = f(\epsilon_g, V_{b\infty})$	$d_p = 0.32 \sim 6$ mm
	$k = 0$, for $\frac{U_l}{U_g} < 0.4$		$f(\epsilon_g, V_{b\infty}) = 180\ \epsilon_g$ (uniform bubbling regime) Graphical presentation (churn-turbulent regime)	$U_l/U_g = 0.4 \sim 20$
Baker et al. (1977)	$k = 1.617\left(\frac{U_l}{U_g}\right)^{0.61}\sigma^{-0.654}$	$x = 0$	$\epsilon_{lf} = 0.148(U_{lf})^{0.38}d_p^{-0.285}\gamma^{0.115}$ γ = generalized viscosity constant Measured bubble velocity Unit: U_{lf} = mm/s, d_p = mm	air/water air/acetone aq. sol. air/sugar aq. sol. air/carboxymethyl cellulose sol $d_p = 1 \sim 6$ mm $U_g = 0 \sim 85$ cm/s U_l = around 10 cm/s $\rho_s = 2.5 \sim 3.0$ g/cm^3 $d_p = 0.273 \sim 2.00$ mm $\mu_l = 1 \sim 6.3$ mg/mm·s $0.07 \le y \le 1.08$
El-Temtamy and Epstein (1978)	$k = k_0\exp(-5.08\ \epsilon_g)$ k_0: relative wake holdup for single bubbles	$x = 1 - 0.877y$ for $0 \le y \le 1.14$ $x = 0$ for $y > 1.14$ where $y = \frac{U_i}{\frac{U_g}{\epsilon_g} - \frac{U_l}{\epsilon_l}}$	Richardson and Zaki equation Measured ϵ_g	

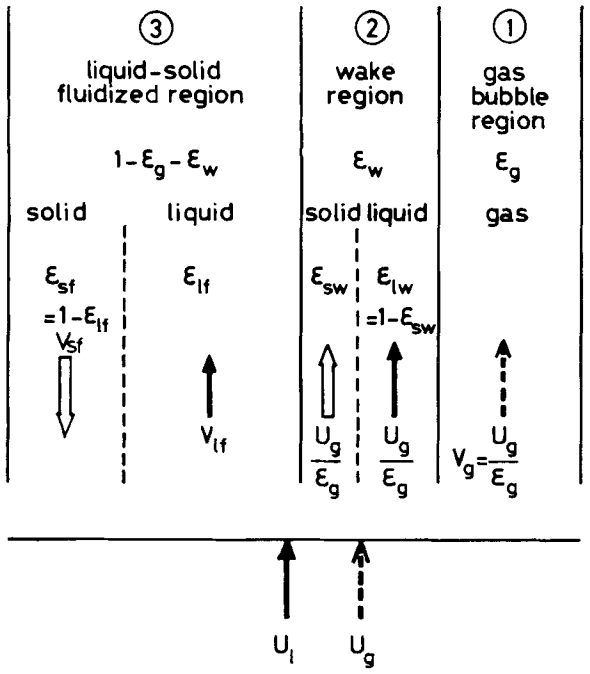

Figure 6. The Generalized Wake Model for the Mode I-a Fluidized Bed Reactor (Bhatia and Epstein, 1974).

shot. In fact, in liquid fluidized beds of such high density particles, well-defined liquid bubbles and slugs are formed and logarithmic plots of voidage against velocity are no longer linear (Richardson, 1971).

Correlations Based on Wake Models and Empirical Correlations for Phase Holdup. In the wake model, the role of the wakes behind the gas bubbles in the liquid flow, as pointed out by Stewart and Davidson (1964), is mathematically formulated to elucidate the bed expansion (or solids holdup) and the liquid holdup behavior. The wake concept considers the three-phase fluidized bed to be composed of: (1) the gas bubble region, (2) the wake region, and (3) the solid-liquid fluidization region. Table 3 summarizes the various correlations of phase holdups based on the wake model. The differences among these correlations lie in the assumptions made in the model for the solids concentration in the wake region, the correlations for the porosity in the liquid-solid fluidization region, and the correlations for the gas holdup or bubble velocity. Based on the wake model, Ostergaard (1965) assumed that the porosity in the liquid-solid fluidization region can be expressed by the Richardson and Zaki equation (1954), the wake region moves at the same velocity as the bubble, and the porosity of the wake is identical to that of the liquid-solid fluidization region, i.e., $x = 1$ as defined in the next paragraph. Ostergaard proposed empirical equations relating the bubble velocity (U_g/ϵ_g) to the wake holdup ϵ_w. However, if the porosity of the wake is the same as that of the liquid-solid fluidization region, the result is a stirring of the bed which does not give rise to bed expansion (Darton and Harrison, 1975). Assuming that the wake is solid-free, Efremov and Vakhrushev (1970) derived a set of equations based on the wake concept which were also independently deduced by Stewart in 1965 in his dissertation. Rigby and Capes (1970b) compared the values of wake volume to bubble volume ratio, k, for wake models with $x = 0$ and 1. Their findings indicate that k increases with an increase of the particle size, an increase of the liquid flow rate, and a decrease of the gas flow rate. By calculating the equivalent wake volume due to the shedding wakes, they showed that the shedding wakes are also responsible for bed expansion.

The generalized wake model was developed by Bhatia and Epstein (1974a). The schematic description of the concept of this model is shown in Figure 6. In this model two key parameters, x and k, are defined as:

$$x = \epsilon_{sw}/\epsilon_{sf} \tag{4}$$

$$k = \epsilon_w/\epsilon_g \tag{5}$$

The model assumes the relative velocity between the liquid and the solid in the liquid-solid fluidized region is related to the bed porosity by the Richardson and Zaki equation (1954). The resultant expression for the liquid holdup and bed porosity can be given, respectively, by:

$$\epsilon_l = \left[\frac{U_l - U_g k(1-x)}{U_t(1-\epsilon_g - k\epsilon_g)}\right]^{1/n} [1 - \epsilon_g(1 + k - kx)] + \epsilon_g k(1-x) \tag{6}$$

$$1 - \epsilon_s = (\epsilon_g + \epsilon_l) = \left[\frac{U_l - U_g k(1-x)}{U_t(1-\epsilon_g - k\epsilon_g)}\right]^{1/n} \times [1 - \epsilon_g(1 + k - kx)] + \epsilon_g(1 + k - kx) \tag{7}$$

The values of k and x need to be known to estimate the bed expansion or liquid holdup based on the generalized wake model, in addition to ϵ_g or mean bubble velocity U_g/ϵ_g. In the solid-free wake model, which assumes $x = 0$, the values of k and ϵ_g need to be known for estimating phase holdups or bed expansion.

With $x = 0$, Eq. 7 reduces to the equation for the bed expansion which was derived by Efremov and Vakhrushev (1970). Darton and Harrison (1975) presented an empirical correlation equation for k based on the solid-free wake model. According to their expression, k becomes negligible at $U_l/U_g < 0.4$, under which condition the bed is highly turbulent due to the flow behavior change in the bubbling regime (Schuman et al., 1965). Darton and Harrison (1975) showed that the values of k for single-bubble systems observed in a two-dimensional column by Rigby and Capes (1970b) decrease with an increase in the bubble volume. Baker et al. (1977) also investigated the effects of liquid viscosity and surface tension on k based on the solid-free wake model. Darton and Harrison (1976) analyzed the liquid and particle streamlines around a bubble based on the two vortex theories, i.e., Hill's spherical vortex and axisymmetric flow towards a stagnation point, to assess the formation of solid-free wakes and to provide a theoretical basis for the estimation of k. Hill's vortex model enables calculation of the motions of the liquid and particles near a bubble in a three-phase system. The axisymmetric flow model, or alternatively the flat topped wake model, predicted a horizontal voidage discontinuity in the wake behind the bubble with reasonable accuracy (Darton and Harrison, 1976; Davidson et al., 1977). The solid-free wake model was also applied to a multistage, three-phase fluidized bed by Schmidt (1976).

Based on the generalized wake model, however, one is unable to evaluate the values of k and x independent of the holdup data. Bhatia and Epstein (1974a) presented a heuristic equation for k assuming that the wake behavior in the three-phase system is analogous to that in a liquid-liquid dispersion system (Letan and Kehat, 1968). El-Temtamy and Epstein (1977, 1978) obtained the value for k by assuming that the sphere-completing volume of spherical cap bubbles is the effective volume of the bubble wake. Henriksen and Ostergaard (1974a) found that the included angle, θ, of the spherical cap bubble is a unique function of the kinematic viscosity of the medium surrounding the bubble. The apparent viscosity, μ_0, of a liquid-solid fluidized bed surrounding the bubble can be estimated from correlation equations presented by several investigators (e.g., Hetzler and Williams, 1969). The average density of the liquid-solid fluidized bed, ρ_0, can be easily estimated. Knowing the value μ_0/ρ_0, the included angle, θ, can be read from the figure of θ vs. μ_0/ρ_0 presented by Henriksen and Ostergaard (1974a). Thus, the value of k can be calculated by the following equation (El-Temtamy and Epstein, 1977, 1978).

$$k = k_0 \exp(-5.08\epsilon_g) \tag{8}$$

The value for x can be calculated from the holdup data. An empirical correlation equation for x is presented by El-Temtamy and Epstein (1977, 1978) as:

TABLE 4. EMPIRICAL CORRELATIONS OF PHASE HOLDUPS FOR THREE-PHASE FLUIDIZATION

Investigators	Correlation Equations	Gas-Liquid	Solid	Column Dimension	Remarks
Viswanathan et al. (1964)	$\frac{\epsilon_l + \epsilon_g}{\epsilon_g} = \frac{1 - \epsilon_s}{\epsilon_g} = \frac{1}{k_b}\frac{U_l}{U_g} + \frac{1}{k_b}$ k_b = Bankoff's two-phase flow factor	air/water	quartz particles (0.928 and 0.649 mm)	50.8 mm I.D.	poor correlation
Ostergaard and Michelsen (1968)	$\epsilon_l = 0.705U_l^{0.211}\,10^{-0.018U_g}$ d_p = 0.25 mm, $0.35 < U_g < 1.7$ cm/s, $0.5 < U_l < 1.25$ cm/s $\epsilon_l = 0.347U_l^{0.397}\,10^{-0.023U_g}$ d_p = 1 mm, $0 < U_g < 2.2$ cm/s, $2 < U_l < 10.5$ cm/s $\epsilon_l = 0.2092U_l^{0.415}\,10^{-0.011U_g}$ d_p = 6 mm, $0 < U_g < 2.2$ cm/s, $9 < U_l < 18$ cm/s Unit: U_l = cm/s, U_g = cm/s	air/water	glass beads (0.25, 1 and 6 mm)	216 mm I.D.	purely empirical data were taken also for axial mixings of gas and liquid
Ziganshin and Ermakova (1970)	$1 - \epsilon_g = \frac{1}{1 + 1{,}000\nu_l^{0.5}U_g}$ Unit: ν_l = m²/s, U_g = m/s	air/water air/aqueous glycerin solution	glass spheres (0.7 to 2.0 mm)	100 and 200 mm I.D.	gas holdup only effect of viscosity of liquid was considered purely empirical
Vail, Manakov and Manshilin (1970)	$\epsilon_g = k'(1 - \epsilon_s)^{m'}\left(\frac{U_g}{U_l}\right)^{n'}$ k', m' and n' = adjustable parameters for different particles 0.73 mm glass beads: k' 0.1026, m' 0.780, n' 2.09 0.77 mm Al-Si cat.: 0.108, 0.630, 3.01 0.74 mm Co-Mo cat.: 0.0526, 0.670, 1.69	air/water	glass beads (0.73 mm) spherical alumino-silicate catalyst (0.77 mm) spherical alumino-cobalt-molybdenum catalyst (0.74 mm)	146 mm I.D.	gas holdup only purely empirical
Mach (1970)	$7.4 \times 10^{-3} = Fr_l'\sigma^{2/3}\mu_l^{1/15}d_p^{-1/4}(\epsilon_g + \epsilon_l)^{-3}\rho_l^{-2/3}$ $3 \times 10^{-3} < d_p < 8 \times 10^{-3}$ m, $0.8 < (\epsilon_g + \epsilon_l) < 0.98$ $7{,}000 < \rho_s < 11{,}000$ kg/m³ $10^{-3} < \mu_l < 12.7 \times 10^{-3}$ kg/m·s, $800 < \rho_l < 1{,}200$ kg/m³ $0.027 < \sigma < 0.072$ N/m $Fr_l' = \frac{U_l^2}{d_p g}\frac{1}{(\epsilon_g + \epsilon_l)^2}\cdot\frac{\rho_l}{\rho_s - \rho_l}$ Unit: S.I. unit	air/water air/glycerin aq. sol air/gear oil air/spindle oil air/benzene air/diesel oil air/ethanol air/methanol	lead particle (2.5, 5 and 8 mm) steel particle (2, 4.5 and 7 mm)	44 and 60 mm I.D.	bed expansion only effect of surface tension effect of viscosity empirical correlation
Dakshinamurty et al. (1971)	$\epsilon = (\epsilon_g + \epsilon_l) = k''\left(\frac{U_l}{U_t}\right)^{m''}\left(\frac{U_g\mu_l}{\sigma}\right)^{n''}$ $n'' = 0.08$ $k'' = 2.12$, $m'' = 0.41$ for $Re_t < 500$ $k'' = 2.65$, $m'' = 0.60$ for $Re_t > 500$	air/water air/kerosene	rockwool shot (1.3 mm) sand (1.06 and 2.235 mm) glass beads (0.335, 6.84 and 4.89 mm) iron shot (3 mm)	56 mm I.D.	bed expansion only purely empirical
Dakshinamurty et al. (1972)	$(\epsilon_g + \epsilon_l) = 2.85\left(\frac{U_l}{U_t}\right)^{0.60}\left(\frac{U_g\mu_l}{\sigma}\right)^{0.08}$ for $R_t > 500$	air/water air/electrolyte solution	lead shot (2.13 mm) rockwool shot (1.3 mm) glass beads (3.35, 4.18, 6.03 and 6.84 mm)	circular and annular column	bed expansion only purely empirical
Kim et al. (1972)	$(\epsilon_l)_{U_g=0} - \epsilon_l = 0.0025\left(Fr_l\frac{\rho_s}{\rho_l}\right)^{0.149}\left(Fr_g\frac{\rho_s}{\rho_g}\right)^{0.161} \times (Re_l \cdot Re_g)^{0.259}$	air/water	glass beads (6 mm) irregular gravel (2.6 mm)	660.4 × 25.4 mm rectangular cross section column	two dimensional column data were taken also for liquid mixing purely empirical

$$(\epsilon_l)_{Ug=0} = 0.409\left(Fr_l\frac{\rho_s}{\rho_l}\right)^{0.193}(Re_l)^{0.074}$$

$$\left(\frac{H}{H_0}\right) - \left(\frac{H}{H_0}\right)_{U_g=0} = 0.0026\left(Fr_l\frac{\rho_s}{\rho_l}\right)^{0.178}\left(Fr_g\frac{\rho_s}{\rho_l}\right)^{0.345} \times (Re_l Re_g)^{0.252}$$

$$\left(\frac{H}{H_0}\right)_{U_g=0} = 1.80\left(Fr_l\frac{\rho_s}{\rho_l}\right)^{0.202}(Re_l)^{-0.012}$$

Razumov et al. (1973)	$\epsilon_s = 0.578 - 3.198U_l - 0.538U_g$ $\epsilon_l = 0.422 + 0.135U_l/d_p^{0.562} - 1.82U_g$ Unit: S.I. unit	air/water	sand particles and slag beads (0.49 to 1.27 mm)	300 mm I.D.	purely empirical limited liquid and gas velocities
Kim et al. (1975)	$(\epsilon_g + \epsilon_l) = 1.40(Fr_l)^{0.170}\left(\frac{U_g\mu_l}{\sigma}\right)^{0.078}$ for expanded beds $(\epsilon_g + \epsilon_l) = 1.301(Fr_l)^{0.128}\left(\frac{U_g\mu_l}{\sigma}\right)^{0.073} \times \exp\left[0.031\left(\frac{U_l}{U_g}\right)(\epsilon_l)_{U_g=0}\right]$ for contracted beds $(\epsilon_l)_{U_g=0} = 1.353(Fr_l)^{0.206}(Re_l')^{-0.100}$ $\epsilon_l = 1.504(Fr_l)^{0.234}(Fr_g)^{-0.086}(Re_l')^{-0.082}\left(\frac{U_g\mu_l}{\sigma}\right)^{0.092}$ $Fr_l = \frac{U_l^2}{d_p g}, Fr_g = \frac{U_g^2}{d_p g}, \mu_l = k/(du/dy)^{1-\bar{n}}, Re_l' = \frac{U_l^{2-\bar{n}}d_p^{\bar{n}}}{\nu_l}$	air/sugar solution air/carboxymethyl cellulose air/water-acetone	glass beads (6 mm) irregular gravel (2.6 mm)	660.4 × 25.4 mm rectangular cross section column	two-dimensional column purely empirical
Blum and Toman (1977)	$\frac{(\epsilon_g + \epsilon_l) - (\epsilon_l)_{U_g=0}}{1 - (\epsilon_l)_{U_g=0}} = f(U_g)$	N_2/light mineral oil	cylindrical catalyst Dia. (mm) / Length (mm) 3.18 / 3.18 4.76 / 2.38 4.76 / 4.76	101.6 mm I.D.	graphical description for $f(U_g)$
Soung (1978)	$\left(\frac{H_0}{H}\right)\Big/\left(\frac{H_0}{H}\right)_{U_g=0} = 1.50 + 0.16\,ln\left(\frac{U_l}{U_g}\right) - 0.065\,ln(\phi_s Re_t)$ for $0.06 \le \frac{U_l}{U_g} < 0.6$ $\left(\frac{H_0}{H}\right)\Big/\left(\frac{H_0}{H}\right)_{U_g=0} = 2.09 - 0.17\,ln(\phi_s Re_t)$ for $0.6 \le \frac{U_l}{U_g} < 5$ $\left(\frac{H_0}{H}\right)_{U_g=0} = 1 - 4.50\left(\frac{U_l}{U_t}\right)^{2.15}$ for $\frac{U_l}{U_t} \le 0.25$ $\left(\frac{H_0}{H}\right)_{U_g=0} = 1 - 1.22\left(\frac{U_l}{U_t}\right)^{1.20}$ for $\frac{U_l}{U_t} > 0.25$	N_2/n-heptane	Co-Mo catalyst (0.635, 1.27 and 1.6 mm)	127 and 152.4 mm I.D. columns	purely empirical

TABLE 4. (*Continued*)

Investigators	Correlation Equations	Gas-Liquid	Solid	Column Dimension	Remarks
Begovich and Watson (1978a)	$Re_t = d_p U_l \rho_l / \mu_l$, ϕ_s = sphericity of the catalyst $(\epsilon_g + \epsilon_l) = (0.371 \pm 0.017) U_l^{(0.271 \pm 0.011)}$ $\times U_g^{(0.041 \pm 0.005)} (\rho_s - \rho_l)^{(-0.316 \pm 0.011)}$ $\times d_p^{(-0.269 \pm 0.010)} \mu_l^{(0.055 \pm 0.008)}$ $\times D_c^{(-0.033 \pm 0.013)}$ $\epsilon_g = (0.048 \pm 0.010) U_g^{(0.72 \pm 0.028)} d_p^{(0.168 \pm 0.061)}$ $\times D_c^{(-0.125 \pm 0.088)}$ Units: U_l = cm/s, U_g = cm/s, ρ_s and ρ_l = g/cm^3, d_p = cm, D_c = cm, μ_l = g/cm·s	air/water	alumina beads (6.2 mm) glass beads (4.6 and 6.2 mm) alumino-silicate (1.9 mm) Plexiglas (6.3 mm)	76.2 and 152 mm I.D.	purely empirical 2,381 points for $\epsilon_g + \epsilon_l$ 913 points for ϵ_g
Kato et al. (1981)	$\left(\frac{U_l}{U_l}\right) = (\epsilon_l / \epsilon_l^*)^n$ $\epsilon_l^* = 1 - 9.7(350 + Re_t^{1.1})^{-0.5} (\rho_l U_g^4 / g\sigma)^{0.092}$ $\frac{5.1 + 86.2(\rho_l U_g^4 / g\sigma)^{0.285} - n}{n - 2.7} = [0.1 + 0.443(\rho_l U_g^4 / g\sigma)^{0.165}] \times Re_t^{0.9}$	air/water air/carboxymethyl cellulose sol.	glass sphere 0.42, 0.66, 1.2 and 2.2 mm	52 and 120 mm I.D.	modified from the correlation of Garside and Al-Dibouni (1977)

$$x = 1 - 0.877 \frac{U_t}{\frac{U_g}{\epsilon_g} - \frac{U_l}{\epsilon_l}}, \quad \text{for} \quad \frac{U_t}{\frac{U_g}{\epsilon_g} - \frac{U_l}{\epsilon_l}} \leq 1.14 \tag{9a}$$

$$x = 0, \quad \text{for} \quad \frac{U_t}{\frac{U_g}{\epsilon_g} - \frac{U_l}{\epsilon_l}} > 1.14 \tag{9b}$$

The equation shows that x increases as the particle size or the superficial liquid velocity decreases, and the liquid viscosity or superficial gas velocity increases. As pointed out by Dhanuka and Stepanek (1978), the value of x is virtually zero for glass particles with a size larger than 2 mm. Vasalos et al. (1979, 1980) and Rundell et al. (1980) applied Bhatia and Epstein's generalized wake model to explain the holdup data from the H-Coal process.

In the wake models, several types of correlation equations for ϵ_g have been presented: some of them are based on the gas-liquid two-phase flow theory, while others are purely empirical in nature. Ostergaard (1965) obtained an empirical equation for the bubble velocity. Bhatia and Epstein (1974a) employed correlation equations for the bubble velocity proposed for gas-liquid two-phase flow directly to predict the gas holdup in the three-phase system. Darton and Harrison (1975) applied the drift flux theory developed by Wallis (1969) for gas-liquid two-phase flow to describe the three-phase system. The same method is employed by Dhanuka and Stepanek (1978) who, however, defined the drift flux differently from that of Darton and Harrison (1975). Efremov and Vakhrushev (1970) presented an empirical equation for estimating ϵ_g. Baker et al. (1977) used the measured bubble velocity to calculate k for the wake model.

To estimate the liquid holdup and the bed porosity (or the solid holdup), the correlation based on the generalized wake model by El-Temtamy and Epstein (1978) and that based on the solid-free wake model by Darton and Harrison (1975) are recommended because of the reasonable accuracy. However, in calculations using the wake models, a potential difficulty exists in the estimation of the gas holdup for the model.

Correlation equations other than those based on the wake models for phase holdups in cocurrent three-phase fluidized beds are summarized in Table 4. Most of these correlations are purely empirical in nature and are usually obtained without considering whether the bed initially contracts or expands. Recently, Vasalos et al. (1982) and Schaefer et al. (1983) studied holdups in a slurry-solid fluidized bed to simulate the H-Coal reactor. Vasalos et al. (1982) showed that the bed porosity in the slurry-solid fluidized bed (without gas flow) can be well represented by the bed porosity correlations proposed for liquid-solid fluidized beds. Using kerosene as the liquid phase, Schaefer et al. (1983) showed that the gas holdup decreases with an increase of the fines loading at high gas velocity conditions while fines loading has little effect on gas holdup at low gas velocity conditions. Schaefer et al. (1983) further indicated that the gas holdup and bed expansion distinctly increase with an increase of the bed pressure.

The gas holdup in a three-phase fluidized bed with fine particles is lower than that in the corresponding solid-free systems observed by Adlington and Thompson (1965) and Viswanathan et al. (1964). The reduction in the gas holdup due to the presence of the solid is commonly observed in bubble column slurry reactors (Kato et al., 1963; Kurten and Zehner, 1979). The gas holdup behavior is strongly dependent upon the flow regimes (Michelsen and Ostergaard, 1970). That is, in the regime of bubble coalescence, considerable reduction in the gas holdup takes place. Furthermore, the physical properties of the liquid, such as viscosity and surface tension, affect the bubble characteristics and phase holdup behavior (Kim et al., 1975). Blum and Toman (1977) reported an extremely high gas holdup existing in a nitrogen/light mineral oil/coarse catalyst particles system. The gas holdup was observed to increase linearly up to 50% as the gas velocity increased to 14 cm/s in the system where the liquid and gas velocities are identical and a foam phase is formed.

The liquid holdup behavior is less complicated than the bed expansion or gas holdup. The liquid holdup decreases monotoni-

cally with increasing gas velocity and increases with increasing liquid velocity (Michelsen and Ostergaard, 1970). Empirical equations of the liquid holdup were presented for particle sizes of 0.25, 1 and 6 mm in diameter, by Ostergaard and Michelsen (1968). Kim et al. (1972) have taken into account the effect of liquid viscosity and surface tension in the expression for their liquid holdup correlation. An empirical correlation for the liquid holdup in a bed of fine particles was given by Razumov et al. (1973). Recently, Kato et al. (1981) developed a correlation for liquid holdup in the three-phase fluidized bed by modifying the empirical equation proposed by Garside and Al-Dibouni (1977) for the liquid holdup in the liquid-solid fluidized-bed system.

In summary, for independent estimation of porosity in a bed containing relatively large particles, the correlation of Dakshinamurty et al. (1971) and that of Begovich and Watson (1978a) can be employed, since these correlations are based on a large number of data obtained with various properties of particles. For liquid holdup estimation, the correlation of Kato et al. (1981) is recommended because of the wide coverage of particle size and liquid viscosity and the unified expression they developed in terms of dimensionless parameters. The gas holdup varies significantly with the flow regimes, and no satisfactory unified, independent correlation is available yet. However, the drift flux approach of Wallis (1969) and the Nicklin model (1962) provide a basic framework for the gas holdup analysis for the cocurrent three-phase system (Darton and Harrison, 1975; Chern et al., 1982). An analysis based on such models is recommended in the attempt to correlate gas holdup. To accurately evaluate the gas holdup in an industrial system, direct measurement using a column with a diameter greater than 15 cm is needed.

Criterion for Initial Bed Contraction and Effects of Solids Wettability. As indicated earlier, the bed may either contract or expand when a low flow rate of gas in introduced into a liquid-solid fluidized bed. According to Darton and Harrison (1975), the bed contracts if

$$\frac{\partial}{\partial U_g}(\epsilon_g + \epsilon_l)\bigg|_{U_g \to 0} < 0 \tag{10}$$

Based on the solid-free wake model, mathematical descriptions for the criterion of the contraction-expansion behavior were presented by Darton and Harrison (1975), Epstein and Nicks (1976), and Epstein (1976). Recently El-Temtamy and Epstein (1979) developed the criterion based on the generalized wake model of Bhatia and Epstein (1974a). They showed that bed contraction occurs when ψ, defined as:

$$\psi = \left(\frac{n}{n-1} + k\right)\frac{U_l}{\epsilon_l} + \frac{xk(U_g/\epsilon_g)}{n-1} - \left[(1+k)U_l + \frac{k}{n-1}\left(\frac{U_g}{\epsilon_g} - \frac{U_l}{\epsilon_l}\right)\right] \tag{11}$$

is negative. The results of these investigations indicate that a large value for k, a high bubble velocity or a high liquid viscosity favors bed contraction, whereas large particle size or high particle density favors bed expansion. These indications are quantitatively consistent with the experimental observation of the holdup behavior by Kim et al. (1975), who measured phase holdup characteristics with varying viscosity and surface tension of the liquid.

Bhatia et al. (1972) investigated the effect of the wettability of the particles on bed expansion using 1 mm glass beads coated with Teflon spray, giving rise to almost nonwettable conditions on the particle surface. They observed that a bed of nonwettable beads always expands upon the introduction of gas. In contrast, a bed of clean, wettable beads contracts upon the introduction of gas at low gas velocity. By rendering the solids nonwettable, the formation of liquid wakes is probably inhibited; thus, beads of small nonwettable particles expand upon the introduction of gas.

Using large particles (6 mm glass beads) with and without Teflon coating, Armstrong et al. (1976a) investigated the effect of solid wettability on holdup behavior. The nonwettable particles exhibited greater bed expansion or smaller solids holdup. The gas holdup for the Teflon-coated beads was much lower than that for the uncoated beads. These results imply that by rendering the solids nonwettable, the increased gas-solid contact results in adherence of the bubbles to the solids; thus, the breakup of the bubbles is reduced.

The work of adhesion, W_{SLV}, which represents the energy required per unit interfacial area to separate a liquid from a solid, is given by:

$$W_{SLV} = \sigma(1 + \cos\theta') \tag{12}$$

where σ is the liquid-gas surface tension and θ' is the contact angle. The solid tends to be nonwettable as θ' increases. As shown by Eq. 12, the surface tension may also affect the tendency toward direct contact between gas and solid. The use of a low surface tension liquid causes bed expansion rather than bed contraction, as shown experimentally by Dakshinamurty et al. (1971). The wake volume is relatively insensitive to the surface tension in a bed of small particles (Baker et al., 1977). Some discussions were made on the effect of surface tension and solid wettability on x by El-Temtamy and Epstein (1979). However, little consideration has been made of the effect of surface tension on phase holdups (Mach, 1970; Kim et al., 1975). Thus, additional study is required to elucidate the effect of surface tension and solid wettability on the phase holdup behavior in three-phase fluidized beds.

Flow Models Other than the Wake Model and Incipient Fluidization. A simplified flow theory to correlate the phase holdups in both two- and three-phase transport systems was developed by Bhaga and Weber (1972a,b). The linear relations between the velocities of the individual phases and the gas and solids holdup in the gas-liquid-solid flow system were deduced by assuming that the local relative velocity of each of the dispersed phases (gas and solid) is a function only of the dispersed-phase concentration and the physical properties of the system. The theory was successfully compared with the experimental data for individual phase holdups which were taken under limited experimental conditions, involving relatively low gas flow rates varying up to 2.5 cm/s and low solids holdups varying up to only 6%. The model, however, does not take into account the flow phenomena of the wakes behind the bubbles and hence it cannot predict bed contraction in three-phase fluidized-bed operation.

A cell model for three-phase fluidization at creeping flow was developed by Bhatia et al. (1974). The model assumes that two different spherical cells, which consists of a gas-liquid cell defined by Gal-Or and Waslo (1968) for the cocurrent gas-liquid flow and a liquid-liquid cell defined by Happel and Brenner (1965) for liquid fluidized systems, can be coupled. This model, however, cannot be verified since the experimental data available in the literature are mainly in the intermediate or high Reynolds number flow region. Furthermore, the model always predicts bed expansion upon the introduction of gas in the liquid-solid fluidized bed.

All the flow models described above assume the holdups and the velocities of individual phases to be uniform across the entire cross section of the column. However, the distributions of the holdups and velocities are not uniform in the radial direction in circular columns as shown experimentally by Rigby et al. (1970a) for the gas holdup, and by Morooka et al. (1982) for the gas holdup and the liquid velocity. Morooka et al. (1982) found that the flow pattern of the liquid phase in the three-phase fluidized bed is similar to that of the bubble column: i.e., the liquid flows upward in the central region and downward in the peripheral region. They proposed a circulating flow model similar to that of Ueyama and Miyauchi (1979) for a gas-liquid bubble column to simulate the lateral distributions of gas holdup and liquid average linear velocity.

The behavior of incipient fluidization for beds of fine particles is considerably different from that for beds of coarse particles. For three-phase fluidization utilizing small particles, Ermakova et al. (1970a) defined three hydrodynamic states: fixed bed, heterogeneous fluidized bed, and homogeneous fluidized bed. The regions of these states as functions of the gas and liquid flow rates are given in Figure 7.

Ermakova et al. (1970a) proposed empirical correlations for the onset liquid velocity for both heterogeneous and homogeneous fluidization. In the region of heterogeneous fluidization some pe-

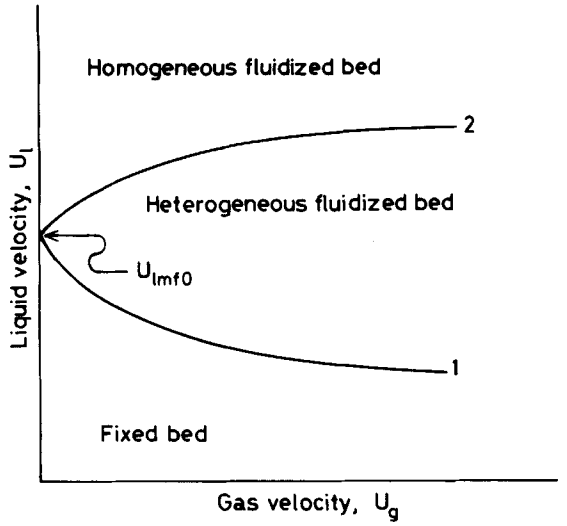

Figure 7. Hydrodynamic States of Three-Phase Fluidization for the Bed of Fine Particles (Ermakova et al., 1970).

culiar behavior of the pressure drop and the wall heat transfer have been noted. This includes the exhibition of local maximum and minimum points on the curve of total pressure drop vs. liquid flow rate at a constant gas velocity (Muroyama, 1976), as well as on the wall heat transfer coefficient vs. liquid velocity curve (Kato et al., 1978, 1980). The heterogeneous fluidization region that exists in beds of small particles does not exist in beds of large particles. In the case of large particle fluidization, the bed expands uniformly with either an increase of the liquid velocity or the gas velocity beyond the onset fluidization condition. The liquid velocity required for the onset of fluidization in a bed of coarse particles decreases with an increase of the gas velocity (Begovich and Watson, 1978a; Lee and Al-Dabbagh, 1978). Empirical correlations of the liquid velocity for the onset of fluidization were developed for beds of coarse particles by Begovich and Watson (1978a). By comparing the experimental data for pressure drop with the prediction based on the equation proposed by Turpin and Huntington (1967) for cocurrent gas-liquid beds, Lee and Al-Dabbagh (1978) concluded that the onset of fluidization occurs when the pressure drop in the packed bed is equal to the effective weight of the particles. Fan et al. (1982d) studied incipient fluidization characteristics of a cocurrent upward gas-liquid-solid fluidized bed containing a binary mixture of particles of varying sizes and/or densities. The particles used were glass beads (3, 4 and 6 mm) and aluminum particles (5.5 mm). The incipient fluidization velocity of the mixture, U_{lmf}, was found to vary with that of flotsam particles $(U_{lmf})_1$, that of jetsam particles, $(U_{lmf})_2$, and the weight fraction of the jetsam particles, x_2, by $U_{lmf}/(U_{lmf})_1 = \{(U_{lmf})_2/(U_{lmf})_1\}^{x_2^{1.69}}$.

Local Holdups and Entrainment of Solid Particles in the Disengagement Section. The carryover of particles, which would pose a serious practical problem for operation of a three-phase fluidized bed, may occur if the height of the disengagement (free board) section is not adequate. The measurement of the local holdups and the analysis of the mechanism of particle entrainment and deentrainment in the free board region are, consequently, important for design and optimal control of three-phase fluidized-bed systems.

Fundamental aspects of particle entrainment and deentrainment in the transition region of the freeboard were phenomenologically investigated by Page and Harrison (1974) using a two-dimensional column. They observed that the particles are pulled from the upper surface of the fluidized bed and carried by the wake behind the bubble into the freeboard where vortices of particles are shed from the wake. Since the liquid velocity in the freeboard is less than the particle terminal velocity, the shed particles settle back into the bed. They reported that particle entrainment decreases with decreasing bubble size and bubble frequency and with increasing liquid velocity and particle size. They also reported that entrainment is considerably reduced by inserting a wire mesh baffle into the freeboard section. The axial distributions of the gas and solids holdups in the transition region were found by Begovich and Watson (1978a,b) to be represented by the error functions involving several adjustable parameters. Recently, El-Temtamy and Epstein (1980b) presented a stagewise partition process model for the entrainment of the solid in the freeboard region, postulating that the solid particles are carried by the wake behind the bubble and settle with a slip velocity as given by Lapidus and Elgin (1957) in the surrounding liquid-solid region. The model compares well with the local solids holdup data.

Properties of Gas Bubbles. The flow behavior of a single bubble was first investigated by Massimilla et al. (1961), who measured the rise velocity of single gas bubbles with respect to the injected gas volume at a constant expansion state in a 3.5 in. (89 mm) I.D. cylindrical, liquid fluidized bed of fine particles. It was found that the bubble rise velocity increases with an increase of the bubble volume in an identical manner as that for gas bubble rise in highly viscous liquids. The rise velocity was observed to increase with an increase of the bed expansion in their experiment.

Henriksen and Ostergaard (1974a), employing a cine photograph technique, measured the rise velocity of large single bubbles in a two-dimensional column. They utilized water and aqueous solutions of methanol and glycerol as the fluidizing liquids and glass beads of 0.2, 1 and 3 mm as the fluidized solids. They found that the relationship between the bubble rise velocity and the bubble size can be represented by an equation similar to that obtained by Davies and Taylor (1950) for spherical cap bubbles rising through inviscid liquids as:

$$V_{b\infty} = K(gR)^{1/2} \tag{13}$$

For spherical cap bubbles in gas-liquid systems, Davies and Taylor (1950) showed that the value for K is 2/3. Henriksen and Ostergaard (1974a) reported that the surface tension of liquid has no noticeable effect on the bubble rise velocities. They observed that the shape of the bubble is commonly a cylindrical cap and the included angle increases with an increase in viscosity of the fluidized bed. The same conclusion for the bubble shape was made by Ostergaard (1966). Vandershuren et al. (1974) reported that the bubbles have a spherical cap shape, and the included angle decreases with an increasing liquid flow rate.

The rise velocity of single bubbles through a liquid fluidized bed was also studied by Darton and Harrison (1974b). The equivalent diameter of the bubble, d_B, was found to vary from 5 to 25 mm in a water fluidized bed of either 500 μm or 1 mm sand particles. The drag coefficient for spherical cap bubbles was correlated by the following equation:

$$C_D = \frac{4}{3} g \frac{d_B}{{U_B}^2} = 2.7 + \frac{B}{\rho U_B d_B} \tag{14}$$

where

$$U_B = U_b - \frac{U_l}{\epsilon_l} \tag{15}$$

The constant B in Eq. 14 was found to be a function of the bed expansion and the particle size. The data for a bed of 500 μm particles showed a higher drag coefficient for small bubbles than for large bubbles.

El-Temtamy and Epstein (1980a) compared the bubble rise velocity predicted from the Davies and Taylor relationship with the experimental data of Darton and Harrison (1974b), and estimated the radius of the spherical cap bubble, R, from the information on the included angle reported by Henriksen and Ostergaard (1974a). They showed that the predictions of the bubble rise velocity based on the Davies and Taylor equation is quite satisfactory, provided the bed voidage is greater than about 0.5. The discrepancy at low bed voidage was attributed to the non-Newtonian behavior of the concentrated solid suspension.

Massimilla et al. (1961) reported that the bubble diameter increases considerably with the distance above the gas distributor in beds of small particles with diameters ranging from 0.22 to 1.1 mm.

This is due to the fact that bubbles coalesce as they move up the bed. Adlington and Thompson (1965) also observed considerable bubble coalescence taking place in a three-phase fluidized bed containing distributed sizes of alumina particles. Ostergaard (1964) observed that the bubble size at low liquid flow rates is larger than that at high liquid flow rates.

On the contrary, Lee (1965) reported that breakup of bubbles takes place in a three-phase fluidized bed when the size of the particle is comparable to that of the bubble. Utilizing 6 mm glass beads and a gas distributing device which provides rather large bubbles, he observed that the bubble diameter decreases with an increase in the bed height. The measurement of the bubble diameter was made immediately above the bed, which was maintained at a constant expansion ratio. In such a bed of coarse particles, the bubbles emerging from the surface of the bed appear to be of uniform size (Ostergaard, 1969).

For beds of small particles, Ostergaard (1966) measured the bubble frequency from a single orifice and the bubble frequency at the bed surface. It was noted that the rate of coalescence decreases as the bed porosity increases and the change in bubble frequency takes place within a relatively short distance from the orifices. Rigby et al. (1970a) measured the local frequency, average size, size distribution, rise velocity and local holdup of gas bubbles in three-phase fluidized beds of 10 cm I.D. by electroresistivity probes. They utilized rather fine particles with diameters ranging from 0.12 to 0.775 mm. The average bubble size increased with a decrease of the liquid flow rate and an increase of the axial distance in a manner similar to that reported by Massimilla et al. (1961). Furthermore, the distribution of the bubble sizes became wider with an increase of the axial distance or with a decrease of the liquid flow rate. They found that the bubble velocity obtained experimentally for the multibubble system is much higher than that predicted by the Davies and Taylor relationship for the single bubble system, and the trends of variation between the two bubbles velocities are quite different. An empirical correlation was developed for the bubble velocity as:

$$[U_b - (U_g + U_l)]\left(\frac{1-\epsilon}{\epsilon}\right)^2 = 32.5\,(l)^{1.53} \tag{16}$$

where U_b, U_g and U_l are in cm/s and l is in cm.

Using a photographic technique, Page and Harrison (1972) examined the size distribution of bubbles leaving a three-phase fluidized bed of 500 μm particles. They found that the logarithmic cumulative distribution function varies linearly with the bubbles size. Furthermore, they reported that at the higher liquid velocity (1.43 cm/s) the bubble size distribution was independent of gas flow rate and of the design of the gas distributor. At the low liquid velocity (0.85 cm/s) the gas distributor again had no effect on the bubble size distribution, but the bubble size markedly decreased with an increase of the gas flow rate. Using an impedance double-probe, Darton and Harrison (1974a) reported that the bubble size in a three-phase fluidized bed of 500–600 μm sand particles follows a log-normal distribution, with a variance which increases with an increase of the gas flow rate.

Bruce and Revel-Chion (1974) investigated the average size of bubbles emerging at the surface of a fluidized bed of large glass particles ranging from 2 to 8 mm in diameter. They observed that the bubble diameter decreases with an increase of the particle size in the range of 2 to 4 mm, reaches a minimum at a particle size of 6 mm and then increases at the size of 8 mm. For the 6 and 8 mm particles, the size of the gas bubbles decreases as the liquid velocity increases, reaching a minimum at a liquid velocity around 13.2 cm/s. A further increase in the liquid velocity increases the size of the gas bubbles. They also reported that the bubble diameter for a bed of 2 mm particles was virtually independent of the gas flow rate, while for a bed of 6 mm particles it markedly increased linearly with an increase of the gas flow rate. Lee et al. (1974) reported that the bubble size decreases with increasing particle diameter. Lee and Buckley (1981) proposed an empirical correlation equation which expresses the bubble diameter in a bed of 6 mm particles in terms of the energy consumption in the liquid phase (Calderbank, 1967). The effects of the surface tension and viscosity on the average bubble size and average bubble rise velocity were investigated in detail by Kim et al. (1977). The measurements were made by cine photography in a two dimensional column using 1.0 mm glass beads, 2.6 mm irregular gravel, and 6 mm glass beads. They indicated that the clouds of bubbles rise considerably faster than a single isolated bubble expressed by the Davies and Taylor relationship. It was reported that both the size and rise velocity of the bubble increased with the gas velocity, but size and velocity are relatively insensitive to the liquid velocity, viscosity and surface tension. The correlation equations for the average bubble size d_B and the rise velocity of the bubble relative to that of the liquid, U_B, were given as follows.

$$d_B = 13.4 U_l^{0.052} U_g^{0.248} \gamma^{0.008} \sigma^{0.034} \tag{17}$$

$$U_B = U_b - \frac{U_l}{\epsilon_l} = 83.1 U_l^{0.065} U_g^{0.339} \gamma^{0.025} \sigma^{0.179} \tag{18}$$

or

$$U_B = 18.0 d_B^{0.989} \tag{19}$$

Here d_B is in mm, U_l and U_g in mm/s, σ in dyne/cm, and γ in $Ns^{\bar{n}}/m^2$. It should be noted that some wall effects may exist in these correlations due to the fact that the experimental column had a rectangular cross section with a rather narrow width. The in-bed bubble property distributions in a fluidized bed of large particles were recently measured using a dual electrical resistivity probe by Matsuura and Fan (1983). They reported that the bubble rise velocity in the slugging regime exhibits the broadest distribution which is followed by that in the coalesced bubble regime and the dispersed bubble regime. It was noted that a small mean bubble size is associated with a small variance in the dispersed bubble regime while a large mean bubble size is associated with a large variance in the coalesced bubble regime as well as slugging regime.

The presence of small particles in a gas-liquid system commonly results in considerable bubble coalescence. This has been attributed to the effect of the liquid-solid suspension, which behaves as a pseudohomogeneous medium with higher density and viscosity than the liquid medium alone as indicated by several investigators (e.g., Massimilla et al., 1961; Ostergaard, 1966; Rigby et al., 1970a). The bubble size increases with the height above the gas distributor, and extensive bubble coalescence takes place within a short distance above the gas distributor (Ostergaard, 1966). On the other hand, the bubble can be split by turbulent eddies resulting from the agitation of the bed caused by the rising motion of the large bubbles. Thus, the size distribution of the bubbles emerging from a three-phase fluidized bed of fine particles is a product of the competing effects of bubble splitting and bubble coalescence. The size distribution of the bubbles is virtually independent of the initial size of the bubbles immediately above the distributor (Page and Harrison, 1972). The fundamental, physical mechanisms of these phenomena, however, are not well understood and need to be analyzed more extensively.

In a bed of coarse particles, bubble breakup takes place as first reported by Lee (1965). The bubbles emerging from the surface of such a fluidized bed are quite uniform and relatively small in size compared to those observed in a solid-free gas-liquid system (Ostergaard, 1969; Lee et al., 1974; Bruce and Revel-Chion, 1974). The several mechanisms proposed to date on bubble splitting in three-phase fluidized beds have been mainly concerned with coarse particles. Lee (1965) and Lee et al. (1974) assumed that bubble breakup occurs when particles with high momentum penetrate into the bubble. According to their simple theory, bubble breakup occurs when

$$We = \frac{\rho_s U_b^2 d_p}{\sigma} > 3 \tag{20}$$

In their theory, the viscous force is neglected. Roszak and Gawronski (1979) considered a similar mechanism for the breakup of liquid drops in a liquid-liquid-solid fluidized bed. Henriksen and Ostergaard (1974b) reported, however, that in experiments where

a single 5 mm steel sphere particle, or a 3 or 6 mm glass sphere particle was released above a bubble, none of the bubbles disintegrated when the spheres fell through the bubble roofs. For the multiparticle system the bubble can possibly be split by groups of particles (Page and Harrison, 1972; Lee and Al-Kaisi, 1976).

Henriksen and Ostergaard (1974b) suggested that the bubbles in pure liquids and in three-phase fluidized beds are broken up as a result of the Taylor instability on the roof of the bubbles (Bellman and Pennington, 1954) and the particles penetrating a large bubble will not cause bubble breakage if the particle diameter is smaller than the half of the wavelength of the smallest unstable wave. This theory estimates that bubble splitting due to penetration by the particle through the bubble roof proposed by Lee et al. (1974) can take place in the air-water-glass spheres system only when the diameter of the particles exceeded 8.5 mm, which is much larger than 2.5 mm experimentally determined by Kim et al. (1977) for air-water-glass particle beds. Considering the fluid percolation through the gas bubble, the bubble splitting mechanism based on the Taylor instability concept was modeled and analyzed by Clift et al. (1974) for the gas-solid fluidization system. The modification of this instability model to the three-phase fluidization system was discussed by Bhatia (1976). However, the validity of the modification was questioned by Clift et al. (1976), as the fluid percolation through the gas bubble does not occur in three-phase fluidization systems.

Semifluidized Bed and Draft Tube Spouted Bed. Studies of semifluidization have been mildly concerned with liquid-solid or gas-solid systems (e.g., Fan and Wen, 1959). Recently, Chern et al. (1982) investigated the hydrodynamic behavior of the cocurrent gas-liquid-solid semifluidized bed where liquid is the continuous phase. The gas holdup and friction factor of the packed bed section of the semifluidized bed were analyzed based on the phase separation flow model. The generalized wake model, proposed by Bhatia and Epstein (1974a) and refined further by El-Temtamy and Epstein (1978), was adapted to account for the bed expansion of the fluidized bed section of the semifluidized bed.

The hydrodynamic behavior of a draft tube three-phase spouted bed including flow modes, pressure profile and pressure drop, bubble penetration depth, overall gas holdup, apparent liquid circulation rate, and bubble size distribution was studied only recently by Fan et al. (1984a,d). They identified three flow modes of operation: a packed bed mode, a fluidized bed mode, and a circulated bed mode. They reported that at high gas flow conditions, an optimal solids loading exists which yields a maximum apparent liquid circulation rate. The average bubble size in the draft tube region is higher than that in the annular region for both the dispersed bubble regime and the coalesced bubble regime in the draft tube region. The fundamental study of the draft tube spouted bed is of considerable importance because of its potential applicability in chemical and biochemical processing. Further study is needed in this area.

Countercurrent Gas-Liquid-Solid Fluidization

Countercurrent three-phase fluidization with gas as the continuous phase has been given a variety of names. Kielback (1959) was the first researcher to describe this type of fluidization in an application to gas scrubbing processes and termed the phenomenon "floating bed scrubber." This fluidization mode has also been called a "turbulent bed contactor" (TBC) by Douglas (1964), a "mobile-bed contactor" by Tichy et al. (1972), and a "fluidized packing contactor" by O'Neill et al. (1972). The Russian literature refers this type of fluidization as a "tower with fluidizing packing" or a "column with mobile packing." The process has been widely used in industry to absorb gases into the liquid phase, and the term "turbulent contact absorber" (TCA) has become the most popular English designation. Countercurrent three-phase fluidization with liquids as the continuous phase is termed "inverse gas-liquid-solid fluidization."

Turbulent Contact Absorber. A TCA consists of a mass of particles confined between two retaining grids. The particles typically consist of hollow, molded polyethylene or polypropylene spheres

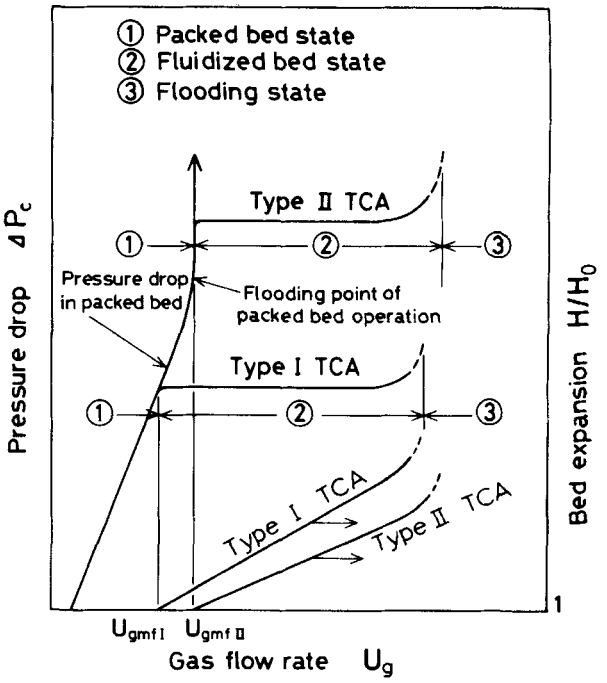

Figure 8. Pressure Drop and Bed Height as Functions of Superficial Gas Velocity for a Given-Liquid Flow Rate for a TCA.

or foam polystyrene spheres with a density between 100 and 400 kg/m^3 and diameters between 10 and 38 mm. The open area of the lower retaining grid in industrial units is normally greater than 70%. This large open area also allows the liquid to be drained by gravity. The distance between the lower and upper retaining grids is usually set at about three times the static bed height of the particles. The gas flows upward in a TCA as a continuous phase, while the liquid is ordinarily sprayed over the top of the fluidized bed and flows downward by gravity. A crosscurrent scheme to the liquid flow is, however, also possible in the TCA operation as employed by Mrowiec and Laszuk (1974) who sprayed the liquid through the side holes on the column wall, located just above the retaining grid, and withdrew it from the bottom of the column.

As the gas flow rate is increased at a constant liquid flow rate in a TCA, three successive hydrodynamic states are observed: the static bed, the fluidized bed, and the flooding bed states. The variations of the pressure drop in TCA columns are shown qualitatively in Figure 8 (O'Neill et al., 1972; Vunjak-Novakovic et al., 1980). O'Neill et al. (1972) explained that two types of fluidization are possible: i.e., the onset of fluidization for beds with very low density packings occurs at a gas velocity before the flooding velocity for the equivalent countercurrent packed bed, while the onset of fluidization for packings with a density higher than about 300 kg/m^3 (for air/water systems) always occurs at the flooding point. The former mode of fluidization is termed Type I TCA—fluidization without flooding and the latter is called Type II TCA—fluidization with flooding. O'Neill et al. (1972) indicated that any operating point in a Type II TCA occurs at flooding conditions. As the gas flow rate is increased further, the "true" flooding bed state is finally reached when the particles are pushed up to the upper retaining grid where they form a packed bed (Barile et al., 1975). In such a bed the pressure drop sharply increases with increasing gas velocity, and the liquid is entrained in the exhaust gas stream (Douglas et al., 1963). Due to intense liquid turbulence and high mass transfer effects, a TCA is preferably conducted under the Type II operating condition for chemical reaction application unless the pressure drop is too high to be acceptable (Viswanathan and Leung, 1984).

Recently, Uchida et al. (1980) showed that the onset of the true flooding condition for the Type I TCA can be estimated from the flooding chart for the packed bed. On the other hand, Gel'perin et al. (1968b) claimed that the flooding condition of the TCA is also

dependent upon the open area and geometry of the grid. They proposed an empirical correlation equation to estimate the flooding condition of the TCA with grid openings of 25 to 70%.

The mode of fluidization for shallow beds is considerably different from that for deep beds. Uniform fluidization occurs in beds with static bed heights shorter than the column diameter, while slugging phenomena are commonly observed in deep beds (Barile et al., 1971). A flow regime map for a TCA using ½- and ¾-in. (13- and 19-mm) packings was presented by Barile et al. (1975), who showed that the stable operation regime narrows with increasing static bed height.

It has been observed that the open area of the supporting grid strongly affects the hydrodynamics of the system (Gel'perin et al., 1968b; Kito et al., 1976a,d, 1978). The data on the hydrodynamics of the TCA, reported by Gel'perin et al. (1966), Blyakher et al. (1967), Aksel'rod et al. (1969), and Balabekov et al. (1969a, 1969b), were obtained for grids with small open areas of 34.7–51.7%, 41%, 35.5–56.8% and 30–60%, respectively. Wall effects may also be significant for small ratios of the column diameter to the packing diameter.

A steady-state macroscopic force balance for the TCA is given by (Wozniak, 1977):

$$\Delta P_c = (\rho_s \epsilon_s + \rho_l \epsilon_l + \rho_g \epsilon_g) gH + \Sigma F \qquad (21)$$

and

$$\Sigma F = F_g + F_\sigma + F_w \qquad (22)$$

Information about F_σ is not available in the literature. A number of authors have observed that F_g is strongly affected by grid geometry, and correlations for F_g were developed by Blyakher et al. (1967), Gel'perin et al. (1968b), Levsh et al. (1968b) and Mayak and Matrozov (1969). Tichy et al. (1972) found that F_g was negligible for a grid with an opening of 83%. When the *pressure drop* is considered only for the fluidized bed section, F_g does not have to be taken into account. Kito et al. (1976e) stated that F_g can be neglected when a stagnant liquid layer is not present on the lower retaining grid. Wozniak (1977) and Uysal (1978) concluded that for a large diameter column F_w is very small and can be virtually neglected.

Neglecting the effects of the grids, the wall, the surface tension and the gas phase static head, Eq. 21 can be reduced to

$$\Delta P_c = (\rho_s \epsilon_s + \rho_l \epsilon_l) gH = (\rho_s \epsilon_{s,st} + \rho_l \epsilon_{l,st}) gH_0 \qquad (23)$$

$\epsilon_{l,st}$ and $\epsilon_{s,st}$ in Eq. 23 are defined respectively by $\epsilon_{l,st} = (H/H_0)\epsilon_l$ and $\epsilon_{s,st} = 1 - \epsilon_0 = (H/H_0)\epsilon_s$. Equation 23 was employed by Barile and Meyer (1971) and Tichy and Douglas (1973) to correlate pressure drop data. The pressure drop due to the weight of dry packing is always constant, while that due to the liquid holdup is a strong function of operating conditions and the geometry of the system.

In the fully-fluidized state where the pressure drop is almost independent of gas velocity, Tichy et al. (1972) found the pressure drop to be independent of packing size. Barile and Meyer (1971), however, reported pressure drop data which increase with decreasing packing size. Packing height also affects the pressure drop (Wozniak, 1977; Kito et al., 1976e). This is a result of the fact that the liquid holdup depends on the static bed height, as will be shown later.

Experimental data on the pressure drop of TCA's were reported by several authors (Douglas et al., 1963; Gel'perin et al., 1966; Balabekov et al., 1969b; Miconnet et al., 1982). Macroscopic models attempting to correlate the pressure drop in the TCA were proposed by several investigators (Blyakher et al., 1967; Gel'perin et al., 1968b; Levsh et al., 1968a,c; Chen and Douglas, 1968; Barile and Meyer, 1971; Kito et al., 1976e; Wozniak, 1977; Uysal, 1978). Blyakher et al. (1967) and Gel'perin et al. (1968b) obtained empirical correlations for pressure drop due to the hydraulic head of liquid.

The correlations for pressure drop in a TCA are summarized in Table 5. Some of them are purely empirical in nature, but the majority are developed based on Eq. 21 or 23. It is obvious from

TABLE 5. CORRELATION EQUATIONS FOR PRESSURE DROP IN A SINGLE-STAGE TCA

Investigators	f	ρ_s [kg/m^3]	D_c/dp	Correlation Equations*
Blyakher et al. (1967)	0.41	90, 180	9.2	$\Delta P_c = \xi_g \frac{U_g^2 \rho_g}{2} + (1-\epsilon_0)(\rho_s - \rho_g) gH_0 + \xi_f U_g^{1.75} U_l^{0.5} + \xi_b U_l H_0$ ξ_g, ξ_f and ξ_b are constants
Gel'perin et al. (1968b)	0.345 ~ 0.70	160 ~ 900	1.7 ~ 61.7	$\Delta P_c = \xi'_g \frac{U_g^2 \rho_g}{2(1-\tau')} + (1-\epsilon_0)\rho_s g H_0 + 0.138 U_l^{0.5} H_0^{0.75} d_p^{-0.6} \rho_l g + F_\sigma$
Levsh et al.** (1968a)				$\Delta P_c = \frac{Wg}{S} + 14.0 U_l^{0.55} U_g (14.29 H_0)^m + F_\sigma + F_g$
Tichy et al. (1972)	0.78	155	11.4 ~ 7.5	$\log\left(\frac{2\rho_g \Delta P_c}{G_g^2} \frac{D_c}{H_0} \frac{1}{1+CG_l}\right) = 4.003 - 2.240 G_g + 0.840 G_g^2 - 0.127 G_g^3$ C is a constant which depends on H_0/D_c
Uchida et al. (1977)				$\Delta P_c = (1-\epsilon_0)\rho_s g H_0 + 9.38 \times 10^8 \mu_l^{2.3} f^{-0.42} \left(\frac{d}{D}\right)^{-0.84} d_p^{-0.84} \rho_s^{0.18} H_0 U_l + 788 U_g^{2.91} U_l^{1.27}$
Wosniak (1977)	0.6	266	10.2	$\frac{(\Delta P_c - W\,g/S)}{\rho_g U_g^{\,2}} = 4.672 \times 10^5 \left(\frac{H_0}{D_c}\right)^{0.4515} \left(\frac{d_p U_g \rho_g}{\mu_g}\right)^{-1.798} \left(\frac{d_p U_l \rho_l}{\mu_l}\right)^{0.8261}$
Barile and Meyer (1971)	0.82	109, 160	7.5, 15	
Kito et al. (1976e)	0.71 ~ 0.84	170 ~ 1,250	3.6 ~ 10.3	$\frac{\Delta P_c}{g} = (1-\epsilon_0)\rho_s H_0 + \epsilon_{l,st}\rho_l H_0$ Correlation equations for $\epsilon_{l,st}$ are given in Table 7.
Vunjak-Novakovic et al. (1980)	0.36, 0.52 and 0.78	200, 400 and 700	3.6 ~ 29	

* Use SI units for variables involved in the equations.
** Special type of packing (plastic ring) was used.

TABLE 6. CORRELATION EQUATIONS FOR BED EXPANSION IN A TCA

Investigators	f	ρ_s [kg/m^3]	D_c/d_p	Correlation Equations*/Comments
Blyakher et al. (1967)		See Table 5		$\frac{H}{H_0} = 1.17 + (0.65 + 24.6U_l^{0.75})(U_g - U_{gmf})$
Levsh et al. (1968c)**				$H/H_0 = 4.4U_l^{0.43}U_g^2$ ($U_l < 0.0078$ m/s, $U_g < 2.5$ m/s) $H/H_0 = 2.3U_l^{0.35}U_g^2$ ($U_l > 0.0078$ m/s, $U_g > 2.5$ m/s)
Aksel'rod and Yakovenko (1969)	0.3 ~ 0.6	150 ~ 500	>9.0	$H = 0.933U_l^{0.3}H_0^{0.6}\left(\frac{U_g}{f}\right)^{0.93}$ for $\frac{U_g}{f} \geqq 6$ m/s, $H = 2.16U_l^{0.3}H_0^{0.6}\left(\frac{U_g}{f}\right)^{0.43}$ for $\frac{U_g}{f} < 6$ m/s
Khanna (1971) (quoted from Uysal, 1978)	0.7	155 ~ 458	3.7 ~ 11	$\frac{H}{H_0} = 1 + 0.414\left(\frac{G_g - G_{gmf}}{G_{gmf}}\right)^{1.2}$
Tichy and Douglas (1972)	0.7	155 ~ 458	3.7 ~ 11	$\frac{H}{H_0} = 0.8849 + 0.3166G_g - 18.33d_p + 0.5852G_l^{0.6}d_p^{0.5}$
Uysal (1978)	0.87		7.6 ~ 15.3	$\frac{H}{H_0} = 1 + 0.147\frac{(G_g - G_{gmf})}{H_0}$
O'Neill et al. (1972)				$\frac{H}{H_0} = \frac{1 - \epsilon_0}{1 - \epsilon} = \frac{\epsilon_{s,st}}{\epsilon_s}$ Correlation for ϵ was proposed
Gel'perin et al. (1968b)		See Table 5		$\frac{H}{H_0} = \frac{(1 - \epsilon_0) + \epsilon_{l,st}}{1 - \epsilon_g} = \frac{\epsilon_{s,st} + \epsilon_{l,st}}{1 - \epsilon_g}$
Kito et al. (1976d)		See Table 5		
Uchida et al. (1977)				
Vunjak-Novakovic et al. (1980)		See Table 5		Correlation equations for $\epsilon_{l,st}$ and ϵ_g are given in Table 7

* Use SI units for variables involved in the equations.
** Special type of packing (plastic ring) was used.

these equations that the liquid holdup needs to be correlated in order to be able to estimate the pressure drop.

Clearly, the pressure drop without grid friction can be readily evaluated from Eq. 23 once the liquid phase holdup is known. It should be noted, however, that the pressure drop due to grid friction strongly depends on the geometry of the grid and the fluid through flow velocity. More studies on grid effects are needed.

Bed expansion data were first reported by Gel'perin et al. (1966) who used a supporting grid with an open area of only 34.5%. Chen and Douglas (1968) gave a graphical representation for the bed expansion. The bed height increases linearly with increasing gas velocity and also increases with increasing liquid velocity. Tichy and Douglas (1972) reported that the reduced bed height, H/H_0, is independent of both the static bed height and the packing density for low-density packings.

Experimental data on bed expansion for packings of relatively high density were obtained by Balabekov et al. (1969a) and Strumillo et al. (1974). A rapid increase in bed height has been observed in the region in which the gas velocity is close to the flooding point (Tichy and Douglas, 1973). When the liquid holdup and gas holdup can be estimated, the reduced bed height can be calculated from a simultaneous volume balance on the liquid and solid phases:

$$\frac{H}{H_0} = \frac{1 - \epsilon_0 + \epsilon_{l,st}}{1 - \epsilon_g} \tag{24}$$

Table 6 summarizes correlation equations for bed expansion in a TCA.

A small open area in the distributing grid strongly affects the bed expansion since a liquid layer builds up immediately above the grid, and as a consequence, the liquid holdup varies across the TCA in the axial direction. Levsh et al. (1968b) attempted to correlate the height of the liquid layer. The behavior of such beds may resemble that of a bubble column or sieve tray. Such beds can even be operated with a stationary liquid phase (Kito et al., 1976a,b,c).

In analyzing the pressure drop in the TCA, a number of correlations for the *liquid holdup* have been proposed as summarized in Table 7.

Gel'perin et al. (1968b) defined two liquid holdups: i.e., the liquid holdups in the region near the grid and in the fluidized bed. They presented an empirical correlation for the latter, showing that the liquid holdup is affected by the static bed height. Using a transient-response technique, Chen and Douglas (1968) found that liquid holdup is independent of gas flow rate but increases with increasing liquid flow rate and with decreasing packing size. Their packing diameter was varied from 12.5 to 38 mm in diameter. Barile and Meyer (1971) also presented a correlation of liquid holdup taking into consideration the effect of static bed height in a manner similar to Gel'perin et al. (1968b). The effect of the open area of the supporting grid on the liquid holdup was evaluated by Kito et al. (1976e, 1978) and Kuroda and Tabei (1981). Mayak and Matrozov (1969) also gave a correlation for the liquid holdup in a TCA. Recently, Vunjak-Novakovic et al. (1980) proposed liquid holdup correlations for the two types of fluidization: Type I TCA and Type II TCA.

Relatively little information is available regarding *gas holdup* in a TCA. Gel'perin et al. (1968b) were the first to propose a correlation equation for the gas holdup in a TCA. Kito et al. (1978) reported that the gas holdup is nearly independent of packing density, liquid viscosity and static bed height. They also stated that the gas holdup increases with increasing gas velocity, but it is unaffected by the liquid velocity. According to their results, the opening area of the supporting grid had virtually no effect on the gas holdup. Kito and his coworkers have developed several correlations for gas holdup in the TCA. The first correlation is for a TCA with a stagnant liquid (Kito et al., 1976b). The open area of the supporting grid was varied between 1.27 and 31.5%. The second correlation is for gas holdup in a TCA with countercurrent gas-liquid flow (Kito et al., 1976e). Their third correlation was a dimensionless equation also for a TCA with countercurrent gas-liquid flow (Kito et al., 1978). Vunjak-Novakovic et al. (1980) also proposed an empirical correlation for gas holdup in a TCA. Kito et al. (1976a) have also reported that the gas holdup may vary linearly with the gas-liquid interfacial area.

TABLE 7. CORRELATION EQUATIONS FOR LIQUID AND GAS HOLDUPS IN A TCA

Investigators	f	ρ_s [kg/m^3]	D_c/d_p	Correlation Equations*
Chen and Douglas (1968)	0.80	156 ~ 170	8 ~ 24	$\epsilon_l = 0.02 + 2.371 \times 10^{-3} G_l^{0.6} d_p^{-0.5}$
Gel'perin et al. (1968b)		See Table 5		$\epsilon_{l,st} = 0.138 U_l^{0.5} H_0^{-0.25} d_p^{-0.6}$ $\epsilon_g = 0.93 \left(\frac{d_p U_g \rho_g}{\mu_g}\right)^{0.4} \left[\frac{d_p^3(\rho_s - \rho_g)\rho_g g}{\mu_g^2}\right]^{-0.2}$
Barile and Meyer (1971)		See Table 5		$\epsilon_{l,st} = 1{,}160 \left(\frac{G_l^2}{d_p g \rho_l^2}\right)^{0.78} \left(\frac{d_p G_l}{\mu_l}\right)^{-0.51} \left(\frac{H_0}{d_p}\right)^{-0.36}$
Kito et al (1976a,b)**	0.0127 ~ 0.315	300 ~ 1,100	1.89 ~ 9.09	$\frac{\epsilon_g}{\{\epsilon_g(1-\epsilon_g)^2\}^{0.44}} = 0.5 \left(\frac{D_c U_g^2 \rho_l}{\sigma}\right)^{0.11} \left(\frac{U_g}{\sqrt{g D_c}}\right)^{0.22}$
Kito et al. (1976e)		See Table 5		$\epsilon_{l,st} = 0.06 + 3.018 \times 10^{-3} \left(f\frac{d}{D}\right)^{-0.84} d_p^{-0.84} \rho_s^{0.18} H_0^{-0.4} U_l$ $\epsilon_g = 0.417 U_g^{0.44}$
Kito et al. (1978)		Same as those of Kito et al. (1976e)		$\epsilon_{l,st} = 12.8 \left(\frac{H_0}{d_p}\right)^{-0.4} \left(f\frac{d}{D}\right)^{-0.58} \left(\frac{g d_p^3 \rho_s^2}{\mu_l^2}\right)^{0.09} \left(\frac{U_l}{\sqrt{g d_p}}\right)^{1.66} \left(\frac{d_p U_l \rho_l}{\mu_l}\right)^{-0.34} \left(\frac{d_p U_l^2 \rho_l}{\sigma}\right)^{-0.34}$ $\epsilon_g = 0.19 \left(\frac{d_p U_g^2 \rho_l}{\sigma}\right)^{0.11} \left(\frac{U_g}{\sqrt{g d_p}}\right)^{0.22}$
Uysal (1978)		See Table 6		$\epsilon_{l,st} = 1.15 \times 10^{-4} G_l^{0.826} d_p^{-1.289}$
Vunjak-Novakovic et al. (1980)		See Table 5		$\epsilon_{l,st} = 6.4848 Re_l^{-0.1387} Fr_l^{0.4287} \left(\frac{H_0}{D_c}\right)^{-0.5672} + 0.02$ (Type I TCA) $\epsilon_{l,st} = 7.326 Re_l^{-0.0591} Fr_l^{0.4354} \left(\frac{H_0}{D_c}\right)^{0.4328} \left(\frac{\rho_s}{\rho_l}\right)^{0.0904} + 0.02$ (Type II TCA) $\epsilon_g = 0.628 U_g^{0.237}$

* Use SI units for variables involved in the equations.
** Stagnant liquid system.

TABLE 8. CORRELATION EQUATIONS FOR MINIMUM FLUIDIZATION VELOCITY IN TCA COLUMNS

Investigators	f	ρ_s [kg/m^3]	D_c/d_p	Correlation Equations*
Gel'perin et al. (1966)	0.345	250, 500	$\geqq 10$	$U_{gmf} = 0.3837 U_l^{0.28}$
Blyakher et al. (1967)		See Table 5		$U_{gmf} = U_{gmf0}\left[1 + \frac{1{,}587 U_l^{0.9}}{37.5 + 1{,}587 U_l^{0.9}}\right]$ $U_{gmf0} = \frac{0.0579 d_p^{0.715}(\rho_s - \rho_g)^{0.572}}{\mu_g^{0.143}\rho_g^{0.429}}$
Chen and Douglas (1968)		See Table 7		$G_{gmf} = 120.4 d_p^{1.15} 10^{-0.03812 G_l}$
Gel'perin et al. (1968b)		See Table 5		$\frac{U_{gmf}^2}{g d_p} = 4.6 \times 10^3 f^{1.54} \exp\left[-12.6\left(\frac{U_l}{U_{gmf}}\right)^{0.25}\right]$
Khanna (1971) (quoted from Uysal, 1978)		See Table 6		$G_{gmf} = 526.47 d_p^{1.5} 10^{-0.0317 G_l}$
Tichy and Douglas (1972)		See Table 6		$G_{gmf} = 0.36355 + 57.90 d_p - 1.848 G_l^{0.6} d_p^{0.5}$
Strumillo et al. (1974)	0.65	770 ~ 1,050	7 ~ 13.3	$U_{gmf} = (13.3 D_c + 2.24) \exp\left[\frac{-3.6 U_l}{D_c^{0.014}}\right]$
Kito et al. (1976d)	0.04 ~ 0.84	170 ~ 1,160	3.5 ~ 8.62	$\frac{U_{gmf}}{U_{gmf0}} = 16.48\left(f\frac{d}{D}\right)^{0.46} U_l^{-0.36}$ for $f\frac{d}{D} \leq 0.05$ $\frac{U_{gmf}}{U_{gmf0}} = 4.09 U_l^{-0.36}$ for $f\frac{d}{D} > 0.05$ U_{gmf0} can be estimated by using the Ergun equation (Kunii and Levenspiel, 1969).
Uysal (1978)		See Table 6		$G_{gmf} = 10.86 d_p^{0.488} 10^{-0.01985 G_l}$
Kuroda and Tabei (1981)	0.04 ~ 0.84	170 ~ 540	5.13 ~ 8.62	$C_{fl}\left(\frac{\rho_g U_{gmf}^2}{d_p}\right)\left(\frac{1}{\epsilon_{g,mf}^3}\right) = \left(\rho_{wp} - \rho_g\right)$ $\rho_{wp} = \frac{\epsilon_{l,st}}{1 - \epsilon_0}\rho_l + \rho_s$ $C_{fl} = C_{fs}(1 + 800\,\epsilon_{l,mf}^3)$ C_{fl} = apparent friction coefficient C_{fs} = friction coefficient in a gas-liquid packed bed
Vunjak-Novakovic et al. (1980)		See Table 6		$U_{gmf} = 11.3 d_p^{1.2}[(1 - \epsilon_0)(\rho_s - \rho_g) + 1.1 d_p^{-0.5} G_l^{0.6}]^{0.5} \times 10^{-0.0133 G_l}$ for Type I TCA $\log\left(\frac{U_{gmf}}{g}\frac{a_p}{\epsilon^3}\frac{\rho_g}{\rho_l}\mu_l^{0.2}\right) = 0.204 - 1.582\left(\frac{G_l}{G_g}\right)^{0.25}\left(\frac{\rho_g}{\rho_l}\right)^{0.125}$ for Type II TCA

* Use SI units for variables involved in the equations.

To estimate the holdups of liquid and gas, the correlations by Kito et al. (1978) which cover a wide range of physical properties of particles and operating conditions are recommended to use.

Kito et al. (1976d, 1976e) observed that the bed progressively expands prior to achieving the fully fluidized state, and thus it appears that the minimum fluidization velocity defined by the pressure drop method is always greater than that defined by the reduced bed height method as employed by Chen and Douglas (1968).

It has been generally observed that the *minimum fluidization velocity* decreases with increasing liquid flow rate and with increasing packing diameter (Chen and Douglas, 1968; Kito et al., 1976d; Vunjak-Novakovic et al., 1980). Kito et al. (1976d) reported that the minimum fluidization velocity increases with increasing packing density, but is independent of static bed height. Gel'perin et al. (1968b) reported that the minimum fluidization velocity is a strong function of the open area of the grid, but this is in contrast with Kito et al. (1976d) who reported that it is practically independent of grid area.

The geometry of the experimental system, especially the open area of the grid, as well as the operating conditions, must be taken into account to develop reliable correlation equations. The correlation equations for estimating the minimum fluidization velocity are summarized in Table 8. Most of the equations listed are purely empirical in nature, and there are considerable differences in the minimum fluidization velocity estimated by these equations. Differences in the techniques used to determine the minimum fluidization velocity may yield different correlation equations.

O'Neill et al. (1972) established a theory for incipient fluidization in the TCA. For a Type I TCA, the incipient gas fluidization velocity can be obtained by equating the pressure drop through the bed with the wetted particle weight. The incipient gas fluidization velocity for a Type II TCA is independent of packing density and is determined from a flooding chart for countercurrent packed bed operation. Vunjak-Novakovic et al. (1980) have confirmed O'Neill's theory for several packings. Recently Kuroda and Tabei (1981) applied the one-dimensional, two-phase flow model proposed by Wallis (1969) to obtain a correlation of the apparent friction coefficient in a countercurrent packed bed. The minimum fluidization velocity could be estimated by combining the momentum balance equations for both the gas and wetted particle phases. It is also noted that the model proposed by Kuroda and Tabei does not require a distinction between the fluidization modes defined by O'Neill et al. (1972).

The pressure drop method generally provides a feasible approximation to estimate the minimum fluidization velocity. The mechanism of fluidization in a TCA illustrated by O'Neill et al. (1972) has laid a conceptual basis for analysis of the minimum fluidization velocity and the pressure drop. In future studies, correlations for hydrodynamics in a TCA should be established on such a basis.

Inverse Fluidized and Semifluidized Bed. The term "inverse three-phase fluidization" was first introduced by Page in 1970 (Epstein, 1981). Stretton and Stuckey (1971) investigated the dissolution of carbon dioxide bubbles in "inverse" water-fluidized beds of polyethylene chips (specific gravity = 0.925). In the study of three-phase inverse fluidization under the confined condition, Werner and Schugerl (1972) reported that the gas holdup increases appreciably with an increase of the solid content in the column. Fine particles with sizes from 125 to 250 μm were used in their experiments. Using large particles ranging from 6.35 to 10 mm in diameter, Chern et al (1981) and Fan et al. (1982a,b) found that the characteristics of bed expansion and gas holdup were strongly affected by the flow regimes.

The inverse fluidized bed is characterized by high gas holdups and ease in refluidization after power failure when applied to biological wastewater treatment (Edwards, 1981; Shimodaira et al., 1981). Because of the demonstrated industrial application in biological processing, extensive studies on hydrodynamics are needed for the inverse fluidized bed.

Unlike cocurrent upward gas-liquid-solid semifluidized bed operation, the expanded fluidized bed in the countercurrent (inverse) gas-liquid-solid semifluidized bed with a liquid as the continuous phase may not form a packed bed when it first reaches the lower retaining grid. Instead, the solid particles are distributed uniformly throughout the space bounded by the retaining grids, although the free expansion height of the bed far exceeds the bounded height (Fan et al., 1982b). However, when either the liquid or the gas velocity exceeds a certain value, a packed bed above the retaining grid will form.

MIXING OF PHASES IN GAS-LIQUID-SOLID FLUIDIZATION

In three-phase fluidized beds, plug flow can often be assumed for the gas phase. Appreciable backmixing, however, may occur in the liquid phase, especially for beds of fine particles in cocurrent three-phase fluidization. The backmixing of the liquid and solid particles in such a bed is primarily caused by the rising motion of coalesced large gas bubbles. Segregation or stratification phenomena of the solid particles occur in a fluidized bed containing particles with a wide size or density distribution. Such a segregation behavior of the solid phase is particularly pronounced for biological fluidized bed reactors. The solids mixing diminishes the segregation or stratification as the gas flow rate increases in the three-phase fluidized bed.

The axial dispersion model has been most commonly used to describe the backmixing behavior of the fluid phases and to simulate chemical conversion in the three-phase fluidized bed reactor (Ostergaard, 1968; Ermakova et al., 1973, 1977, 1979; Parulekar and Shah, 1980; Shah et al., 1981). An extensive review of fluid mixing in gas-liquid reactors was provided by Shah et al. (1978). In the following, the studies of fluid mixing and solid mixing in cocurrent gas-liquid-solid fluidized beds are described. Fluid mixing in the TCA is also described.

Cocurrent Gas-Liquid-Solid Fluidization

Liquid Mixing. Vail et al. (1968) measured liquid mixing in a cocurrent three-phase fluidized bed using the steady-state tracer injection method. They determined the height of a unit of perfect mixing for three-phase fluidized beds with 0.86 mm molten sludge particles in a 146 mm I.D. column. Ostergaard and Michelsen (1968) and Ostergaard (1969) studied axial mixing of both the liquid and gas phases in a three-phase fluidized bed with 0.25, 1 and 6 mm glass beads in a 0.216 m I.D. column. An imperfect tracer pulse method was employed utilizing gamma ray emitting isotopes bromine-82 and argon-41 as the liquid phase tracer (aqueous ammonium bromide solution) and the gas phase tracer, respectively. They employed the transfer function to evaluate the mixing parameters based on the axial dispersion model instead of the model based on the methods of first and second moments. This is because the calculated moments were very sensitive to small measurement errors in the tails of the residence time distribution curves and consequently significant errors could be caused in the calculation (Ostergaard and Michelsen, 1969; Michelsen and Ostergaard, 1970).

Ostergaard and Michelsen (1968) and Ostergaard (1969) reported that the degree of axial liquid mixing in a bed of 0.25 and 1 mm particles at high liquid flow rates was comparable to that in the corresponding gas-liquid flow, both in intensity and in trend. However, the intensity of the axial mixing in a bed of 6 mm particles was found to be much lower than that in the corresponding gas-liquid flow. Michelsen and Ostergaard (1970) measured the axial liquid mixing in a three-phase fluidized bed with 1, 3 and 6 mm glass beads in a 152.4 mm I.D. column, utilizing the same tracer response system previously reported (Ostergaard and Michelsen, 1968; Ostergaard, 1969). The beds of 6 mm particles were characterized by a very low degree of axial liquid mixing in the dispersed bubble flow regime where the superficial gas velocity was lower than 15 cm/s, while the degree of axial liquid mixing increased considerably at gas velocities exceeding 15 cm/s. The bed of 3 mm particles exhibited rather complex behavior with respect to the flow regime. Kim et al. (1972) also measured the height of the liquid phase mixing unit in a 660 mm wide and 25

mm thick two-dimensional three-phase fluidized bed. The particles utilized were 2.6 mm gravel and 6 mm glass beads. An empirical correlation equation for the height of a mixing unit of the liquid was developed as a function of the Reynolds and Froude numbers of both the gas and liquid phases, and of the ratio of the particle density to fluid density.

The axial liquid mixing in the transition regime between a fixed bed and a fully developed fluidized bed with a cocurrent gas-liquid up-flow was investigated by Ohshima et al. (1977). Davidson et al. (1977) showed that, depending on the liquid flow rate, the axial dispersion coefficient, E_{zl}, of the liquid retains a value between about 40 and 120 cm^2/s in the dispersed bubble flow regime; in the coalesced bubble flow regime, E_{zl} retains very high values, varying from 200 to 400 cm^2/s, and increasing with an increase of the gas drift flux. Muroyama et al. (1978) also measured the axial dispersion coefficients of the liquid in three-phase fluidized beds of 60 and 100 mm diameter using an imperfect tracer pulse technique with transfer function analysis. The empirical correlation equation provided by them are

$$Pe' = \left(\frac{V_l D_c}{E_{zl}}\right) = 1.07(U_l)^{0.738}(U_g)^{-0.167}(D_c)^{-0.583} \quad (25)$$

for the coalesced bubble flow regime and

$$Pe' = 26\left(\frac{d_p}{D_c}\right)^{1/2} \quad (26)$$

with the limit of $0.02 < d_p/D_c < 0.12$, for the dispersed bubble flow regime, where U_l and U_g are in cm/s, and D_c and d_p are in cm. The behavior of Pe' in the slug flow regime was found to be similar to that in the coalesced bubble flow regime. Ostergaard (1978) reported that the axial dispersion coefficient in the 228 mm I.D. column was higher by 50% than that reported by Michelsen and Ostergaard (1970) for the 152.4 mm I.D. column with bed particles of 1 mm, and higher by roughly 100% than that with bed particles of 6 mm. These results indicate that the axial dispersion coefficient in three-phase fluidized beds varies with the column diameter to the power of 1.1 to 1.7 which is in reasonably good agreement with results obtained by Muroyama et al. (1978) and is comparable to the value of 1.5 obtained for gas-liquid bubble columns (Towell and Ackerman, 1972). El-Temtamy et al. (1979a) also measured the axial dispersion coefficient of the liquid in three-phase fluidized beds with 50 mm I.D., using the steady-state tracer injection technique as employed by Vail et al. (1968). Glass beads of 0.45, 0.96, 2 and 3 mm average diameter were used as fluidizing particles. They reported that the backmixing measurement could not be made in a bed of 3 mm particles due to the low degree of backmixing. The axial dispersion coefficients of 3 mm particles were obtained by El-Temtamy et al. (1979b) from a measurement of the radial concentration profiles in the downstream liquid caused by a steady flow of the tracer from a point source. They were able to develop an empirical correlation for the axial liquid dispersion coefficient. Recently, a unified correlation of the axial liquid mixing in gas-liquid two phase columns and three-phase fluidized beds was proposed by Joshi (1980), who developed an energy balance model for liquid mixing. The correlation equation has the form:

$$E_{zl} = 0.29(U_l + V_c)D_c \quad (27)$$

where E_{zl} is in m^2/s, D_c in m, and V_c in m/s. V_c can be calculated by:

$$V_c = 1.31\left\{gD_c\left[U_g + U_l - \frac{\rho_l U_l}{\epsilon_s\rho_s + \epsilon_l\rho_l} - \epsilon_s\left(\frac{\rho_s}{\epsilon_s\rho_s + \epsilon_l\rho_l} - 1\right)U_t - \epsilon_g V_{b\infty}\right]\right\}^{1/3} \quad (28)$$

Here, U_g, U_l, U_t and $V_{b\infty}$ are in m/s, and ρ_l and ρ_s are in kg/m. Kim and Kim (1981) examined the effects of the liquid viscosity and surface tension on the axial dispersion coefficient of the liquid in a three-phase fluidized bed. The axial dispersion coefficient slightly increased with the liquid viscosity for a bed of large particles, i.e., 6 mm glass beads, but it decreased with viscosity at high gas flow rates in a bed of small particles, i.e., 1.6 and 3 mm particles. The axial dispersion coefficient increases somewhat with an increase in the surface tension of the liquid. The recent correlation on liquid-phase axial mixing by Kim and Kim (1983) covers a wide range of literature data. However, they did not take into consideration the effect of viscosity and surface tension of the liquid on the axial dispersion coefficient. Their equation is:

$$\frac{d_p U_l}{E_{zl}} = 20.19\left(\frac{d_p}{D_c}\right)^{1.66}\left(\frac{U_l}{U_l + U_g}\right)^{1.03} \quad (29)$$

An experimental study was conducted on radial liquid mixing for cocurrent three-phase fluidization by El-Temtamy et al. (1979b). The radial dispersion coefficient of the liquid in three-phase fluidization was found to be much less than the axial dispersion coefficient. For example, for beds of 3 mm glass beads, the radial dispersion coefficient was roughly $\frac{1}{2}$ to $\frac{1}{10}$ of the axial dispersion coefficient, while for beds of 0.45 and 0.96 mm glass beads the radial dispersion coefficient was roughly $\frac{1}{20}$ to $\frac{1}{30}$ of the axial dispersion coefficient. The axial dispersion coefficient increases with an increase of the gas velocity. However, no conclusive relationship could be identified between the axial dispersion coefficient and the liquid velocity or the particle size. The radial liquid dispersion coefficients in three-phase fluidized beds were also measured by Muroyama et al. (1981) who obtained the coefficient from the effective thermal conductivity data in heat transfer experiments. The Peclet number for radial liquid mixing in three-phase fluidized beds appreciably decreases with an increase of the gas flow rate. However, a minimum exists in the variation of the Peclet number for radial liquid mixing with respect to the liquid flow rate in a manner similar to that observed in liquid-solid fluidized beds (Hanratty et al., 1956; Patel and Simpson, 1977).

To estimate the axial liquid dispersion coefficient in cocurrent three-phase fluidization, the correlations of Muroyama et al. (1978) or Kim and Kim (1983) are recommended to use at this stage. The correlation by Joshi (1980) is applicable only for a bed of small particles. The effect of the bubble flow pattern and the physical properties of particles and liquid on the liquid mixing should be further studied to establish better correlations. Further studies are also needed on the radial liquid dispersion as it directly relates to the radial convective heat transfer. The mixing phenomena under high velocity conditions which are of industrial interest also require further attention.

Gas Mixing. The use of a radioactive gas tracer with very low solubility can be used to measure the gas phase residence time distribution, thereby obtaining the mixing parameter of the gas. Ostergaard and Michelsen (1969) and Michelsen and Ostergaard (1970) used argon-41 as a gaseous tracer and measured the responses of the tracer pulse in the gas phase indirectly from the outside of the column. However, mixing in the gas phase is rather difficult to analyze quantitatively due to the complex effects involved in the absorption of the tracer material into the liquid phase and the redispersion and coalescence features of the gas bubbles. Ostergaard and Michelsen (1969) showed a simplified method to analyze the imperfect pulse response of the radioactive gas tracer which diffuses from the gas bubbles into the liquid in a finite amount. The height of mixing unit of the gas (HMU_g) was determined by Ostergaard (1969) for three-phase fluidized beds of 216 mm I.D. with 0.25, 1 and 6 mm glass beads. The values of HMU_g in three-phase fluidized beds were found to be comparable to those in gas-liquid bubbling columns. Michelsen and Ostergaard (1970), however, reported that the determination of the axial dispersion coefficient suffered from great difficulties since the axial dispersion model was proven to be unsuccessful in accounting for the gas phase mixing in systems with rapid coalescence. In such systems, negative dispersion coefficients were observed. Furthermore, accurate determination of the axial dispersion coefficient for the gas phase is difficult for beds of large particles. This is due to the fact that a large amount of tracer was transferred from the gas to the liquid and, thus, independent measurements of tracer in both phases were required for such systems. Recently, Vasalos et al.

(1979, 1980) measured the gas phase mixing in the H-Coal fluidized-bed reactor (or ebulated bed reactor) by employing the same gas tracer system as that employed by Ostergaard (1969) and Michelsen and Ostergaard (1970). They reported that considerable gas phase mixing exists in the reactor and evaluated the axial dispersion coefficient of the gas.

Gas phase mixing in a cocurrent slurry flow system containing water, air and 250 μm quartz particles in suspension was investigated by Afshar and Schugerl (1968). The solid concentration in their experiment, however, varied up to only 4%. The degree of gas mixing in a bubble column slurry reactor was assessed using the complete mixing tanks in series model (Kolbel et al., 1962).

Solids Mixing. An experimental investigation to assess the rates of motion of the solid and liquid phases in a gas-liquid-solid fluidized system was carried out by Evstropeva et al. (1972). They measured the average velocities and mean square values of the fluctuation velocity components for the rates of motion of light and heavy tracer particles which simulate the motion of the liquid and the fluidized particles, respectively. A qualitative investigation of solids mixing in cocurrent three-phase fluidized beds containing a binary mixture of glass beads was conducted by Fan et al. (1982c, 1984e). They noted that the complete mixing state occurs largely in the coalesced bubble regime and the slugging regime and slightly in the transition regime. The partial intermixing state occurs largely in the dispersed bubble regime and the transition regime and slightly in the coalesced bubble regime. The complete segregation state occurs solely in the dispersed bubble regime. Quantitative studies of solid concentration profiles and degree of mixing and segregation of a binary mixture of particles in a three-phase fluidized bed were recently conducted by Fan et al. (1984f) using multiple shutter plates for column isolation. They found that the degree of particle segregation decreases sharply with an increase in the gas velocity. The degree of solids mixing, however, would be expected to be lower than that of the liquid mixing in three-phase fluidized beds in the same manner as that observed in the liquid-solid fluidized bed by Al-Dibouni and Garside (1979).

The criteria for the onset of stratification in the liquid-liquid and liquid-solid particle mixtures agitated by gas bubbling were defined experimentally by Epstein et al. (1981). The bubble supported bed was operated with a stationary liquid. In principle, the incipient mixing (or stratification) process was viewed as a quasi-static balance of body forces.

Fluid Mixing in the Turbulent Contact Absorber

Axial mixing of the liquid in the TCA was investigated by Chen and Douglas (1969). The liquid phase axial dispersion coefficient, E_{zl}, was found to increase with increasing gas flow rate, increasing liquid flow rate and increasing particle diameter. They also showed that the Peclet number based on the particle diameter, $Pe'' = V_l d_p / E_{zl}$, decreases as the gas flow rate increases. Chen and Douglas (1969) also observed that the excess gas flow rate over that required for incipient bed motion, represented by the quantity $(G_g - G_{gmf})/G_{gmf}$, is a measure of the intensity of bed motion. The ratio of the TCA Peclet number to that of the countercurrent packed bed Peclet number, Pe''/Pe_0'', could be successfully correlated in terms of the excess gas velocity, $(G_g - G_{gmf})/G_{gmf}$, and the ratio of the particle diameter to column diameter as given in Figure 9.

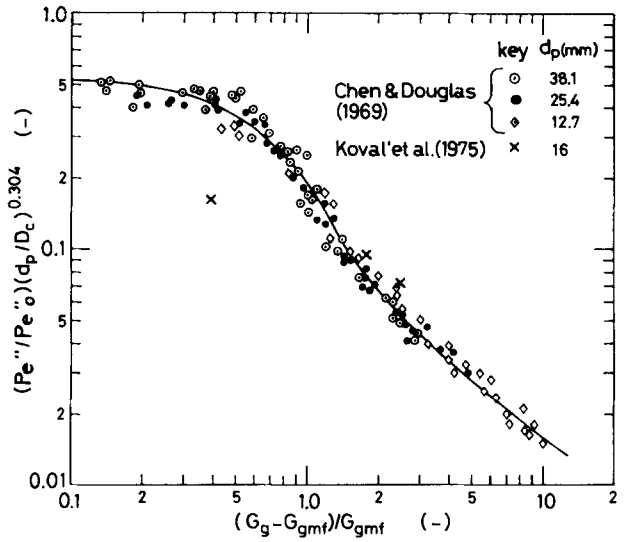

Figure 9. Variation of TCA Peclet Number with Reduced Gas Velocity Defined by Chen and Douglas (1969).

Koval et al. (1975) also measured the axial mixing of the liquid phase in a TCA, using the pulse response tracer technique. The values of Pe'' resemble those of Chen and Douglas (1969) in magnitude and in trend. However, the numerical data reported by Koval et al. (1975) for liquid mixing are quite limited. More experiments should be conducted on the liquid mixing in a TCA for various properties of particles and liquid.

HEAT TRANSFER OF GAS-LIQUID-SOLID FLUIDIZATION

To design and control three-phase fluidized bed reactors, a knowledge of the heat transfer characteristics of the reactor is essential. Heat transfer studies of the fluidized bed have been conducted mainly on gas-solid and liquid-solid fluidized bed systems (Gel'perin and Einstein, 1972; Botterill, 1975; Grace, 1982). Relatively little information on heat transfer is available for three-phase fluidized bed systems.

Cocurrent Gas-Liquid-Solid Fluidization

Van Driesen and Stewart (1964) reported that the temperature distribution is virtually uniform throughout the H-Oil fluidized-bed reactor even when the heat of the reaction is sufficient to raise the temperature of the entire feed by 55.6 K. The uniform temperature distribution within the H-Oil or H-Coal reactor is due to the relatively high degree of internal backmixing and the large recycle flow of the liquid. The thermal stability of an H-Oil reactor during upset conditions such as the total loss of the liquid and hydrogen flow was investigated by Li and Lin (1981). They reported that the fluidized bed reactor is more thermally stable with a lower bed temperature gradient than a trickle bed reactor. The hydrogen quench operation to reduce the temperature rise across coal liquefaction reactors involving the H-Coal fluidized bed or SRC-II slurry reactor was investigated by Shah et al. (1981), and Shah and Parulekar (1982) who presented a mathematical model to illustrate the problem of intrastage quench in an adiabatic multistage reactor.

The heat transfer from the surface of either the column wall or an immersed heater to the three-phase fluidized bed has been studied by several authors. Ostergaard (1964) measured the heat transfer coefficient from the wall to a fluidized bed of 76 mm I.D. containing 0.5 mm glass spheres. The heat transfer coefficient was shown to increase sharply with an increase of the gas flow rate in the lower flow rate range. At higher gas flow rates the heat transfer coefficient did not vary with an increase in gas flow rate. Viswanathan et al. (1964) studied the wall to bed heat transfer in three-phase fluidized beds containing small particles. They measured the overall heat transfer coefficient at a constant bed expansion by varying the ratio of the gas flow rate to liquid flow rate and reported that a maximum heat transfer coefficient occurs as the velocity ratio increases. However, an assessment of the effect of individual operating variables on the heat transfer coefficients is difficult using their unique experimental technique. The effects of individual operating parameters, including the gas and liquid flow rates and particle diameter, on the heat transfer characteristics in three-phase fluidized beds were investigated by Armstrong et al. (1976b) and Baker et al. (1978). They measured the heat transfer coefficients between the surface of an immersion rod heater and

the three-phase fluidized bed. The trend of the variation of the heat transfer coefficient with respect to the gas flow rate was observed to be similar to that reported by Ostergaard (1964). It is noted that the variation of the heat transfer coefficient with the liquid velocity in three-phase fluidized beds exhibits a maximum similar to that observed in liquid-solid fluidized beds. The heat transfer coefficient increases with particle diameter when the particle diameter is greater than about 1 mm (Armstrong et al., 1976b). Kato et al. (1978, 1980, 1981) reported that the wall heat transfer coefficients for a bed of 0.12 m I.D. with small particles exhibits a local maximum and then a minimum during the transition from the fixed bed to a fully developed fluidized bed as the liquid flow rate increases. This behavior of the heat transfer coefficient across the transition regime may be attributed to the heterogeneity in a bed of fine particles operated at a low liquid velocity as reported by Ermakova et al. (1970a). However, such behavior becomes less distinct for beds of coarse particles (Kato et al., 1980). Correlation equations to estimate heat transfer coefficients for a fully developed fluidized bed were presented by Baker et al. (1978), Kato et al. (1981), and Muroyama et al. (1981). The correlation equation of Kato et al. (1981), which takes into consideration the effect of the liquid viscosity on the heat transfer coefficient, is given below:

$$\frac{hd_p\,\epsilon_l}{\lambda_l(1-\epsilon_l)} = 0.044\left\{\frac{d_pU_l\rho_l}{\mu_l(1-\epsilon_l)}\frac{C_{pl}\mu_l}{\lambda_l}\right\}^{0.78} + 2.0\left(\frac{U_g{}^2}{gd_p}\right)^{0.17} \quad (30)$$

A uniform temperature distribution in the phases of three-phase fluidized beds has been observed by various investigators including Viswanathan et al. (1964), Baker et al. (1978), and Kato et al. (1980). Thus, the only resistance considered for heat transfer is in the region very close to the heat transfer surface. It should be noted that the heat transfer coefficients were usually obtained based on the assumption that either the fluid mixing was negligibly small (Viswanathan et al., 1964) or the fluid was completely mixed in the bed (Baker et al., 1978; Kato et al., 1980, 1981). Muroyama et al. (1981), however, took into consideration the effects of fluid mixing in the analysis of the temperature distribution variation in the three-phase fluidized bed. They found that the radial temperature distribution is nearly parabolic in the core area of the bed and has a very steep gradient near the wall similar to that in liquid fluidized beds observed by Wasmund and Smith (1967) and Patel and Simpson (1977).

To estimate the wall-bed heat transfer coefficient, the correlation of Kato et al. (1981), which covers a wide range of the liquid phase Prandtl number, is recommended. Heat transfer characteristics in a bed with internals such as cooling or heating coils or pipes need to be fully explored for practical use. Heat transfer behavior at high velocities, which is of industrial interest, is also in need of extensive study.

Heat Transfer in the Turbulent Contact Absorber

Douglas et al. (1963) examined the simultaneous transfer of heat and mass into liquid water for the condensation of steam and absorption of H_2S from a steam-air-H_2S stream into an aqueous liquid phase. Douglas (1964) also examined simultaneous heat and mass transfer from a water-saturated hot air stream into cooling water. Barile and Meyer (1971) and Barile et al. (1975) studied the performance of a TCA cooling tower designed for cooling hot water from a power plant. They revealed that a 20°F temperature drop could be easily achieved with a packing depth of one foot. They showed that the overall volumetric heat transfer coefficients for cooling are similar to those of NH_3 absorption reported by Douglas (1964) in magnitude and in trend. A correlation equation was developed to account for the overall volumetric mass transfer coefficient or HTU by Barile et al. (1975).

MASS TRANSFER OF GAS-LIQUID-SOLID FLUIDIZATION

Either or both of the mass transfer steps can play an important role in the determination of the overall reaction in three-phase

TABLE 9. GAS-LIQUID MASS TRANSFER STUDIES ON THREE-PHASE FLUIDIZED BEDS WITH COCURRENT GAS-LIQUID FLOW

Investigators	System	Column Size	Particle Size and Density	Flow Range of Gas and Liquid	Correlations or Remarks
Massimilla et al. (1959)	Physical absorption: CO_2-N_2/water/silica particle	30 or 90 mm ID × 100 to 1200 mm height	d_p = 0.22, 0.50 and 0.80 mm	U_g = 2.6 to 4.8 l/min U_l = 4.0 to 11.4 l/min	graphical description absorption efficiency
	CO_2-N_2/water/glass beads (CO_2% = 87%)				
Ostergaard and Suchozebrski (1969)	Physical absorption: CO_2-N_2/water/glass beads (CO_2% = 50.80 and 100%)	15.24 cm ID × 2.91 m height	d_p = 0.125 cm, ρ_s = 2.67 g/cm^3 d_ρ = 0.593 cm, ρ_p = 2.63 g/cm^3	U_g = 0 to 3 cm/s U_l = 6.8 to 17 cm/s	graphical description a very high mass transfer rate for the bed of 6 mm particles
Ostergaard and Fosbol (1972)	Physical absorption: Pure O_2/water/glass beads	15.24 cm ID × 2.91 m height	d_p = 1 and 6 mm	U_g = 0 to 5 cm/s U_l = 1.95 to 16.2 cm/s	graphical description (the variation of kja with the distance from the gas distributor was discussed)
Lee and Worthington (1974)	Physical absorption: CO_2/water/glass beads	5.45 cm ID × 107.6 cm height	d_p = 6 mm	U_g = 0.03 to 1.2 cm/s U_l = 6.4 to 18 cm/s	kja/ϵ_g = 1.53
Dakshinamurty et al. (1974a); Dakshinamurty and Veerabhadra Rao (1976)	Physical absorption: CO_2/water/porcelain beads CO_2/water/sand particle CO_2/water/iron shots CO_2/water/lead shots (CO_2% = 50 and 100%)	5.6 cm ID × 68 cm height	d_p = 1.06 to 6.84 mm ρ_s = 2.4 to 11.18 g/cm^3 (U_t = 12 to 81.5 cm/s)	U_g = 0 to 10 cm/s U_l = 5.0 to 17.2 cm/s	Part I (1974a): graphical description Part II (1976): correlations, $\frac{kad_p^2}{D_A} = K''\left(\frac{d_pU_t\rho_l}{\mu_l}\right)^{3.3}\left(\frac{\mu_lU_g}{\sigma}\right)^{0.7}$ $K'' = 3.946 \times 10^{-7}$ for $Re_t > 2{,}000$ $K'' = 2.33 \times 10^{-5}$ for $Re_t < 2{,}000$

Nishikawa et al. (1977)	Chemical Absorption: air/0.25N sodium sulphite sol. catalyzed by copper ion/glass beads	15 cm ID × 140 cm height (cone angle = 30°)	d_p = 1.01, 2.59 and 4.87 mm ρ_p = 2.6 g/cm^3	U_g = 0 to 19 cm/s U_l = 0 to 6 cm/s	Three-phase spouted bed graphical description
Ostergaard (1978)	Chemical absorption: measurement of $k_l a$; CO_2/Carbonate-Bicarbonate buffer/glass beads measurement of k_l and a; CO_2/Sodium hydroxide/glass beads	0.216 m ID × 8.50 mm height	d_p = 1.1, 3.0 and 6.0 mm		Bubble column; $k_l a = 9.7 U_g$ (1/h), (4.3 > U_g > 12.4) $a = 0.049 U_g^{0.66}$ (1/cm) $k_l = 0.055 U_g^{0.34}$ (cm/s) Bed of 1.1 mm particle: $k_l a = 4.7 U_g^{0.76}$ (1/h), (1.5 < U_l < 4.6) $a = 0.015 U_g^{0.65}$ (1/cm) $k_l = 0.087 U_g^{0.11}$ (cm/s) Bed of 3 mm particle: $k_l a = 7.0 U_l U_g^{0.25}$ (1/h), (4.3 < U_g < 12.8), (4.3 < U_l < 7.3) $a = 0.056 U_g^{0.45}$ (1/cm) $k_l = 0.35 U_l U_g^{-0.20}$ (cm/s) Bed of 6 mm particle: $k_l a = 21.1 U_g^{0.93}$ (1/h), (4.7 < U_g < 12.7) (6.8 < U_l < 9.7) $a = 0.015 U_g^{0.96}$ (1/cm) $k_l = 0.056 U_g^{-0.03}$ (cm/s) where U_g, U_l = cm/s
Fukushima (1979)	See Lee and Worthington (1974)	See Lee and Worthington	See Lee and Worthington	See Lee and Worthington	$\frac{k_l a d_p^2 \epsilon}{D_A \epsilon_g} = 1.4 \times 10^4 Re_l'^{0.38} Re_g'^{-0.2} Sc_l^{1/2} \times \left(\frac{d_p}{D_c}\right)^{2.1}$ $\frac{k_l d_p}{D_A} = 8.9 \times 10^2 Re_l'^{1/3} Re_l'^{0.2} Sc_l^{1/2} \times \left(\frac{d_p}{D_c}\right)^{2.1}$ $\frac{a d_p}{(\epsilon_g/\epsilon)} = 16 Re_l'^{0.05} Re_g'^{-0.4}$
Dharnuka and Stepanek (1980a,b)	Chemical absorption-desorption; CO_2/N_2/Na_2CO_3-$NaHCO_3$ buffer dissociated with O_2/glass beads	50 mm ID × 1.5 m height	d_p = 1.98, 4.08 and 5.86 mm	U_g = 2 to 8 cm/s U_l = 6.1 to 13.8 cm/s	Bed of 1.98 mm beads; $k_l a = 2.37 \times 10^{-3} U_g^{1.0} U_l^{0.45}$ (for pure CO_2) $k_l a = 3.23 \times 10^{-3} U_g^{1.0} U_l^{0.55}$ (for pure N_2) $a = 0.232 U_g^{0.677} U_l^{0.534}$ $k = 0.8118 \times 10^{-3} U_g^{0.4077}$ Bed of 4.08 mm beads; $k_l a = 3.41 \times 10^{-2} U_g^{0.555}$ $a = 1.05 U_g$ $k_l \times 10^2 = 2.355 - 0.1045 U_g$ Bed of 5.86 mm beads; $k_l a = 2.52 \times 10^{-2} U_g$ $a = 1.8 U_g$ $k_l = 0.24 Sc_l^{-2/3}/(E\nu_l)^{1/4}$ where $k_l a$ = 1/s, a = cm^2/cm^3, k_l = cm/s, U_l = cm/s and U_g = cm/s
Alvarez-Cuenca and Nerenberg (1981)	Physical absorption Air/Water/Glass beads	66 cm width × 2.5 cm depth × 250 cm height	d_p = 1, 3 and 5 mm	U_g = 4 to 28 cm/s U_l = 2.5 to 10 cm/s	Local value of $k_l a$ was analyzed based on the plug flow model.

fluidized-bed reactors for catalytic, noncatalytic and biological reactions. The rates of these mass transfer steps are dependent on the hydrodynamic properties of the fluidized bed and hence are strong functions of the operating parameters.

Cocurrent Gas-Liquid-Solid Fluidization

When the catalyst activity is low, the gas-liquid mass transfer is not important in determining the overall rate of reaction. In the experiment of Adlington and Thompson (1965), catalytic desulfurization of residual oils was conducted with the concentration of hydrogen in the bulk liquid estimated to be as high as 90% of its saturation value; under such a condition, the gas-liquid mass transfer resistance can be virtually neglected. However, when the catalyst activity is sufficiently high, the overall conversion rate can be significantly enhanced by lowering the gas-liquid mass transfer resistance or the liquid-solid mass transfer resistance (Ermakova and Ziganshin, 1970b). Examples of reactions which require consideration of this effect include hydrogenation of 1-heptene (Ermakova et al., 1973; and Gartsman et al., 1977). Lee et al. (1974) concluded that an optimum particle size exists which provides a maximum overall conversion in a three-phase fluidized bed reactor where a highly active or moderately active catalytic reaction takes place. The optimum particle size is determined by considering two counteracting effects: an increase in particle size increases the gas-liquid contacting efficiency, but it decreases the effectiveness factor of the catalyst particle for the reaction. They chose hydrogenation of α-methyl styrene (Satterfield et al., 1969) as a model reaction. In their calculation, the mass transfer resistance through a liquid film over the outer particle surface was considered to be negligibly small.

Gas-Liquid Mass Transfer and Interfacial Area. Table 9 summarizes the gas-liquid mass transfer studies. The gas-side mass transfer resistance can generally be neglected in a three-phase fluidized bed with liquid as the continuous phase as well as in a bubble column. Therefore, the liquid-side mass transfer coefficient, $k_l a$, determines the overall gas-liquid mass transfer coefficient.

Ostergaard and Suchozebrski (1969) investigated the effect of individual operating parameters on the volumetric absorption coefficient $k_l a$ using physical absorption of carbon dioxide into water. It was observed that the particle size has a marked effect on $k_l a$. The values of $k_l a$ in a bed of 1 mm particles are about $\frac{1}{5}$ of those in a solid-free bubble column, while the values of $k_l a$ in a bed of 6 mm particles are about two times larger than those in a solid-free bubble column. The increase of $k_l a$ in the 6 mm particle bed is attributed to the break-up of the gas bubbles while the decrease of $k_l a$ in the 1 mm particle bed is attributed to the coalescence of gas bubbles. In the calculation of $k_l a$, they neglected the effect of fluid mixing which should be taken into consideration, especially for a bed of small particles. Ostergaard and Suchozebrski (1969) and Ostergaard and Fosbol (1972) reported that $k_l a$ in a three-phase fluidized bed varies considerably with the axial distance from the gas distributor. In addition, $k_l a$ varies with the particle size. For example, in a bed of 1 mm particles $k_l a$ markedly decreases within a short distance from the gas distributor, while in a bed of 6 mm particles, $k_l a$ sharply increases within a short distance from the distributor, reaches a maximum and then decreases along the axial distance of the bed. Thus, shallow beds containing large particles exhibit particularly high mass transfer rates.

Recently, Alvarez-Quenca and Nerenberg (1981) obtained $k_l a$ averaged over the axial distance from the distributor to various sampling points using a two-dimensional bed. They reported two distinct regions for gas-liquid mass transfer, i.e., the grid region where the mass transfer is excellent and the bulk region at the upper 80% of the bed where the volumetric mass transfer coefficient is much lower than that in the grid region. Using the same two-dimensional column, Alvarez-Quenca et al. (1983) reported that at high gas velocity, the mass transfer rate was the highest in the region between the dense bed region and the dilute bed region. It should be pointed out that the gas distributor in their design would yield poor distribution of bubbles and low mobility of the large particles.

The effects of the size and density of the particles on the average value of $k_l a$ was investigated and correlation equations were developed by Dakshinamurty et al. (1974a,b, 1976). In their calculation, plug flow for the liquid phase was assumed. Vandershuren et al. (1974) measured the absorption of carbon dioxide, ethyl chloride and benzene from single bubbles in a water-fluidized bed of 0.45 mm glass ballotini.

Studies of gas-liquid mass transfer may involve the measurement of the interfacial area. Lee and Worthington (1974) measured the volumetric coefficient $k_l a$ and the interfacial area a, separately. In their experiment, $k_l a$ was measured by the absorption of carbon dioxide into water and into 0.05 M sodium sulfate solution while the gas-liquid interfacial area was measured by the light transmission method applied just above the bed surface. The bubble size was calculated from the relationship $d_B = 6\epsilon_g/a$. The mass transfer coefficient k_l was found to increase with an increase in the bubble size in the same manner as that observed in the gas bubble size transition region in shallow bubble columns and stirred sparged vessels (Calderbank and Moo-Young, 1961). Lee and Worthington (1974) showed that $k_l a$ varies linearly with ϵ_g.

Ostergaard (1978) presented empirical equations for the volumetric coefficient, $k_l a$, the mass transfer coefficient, k_l, and the interfacial area, a, for several particle sizes. Fukushima (1979) developed correlation equations for $k_l a$, k_l and a for the dispersed bubble flow regime, using the data of Lee and Worthington (1974).

Recently, Dhanuka and Stepanek (1980a) measured $k_l a$, k_l and a in a three-phase fluidized bed of 5.86 mm glass beads using a technique involving simultaneous chemical absorption of carbon dioxide and desorption of oxygen which was developed by Robinson and Wilke (1974). They concluded that the particle size has a profound effect on a, little effect on k_l and thus a significant effect on $k_l a$. Both $k_l a$ and a were found to increase with an increase of the gas velocity and an increase of the particle diameter. Furthermore, the liquid velocity had no effect on $k_l a$ and a in beds of 4.08 and 5.86 mm glass beads, while $k_l a$ and a increase with the liquid velocity in a bed of 1.98 mm glass beads.

Correlations for $k_l a$ proposed by several workers lack generality and can be employed only for a very limited conditions. For example, the mass transfer coefficient in the correlation of Dakshinamurty et al. (1974a, 1976) was expressed in proportion to the diffusivity, while that in several other correlations was expressed in proportion to the square of diffusivity. Further efforts are required to obtain a generalized expression for the mass transfer coefficient even though there is a complex dependency of the volumetric mass transfer coefficient on the bubble flow pattern. k_l and a should also be independently evaluated.

Liquid-Solid Mass Transfer. Morooka et al. (1979) measured and correlated the wall-to-bed mass transfer coefficients in liquid-solid and gas-liquid-solid fluidized beds with rectangular cross section using the limiting current method. The mass transfer coefficient in the three-phase system was found to be larger than that in the liquid-solid fluidized bed system. A maximum mass transfer coefficient exists at a given liquid velocity and hence a given bed porosity, similar to the liquid-solid fluidized bed (Beek, 1971).

Liquid-solid particle mass transfer was only recently explored by Arters and Fan (1984). They employed cylindrical particles of benzoic acid (diameter = length = 1.5 to 4 mm) which were fluidized with water and air. Results show that liquid-solid mass transfer in a three-phase fluidized bed is higher than that in a two-phase (liquid-solid) fluidized bed at a given liquid velocity. Furthermore, the Sherwood number for liquid-solid mass transfer increases with increasing gas velocity. Liquid-solid mass transfer in a three-phase fluidized bed appears to be relatively independent of the liquid velocity, as has been noted for a two-phase fluidized bed.

Spouted Bed

Nishikawa et al. (1976) reported that the liquid-solid mass transfer coefficient in a three-phase spouted bed with liquid as the

continuous phase increases with the gas injection rate, reaches a maximum value at a gas velocity of about 0.5 cm/s and gradually decreases with further increases in the gas flow rate. The liquid-solid mass transfer coefficient at the maximum value was about 1.25 times that for the liquid-solid spouted bed without gas. Nishikawa et al. (1977) reported that when the particle size is 1 mm in diameter, the value of the gas-liquid mass transfer coefficient, $k_l a$, in three-phase spouted beds is only 65% of that in the solid-free bubble column. The ratio of $k_l a$ in a three-phase spouted bed to that in a bubble column with identical gas and liquid velocities increases with the particle diameter and the amount of the particles contained in the bed. This ratio exceeds unity when the particle diameter exceeds 3 mm for a fixed particle amount. Recently, Fan et al. (1984b) examined the gas-liquid mass transfer of the three-phase spouted bed under zero liquid flow conditions for application as a bioreactor for wastewater treatment. Over a wide range of the gas velocity considered, they reported that the mass transfer coefficient increases with increasing gas velocity.

A three-phase spouted bed operated under countercurrent conditions with gas as the continuous phase was studied for gas-liquid mass transfer application (Vukovic et al., 1974). The spouted bed and spouted fluidized bed with gas as the continuous phase were developed for various processes in chemical, petrochemical and fertilizer industry (Kono, 1980; Kinno and Nioh, 1983). The products of these types of reactors are granulated solids or gaseous materials. For the draft tube spouted bed Fan et al. (1984b) reported that the mass transfer coefficient increases and then decreases with an increase in the particle loading. Moreover, they reported that, for a given gas velocity at zero and low solids loading conditions, $k_l a$ for the draft tube three-phase spouted bed is higher than that for the three-phase fluidized bed, three-phase spouted bed, inverse three-phase fluidized bed (Yushina and Sata, 1983) and gas-liquid bubble column (with coarse bubble generators).

Gas-Liquid Mass Transfer in the Turbulent Contact Absorber

Douglas et al. (1963) investigated the absorption of CO_2 and SO_2 from a dust laden gas by alkaline process liquors. The volumetric gas side absorption coefficient $k_g a_{st}$, which is based on the static packing volume, was evaluated. They reported that the volumetric mass transfer coefficient in a TCA was two orders of magnitude higher than in packed beds. Subsequently, Douglas (1964) studied the absorption of ammonia into boric acid solutions. The height of the overall mass transfer unit (HTU) for NH_3 absorption was found to be approximately $\frac{1}{3}$ to $\frac{1}{2}$ of that obtained in a packed bed. It was reported that the HTU for mass transfer increases with increasing gas flow rate, decreases with increasing liquid flow rate and increases with increased static bed height.

Zhukov et al. (1977) reported data on the overall volumetric mass transfer coefficient for the physical absorption of SO_2 into water. Levsh et al. (1968b) measured the overall volumetric mass transfer coefficient for the desorption of oxygen from water.

The liquid film volumetric coefficient for mass transfer, $k_l A$, which is based on the unit cross section of the column, was measured by Elenkov and Kosev (1970) who assumed the gas side mass transfer resistance was negligible. They reported that $k_l A$ increases with increasing gas flow rate, increases with increasing static packing height and decreases when the open area of the supporting grid increases. Increasing the liquid flow rate generally caused an increase in $k_l A$, but in some cases $k_l A$ passed through a maximum point with respect to the liquid flow rate. An empirical correlation for $k_l A$ was also proposed by these authors.

Kosev and Elenkov (1973) measured the volumetric gas film mass transfer coefficient, $k_{cg} A$, defined in terms of gas side concentration difference as the driving force instead of the more commonly used partial pressure difference. The general trends for the volumetric gas film coefficient are similar to those of the liquid film mass transfer coefficient previously measured by Elenkov and Kosev (1970). A correlation equation was developed by Kosev and Elenkov (1973) to represent $k_{cg} A$.

The absorption efficiency, which denotes the degree of absorption per stage of TCA bed, has been employed by several investigators to compare the performance of the TCA with that of other types of apparatus. Blyakher et al. (1967) measured the absorption efficiency for the physical absorption of SO_2 and NH_3 into water. Ubaidullaev et al. (1981) correlated the absorption efficiency in terms of pressure drop for the desorption of NH_3 from ammonia-water solution. Miconnet et al. (1982) also used the concept of absorption efficiency to compare the performance between the TCA and the packed bed for the absorption of HCl into water. The concept of plate efficiency was employed by Gel'perin et al. (1968a) who described the effective use of a TCA as a rectification column.

The absorption of SO_2 by alkaline solutions and lime/limestone slurries in a TCA was studied in a small scale scrubber (Borgwardt, 1972) and a large scale scrubber (Epstein et al., 1973). SO_2 removal efficiency in a TCA was reported to be considerably higher compared to both conventional packed towers and venturi scrubbers. The data of TCA scrubber performance for the wet scrubbing of SO_2 from flue gases have been analyzed by Fan (1975) and McMichael et al. (1976) to determine the volumetric gas side mass transfer coefficients and the liquid side volumetric mass transfer coefficients in the lime/limestone chemical absorption system. A logical design procedure for a TCA as a scrubber was recently given by Visvanathan and Leung (1984).

Three kinds of interfacial area have been defined in the literature. They are the effective interfacial area per unit cross section of the column, denoted by A (Kossev et al., 1971; Gel'perin et al., 1972; Strumillo and Kudra, 1977), the effective interfacial area per unit volume of static bed, a_{st} (Wozniak and Ostergaard, 1973; Wozniak, 1977), and the effective interfacial area per unit volume of expanded bed, a (Kossev et al., 1971; Kito et al., 1976a,c). The following relationships hold between these interfacial systems:

$$A = a_{st} H_0 = aH \tag{31}$$

Moreover, the overall volumetric mass transfer coefficient, the gas film volumetric mass transfer coefficient and the liquid film volumetric mass transfer coefficient are uniquely defined for each corresponding interfacial area. Thus, to avoid confusion, caution must be exercised in the interpretation of the data for interfacial areas and mass transfer coefficients in the literature since these quantities might have a different basis.

The interfacial area between the gas and liquid phase in a TCA was first examined by Kossev et al. (1971) using the chemical absorption of carbon dioxide diluted with air into sodium hydroxide solution. The same chemical absorption system was also utilized for measuring the effective interfacial area by Gel'perin et al. (1972), Wozniak and Ostergaard (1973), Wozniak (1977), Kito et al. (1976a,c), and Strumillo and Kudra (1977).

Kossev et al. (1971) determined a for hollow polystyrene spheres with a diameter of 18 mm and a density of 176 kg/m^3. They found that a increases with increasing gas flow rate, passes through a maximum at a gas velocity of about 3 m/s and decreases with a further increase of the gas flow rate. They observed that at higher gas velocities where the decrease in a occurs, the homogeneity of the fluidized bed is disturbed due to considerable pulsing in the bed. Figure 10 shows the variation of a with respect to the gas flow rate. In this figure the data points of Gel'perin et al. (1972) and Strumillo and Kudra (1977) were calculated from their data for a by estimating the expanded bed height from the correlation equation proposed by Kito et al. (1976e, 1978).

The data for a obtained by Kito et al. (1976a,c) for a stagnant liquid flow system also shows a maximum with respect to the gas flow rate. However, the values of a obtained by Kito et al. (1976a,c) are considerably higher than those of other investigators, especially at low gas flow rates. This may be due to the fact that in experiments of Kito et al. the small open area of the grid prevents weeping of the liquid through the supporting grid. In fact, the fraction of the liquid holdup in their system is much greater than that in a typical TCA.

Figure 11 shows the variation of a (or a_{st}) with respect to liquid flow rate. The values of a_{st} measured by Kossev et al. (1971), Wozniak and Ostergaard (1973), Wozniak (1977), and Strumillo and Kudra (1977) are each confined to a narrow range of different

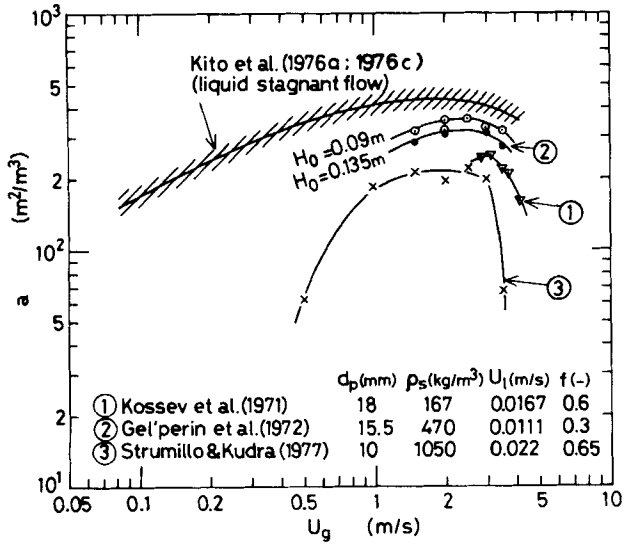

Figure 10. Gas-Liquid Interfacial Area vs. Superficial Gas Velocity for a TCA.

operating conditions. The value of a_{st} generally increases considerably with increasing liquid flow rates, since the increased liquid flow rate increases the liquid holdup and causes increased bed expansion. In Figure 11 the data for a are also shown for comparison. It is observed that the increase of a due to the increase of liquid flow rate is more gradual than that of a_{st}. In some cases, a is virtually independent of liquid flow rate, e.g., the data of a obtained by Wozniak and Ostergaard, (1973). The values of a are $\frac{1}{3}$ to $\frac{1}{2}$ of those of a_{st}, depending on the bed expansion height.

Correlation equations for estimating the interfacial area in the TCA have been developed by several authors. The interfacial area per unit cross section of the column, A, has been correlated by Gel'perin et al. (1972) and Strumillo and Kudra (1977). The empirical equation for A proposed by Strumillo and Kudra (1977) is:

$$A = 16.28 U_g^{0.92} U_l^{0.34} H_0^{0.83} d_p^{-0.94} \tag{32}$$

where U_g and U_l are in m/s, and H_0 and d_p in m. Equation 32 was correlated from a range of gas flow rates up to 2 m/s and for static bed heights up to 0.14 m. The packing diameter was varied between 5 and 10 mm and the particle density up to 1,050 kg/m³.

It is evident that A increases with increasing static bed height. The correlation equation proposed by Gel'perin et al. (1972) indicates that A is also a strong function of the open area of the supporting grid.

Wozniak (1977) proposed a correlation for a_{st} as follows:

$$\frac{a_{st}}{a_{pb}} = 6.189 \times 10^{-7} \left(\frac{\epsilon_g}{1-\epsilon_g}\right)^{0.8022} \left(\frac{H \Delta P_c}{U_g \mu_g}\right)^{0.9337} \tag{33}$$

where a_{pb} is the geometric surface area per unit volume for a packed bed of spheres, ϵ_g is the gas holdup, H is the expanded bed height, ΔP_c is the pressure drop across the column, U_g is the superficial gas velocity, and μ_g is the viscosity of the gas. All of the parameters in Eq. 33 are in SI units.

The interfacial area in a TCA can be estimated from Figure 10 or 11, or Eq. 32 or Eq. 33, but it is important to keep in mind that Eqs. 32 and 33 were developed from data which were obtained under very restricted ranges. Consequently, the reliability of these equations is highly questionable if they are extrapolated beyond the operating ranges investigated.

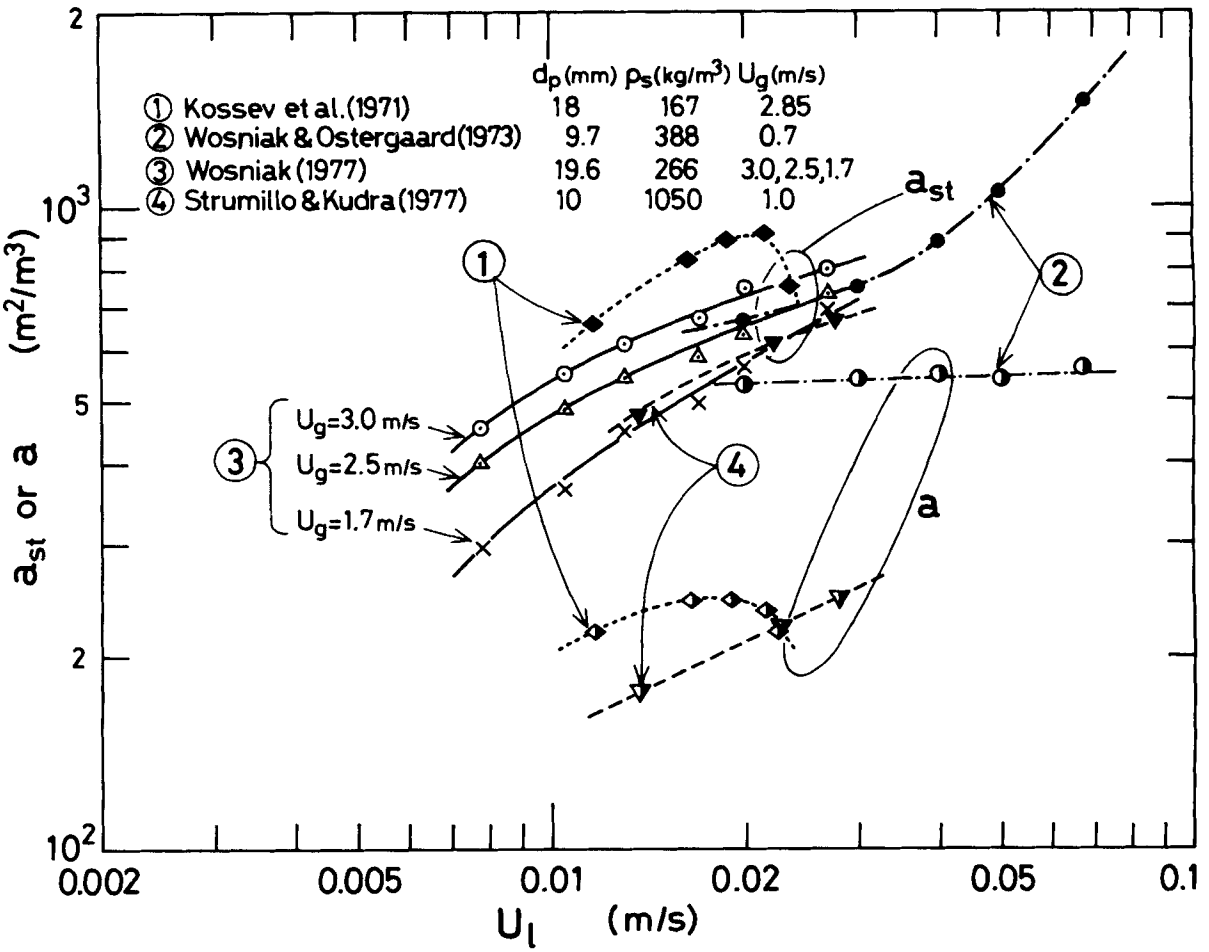

Figure 11. Gas-Liquid Superficial Area vs. Superficial Liquid Velocity for a TCA.

FUTURE STUDY

This review substantiates the information gaps and research needs on fundamentals of three-phase fluidization. Recognizing that fundamental analysis of three-phase fluidization was primarily established on the basis of empirical or semiempirical correlations, approaches based on fluid mechanic theories are deemed necessary. While information derived from air-water systems represented by the majority of the literature work is of importance, proper selection of physical properties of the gas and liquid, such as rheological properties, density and surface tension, compatible with actual process systems is required. Moreover, research is in need on the effect of temperature, pressure, and surfactants on the transport properties of the three-phase fluidized bed.

Correlations of transport properties with operating parameters can be established better if the flow regime of the system in operation could be identified. Research on the generalization of flow regime maps and scaleup of three-phase fluidized beds, which are of practical significance, is encouraged. Furthermore, fundamental research on the behavior of the solids movement, bubble and bubble wake is urged. The mechanistic approach represented by the generalized wake model has provided a basic framework for future modeling efforts. An improved model is sought which takes into consideration the inherent bubble size distribution, solids exchange between the wake and the liquid-solid fluidized bed, and effects of the grid region and the transition region.

Above all, optimal design and operation strategies for three-phase fluidized-bed operation are urgently in need of attention. To this end, it is imperative that new design configurations of the three-phase fluidized bed and associated fundamental analysis be conducted. When the three-phase fluidized bed is intended to be utilized as a chemical or biochemical reactor, the ultimate goal of new design configurations, in most cases, would be to achieve maximum mass and/or heat transfer effects with minimum power input and to maintain optimal fluid mixing for given reaction kinetics.

ACKNOWLEDGMENTS

The assistance of L. E. Beaver, S. H. Chern, and S. J. Hwang in the preparation of this paper is acknowledged. The work was supported by the National Science Foundation Grant Nos. CPE-7911183, CPE-7921068, and CPE-8219160.

NOTATION

A = gas-liquid interfacial area per cross-sectional area of the column
a = gas-liquid interfacial area per unit volume of the bed
a_{pb} = specific surface area of the packing per static bed volume
a_{st} = gas-liquid interfacial area per unit volume of static bed
Ar = Archimedes number, $d_p^3 g(\rho_s - \rho_l)/\rho_l \nu_l^2$
B = constant in Eq. 14
C_D = particle drag coefficient
C_{pl} = specific heat of liquid
D = equivalent diameter for free sectional area of the column
D_A = diffusivity of dissolved gaseous component
D_c = diameter of cylindrical column
d = equivalent diameter of slot or orifice of supporting grid
d_B = equivalent diameter of bubble
d_p = particle diameter
E = rate of energy dissipation defined by $(\Delta P_c/H)(1/\rho_l)(U_l/\epsilon_l)$
E_{zl} = axial dispersion coefficient of the liquid
F_g = pressure drop due to grid
F_w = pressure drop due to column wall
F_σ = pressure drop due to surface tension at gas-liquid interface
f = ratio of the grid open area to the column sectional area
Fr_g = Froude number of the gas, $U_l^2/d_p g$
Fr_l = Froude number of the liquid, $U_g^2/d_p g$
Fr_l' = modified Froude number of the liquid $[U_l^2/d_p g]$ $[1/(\epsilon_g + \epsilon_l)^2]$ $[\rho_l/(\rho_s - \rho_l)]$
G_g = mass flow rate of gas per unit cross section
G_{gmf} = mass flow rate of gas per unit cross section at incipient fluidization
G_l = mass flow rate of the liquid per unit cross section
g = gravitational acceleration
H = effective height of bed expansion
H_0 = static bed height
HMU_l = height of axial mixing unit of the liquid, $2E_{zl}/V_l$
h = heat transfer coefficient
K = constant in the Davies-Taylor equation given in Eq. 13
K' = power law fluid consistency index
k = ratio of wake volume to bubble volume for a multi-bubble system
k_b = Bankoff's two-phase flow factor
k_{cg} = gas-side mass transfer coefficient for concentration driving force
k_g = gas-side mass transfer coefficient for partial pressure driving force
k_l = liquid-side mass transfer coefficient
k_0 = ratio of wake volume to bubble volume for a single bubble system
k_g^p = gas-side mass transfer coefficient in a TCA packed section
k_g^s = gas-side mass transfer coefficient in a TCA spray section
k' = parameter in the correlation equation by Vail et al. (1970)
k'' = parameter in the correlation equation by Dakshinamurty et al. (1971)
l = bubble length
m' = parameter in the correlation equation by Vail et al. (1970)
m'' = parameter in the correlation equation by Dakshinamurty et al. (1971)
n = index in the Richardson and Zaki equation
$\bar{n}$ = power law fluid behavior index
n' = parameter in the correlation equation by Vail et al. (1970)
n'' = parameter in the correlation equation by Dakshinamurty et al. (1971)
Pe' = Peclet number defined by $V_l D_c/E_{zl}$
Pe'' = Peclet number defined by $V_l d_p/E_{zl}$
dP/dz = static pressure gradient
ΔP_c = pressure drop across the column
R = radius of spherical cap bubble
Re_g = gas Reynolds number defined by $d_p U_g \rho_g/\mu_g$
Re_l = liquid Reynolds number defined by $d_p U_l \rho_l/\mu_l$
Re_t = particle Reynolds number defined by $d_p U_t \rho_l/\mu_l$
Re_l' = modified liquid Reynolds number defined by $U_l^{2-\bar{n}} d_p^{\bar{n}}/\nu_l$
Re_g'' = modified gas Reynolds number defined by $d_p V_g \rho_g/\mu_g$
Re_l'' = modified liquid Reynolds number defined by $d_p V_l \rho_l/\mu_l$
S = cross-sectional area of empty column
U_B = relative velocity of the bubble to the liquid
U_b = absolute bubble velocity
U_g = superficial gas velocity
U_{gmf} = minimum fluidization velocity for the gas

U_{gmf0} = minimum fluidization velocity in the gas-solid fluidized bed
U_i = the extrapolated value of U_l as ϵ approaches 1
U_l = superficial liquid velocity
U_{lf} = liquid velocity based on the area of liquid-solid fluidization region
U_{lmf} = minimum fluidization velocity for the liquid
U_{lmf0} = minimum fluidization velocity in the liquid-solid fluidized bed
$(U_{lmf})_1$ = minimum fluidization velocity for the liquid in a fluidized bed containing flotsam particles alone
$(U_{lmf})_2$ = minimum fluidization velocity for the liquid in a fluidized bed containing jetsam particles alone
U_t = terminal velocity of solid particle
$V_{b\infty}$ = rising velocity of isolated bubble in stagnant fluid
V_c = average liquid circulation velocity defined by Eq. 28
V_g = bubble rise velocity in a multibubble system or linear gas velocity
V_l = linear liquid velocity
W = weight of solid particles in the bed
W_{SLV} = work of adhesion
We = Weber number defined by $\rho_s U_b^2 d_p/\sigma$
x = ratio of solid holdup in the wake to that in the liquid-solid fluidized region expressed by $\epsilon_{sw}/\epsilon_{sf}$
x_2 = weight fraction of jetsam particles

Greek Letters

ϵ = bed porosity
ϵ_g = gas holdup
$\epsilon_{g,mf}$ = gas holdup at incipient fluidization
ϵ_l = liquid holdup
$\epsilon_{l,mf}$ = liquid holdup at incipient fluidization
ϵ_{lf} = liquid holdup in the liquid-solid fluidized region
$\epsilon_{l,st}$ = liquid holdup per unit static bed volume
ϵ_s = solid holdup
$\epsilon_{s,st}$ = solid holdup in a static bed
ϵ_{sf} = solid holdup in the liquid-solid fluidized region
ϵ_{sw} = solid holdup in the wake region
ϵ_w = volume fraction of the wake in the fluidized bed
ϵ_0 = porosity in the packed bed
ϵ_l^* = parameter defined in the correlation equation by Kato et al. (1981)
γ = generalized viscosity constant
θ = included angle of a spherical cap bubble
θ' = contact angle
λ_l = thermal conductivity of the liquid
μ_g = viscosity of gas
μ_l = viscosity of liquid
μ_0 = apparent viscosity of a liquid-solid fluidized bed
ν_l = kinematic viscosity of liquid
ρ_g = gas density
ρ_l = liquid density
ρ_s = solid density
ρ_{wp} = density of wetted packing
ρ_0 = apparent density of a liquid-solid fluidized bed
σ = surface tension
τ = residence time
τ' = ratio of the area occupied by liquid to the total open cross section of grid
ϕ_s = sphericity of the solid particle
ψ = parameter defined by Eq. 11

LITERATURE CITED

Adlington, D., and E. Thompson, "Desulphurization in Fixed and Fluidized Bed Catalyst System," *Proc. 3rd European Symp. Chem. React. Eng.*, 203, Pergamon Press, Oxford (1965).

Afschar, A. S., and K. Schugerl, "Eigenscharften von Dreiphasen-Friepbetten mit Gleichstrom von Wasser and Luft," *Chem. Eng. Sci.*, **23**, 267 (1968).

Aksel'rod, L. A., and M. M. Yakovenko, "Certain Hydrodynamic Aspects of Mass Transfer Equipment with Mobile Spherical Packing," *Theor. Found. Chem. Eng.*, **3**, 124 (1969).

Al-Dibouni, M. R., and J. Garside, "Particle Mixing and Classification in Liquid Fluidized Beds," *Trans. Inst. Chem. Engrs.*, **57**, 94 (1979).

Alvarez-Cuenca, M., and M. A. Nerenberg, "The Plug Flow Model for Mass Transfer in Three-Phase Fluidized Beds and Bubble Columns," *Can. J. Chem. Eng.*, **59**, 739 (1981).

Alvarez-Cuenca, et al., "Oxygen Mass Transfer in Three-Phase Fluidized Beds Working at Large Flow Rates," *Can. J. Chem. Eng.*, **61**, 58 (1983).

Armstrong, E. A., C. G. J. Baker, and M. A. Bergougnou, "The Effects of Solids Wettability on the Characteristics of Three Phase Fluidization," *Fluidization Technology*, D. L. Keairns, Ed., **I**, 405, Hemisphere (1976a).

Armstrong, E. A., C. G. J. Baker, and M. A. Bergougnou, "Heat Transfer and Hydrodynamic Studies on Three Phase Fluidized Beds," *Fluidization Technology*, D. L. Keairns, Ed., **I**, 453, Hemisphere (1976b).

Arters, D., and L.-S. Fan, "Liquid-Solid Mass Transfer in a Gas-Liquid-Solid Fluidized Bed," AIChE Mtg., San Francisco (Nov. 25–30, 1984).

Baker, C. G. J., S. D. Kim, and M. A. Bergougnou, "Wake Characteristics of Three-Phase Fluidized Beds," *Powder Technol.*, **18**, 201 (1977).

Baker, C. G. J., F. R. Armstrong, and M. A. Bergougnou, "Heat Transfer in Three-Phase Fluidized Beds," *Powder Technol.*, **21**, 195 (1978).

Balabekov, O. S., et al., "Operating Conditions of Columns with Wetted Moving Spherical Packings," *J. App. Chem. U.S.S.R.*, **42**, 1454 (1969a).

Balabekov, O. S., et al., "Hydrodynamic Characteristics of Columns with Wetted Fluidized Spherical Packings," *J. App. Chem. U.S.S.R.*, **42**, 2128 (1969b).

Barile, R. G., and D. W. Meyer, "Turbulent Bed Cooling Tower," *Chem. Eng. Prog. Symp. Ser.*, No. 119, **67**, 134 (1971).

Barile, R. G., J. L. Dengler, and T. A. Hertwig, "Performance and Design of a Turbulent Bed Cooling Tower," *AIChE Symp. Ser.*, **70**, 154 (1975).

Beaver, L. E., L.-S. Fan, and K. Muroyama, "Sulfur Dioxide Absorption into a Calcium Carbonate Slurry Using a Constrained, Cocurrent Gas-Liquid-Solid Fluidized Bed," AIChE Mtg., Cleveland, OH (Aug. 29–Sept. 3, 1982).

Beaver, L. E., and L.-S. Fan, "Experimental Observations in a Cocurrent Gas-Liquid-Solid Semifluidized Bed with Gas as the Continuous Phase," J. Chinese Institute of Chemical Engineers, **15**, 159 (1984).

Beek, W. J., "Mass Transfer in Fluidized Beds," *Fluidization*, J. F. Davidson and D. Harrison, Eds., 431, Academic Press, London (1971).

Begovich, J. M., and J. S. Watson, "Hydrodynamic Characteristics of Three-Phase Fluidized Beds," *Fluidization*, J. F. Davidson and D. L. Keairns, Eds., 190, Cambridge Univ. Press (1978a).

Begovich, J. M., and J. S. Watson, "An Electroconductivity Technique for the Measurement of Axial Variation of Hold Up in Three-Phase Fluidized Beds," *AIChE J*, **24**, 351 (1978b).

Bellman, R., and R. H. Pennington, "Effects of Surface Tension and Viscosity on Taylor Instability," *Quart. Appl. Math.*, **12**, 151 (1954).

Bhaga, D., and M. E. Weber, "Hold Up in Vertical Two and Three Phase Flow, Part I: Theoretical Analysis," *Can. J. Chem. Eng.*, **50**, 323 (1972a).

Bhaga, D., and M. E. Weber, "Hold Up in Vertical Two and Three Phase Flow, Part II" *Can. J. Chem. Eng.*, **50**, 329 (1972b).

Bhatia, V. K., K. A. Evans, and N. Epstein, "Effects of Solids Wettability on Expansion of Gas-Liquid Fluidized Beds," *Ind. Eng. Chem. Process Des. Dev.*, **11**, 151 (1972).

Bhatia, V. K., G. H. Neale, and N. Epstein, "A Cell Model for Three-Phase Fluidization at Low Reynolds Numbers," *Int. Chem. E. Symp. Ser.*, No. 38, **I**, The Inst. Chem. Engrs. London (1974).

Bhatia, V. K. and N. Epstein, "Three Phase Fluidization: A Generalized Wake Model," *Fluidization and Its Applications*, H. Angelino et al., Eds., 372, Cepadues-Editions, Toulouse (1974a).

Bhatia, V. K., and N. Epstein, Discussions, "Fluidization and Its Applications," H. Angelino et al., Eds., 709, Cepadues-Editions, Toulouse (1974b).

Bhatia, V. K., "Stability of Bubbles in Fluidized Beds," *Ind. Eng. Chem. Fundam.*, **15**, 86 (1976).

Blum, D. B., and J. J. Toman, "Three-Phase Fluidization in a Liquid Phase Methanator," *AIChE Symp. Ser.*, No. 161, **73**, 115 (1977).

Blyakher, I. G., L. Ya. Zhivaikin, and N. A. Yurovskaya, "Investigation of Hydrodynamics and Mass Transfer in Equipment with Movable Packing," *Int. Chem. Eng.*, **7**, 485 (1967).

Borgwardt, R., "Limestone Scrubbing of SO_2 at EPA Pilot Plant," U.S. E.P.A. Report (Aug., 1972).

Botterill, J. S. M., *Fluid-Bed Heat Transfer*, Academic Press (1975).

Bruce, P. N., and L. Revel-Chion, "Bed Porosity in Three-Phase Fluidization," *Powder Technol.*, **10**, 243 (1974).

Calderbank, P. H., and M. B. Moo-Young, "The Continuous Phase Heat and Mass-Transfer Properties of Dispersions," *Chem. Eng. Sci.*, **16**, 39 (1961).

Calderbank, P. H., "Gas Absorption from Bubbles," *The Chem. Eng.*, CE 209 (1967).

Chen, B. H., and W. J. M. Douglas, "Liquid Hold-up and Minimum Fluidization Velocity in a Turbulent Contactor," *Can. J. Chem. Eng.*, **46**, 245 (1968).

Chen, B. H., and W. J. M. Douglas, "Axial Mixing of Liquid in a Turbulent-Bed Contactor," *Can. J. Chem. Eng.*, **47**, (2) 113 (1969).

Chern, S.-H., K. Muroyama, and L.-S. Fan, "Hydrodynamics of Constrained Inverse Fluidization and Semifluidization in a Gas-Liquid-Solid System," *Chem. Eng. Sci.*, **38**, 1167 (1983).

Chern, S.-H., L.-S. Fan, and K. Muroyama, "Hydrodynamics of Cocurrent Gas-Liquid-Solid Semifluidization with a Liquid as the Continuous Phase," *AIChE J.*, **30**, 288 (1984).

Clift, R., J. R. Grace, and M. E. Weber, "Stability of Bubbles in Fluidized Beds," *Ind. Eng. Chem. Fund.*, **13**, 45 (1974).

Clift, R., J. R. Grace, and M. E. Weber, "Stability of Bubbles in Fluidized Beds," *Ind. Eng. Chem. Fund.*, **15**, 87 (1976).

Cooper, P. F., and B. Atkinson, *Biological Fluidized Bed Treatment of Water and Wastewater*, Ellis Horwood Publishers, Chichester, England (1981).

Dakshinamurty, P., V. Sabrahmanyam, and J. N. Rao, "Bed Porosities in Gas-Liquid Fluidization," *Ind. Eng. Chem. Process Des. Dev.*, **10**, 322 (1971).

Dakshinamurty, P., et al., "Bed Porosities in Gas-Liquid Fluidization," *Ind. Eng. Chem. Process Des. Dev.*, **11**, 318 (1972).

Dakshinamurty, P., P. Kameswara Rao, and K. Veerabhadra Rao, "Gas-Liquid Mass Transfer in Gas-Liquid Fluidized Beds: Part I: Liquid Phase Volumetric Absorption Coefficients for Carbon Dioxide-Water System," *Indian J. Technol.*, **13**, 376 (1974a).

Dakshinamurty, P., et al., "Studies of Gas-Liquid Mass Transfer in Gas-Liquid Fluidized Beds," *Fluidization and Its Applications*, H. Angelino et al., Eds., 429, Cepadues-Editions, Toulouse (1974b).

Dakshinamurty, P., and K. Veerabhadra Rao, "Gas-Liquid Mass Transfer in Gas-Liquid Fluidized Beds: Part II," *Indian J. Techn.*, **14**, 9 (1976).

Darton, R. C., and D. Harrison, "Some Properties of Gas Bubbles in Three-Phase Fluidized Beds," *Int. Chem. E. Symp. Ser.*, No. 38, **I**, The Inst. Chem. Engrs., London (1974a).

Darton, R. C., and D. Harrison, "The Rise of Single Gas Bubbles in Liquid Fluidized Beds," *Trans. Inst. Chem. Engrs.*, **12**, 301 (1974b).

Darton, R. C., and D. Harrison, "Gas and Liquid Hold-up in Three-Phase Fluidization," *Chem. Eng. Sci.*, **30**, 581 (1975).

Darton, R. C., and D. Harrison, "Bubble Wake Structure in Three-Phase Fluidization," *Fluidization Technology*, D. L. Keairns, Ed., **I**, 399, Hemisphere (1976).

Davidson, J. F., et al., "Three-Phase Systems," *Chemical Reactor Theory: A Review*, Lapidus and Amundson, Eds., Chapter 10, 655, Prentice-Hall (1977).

Davies, R. M., and G. I. Taylor, "The Mechanics of Large Bubbles Rising Through Extended Liquids and Through Liquids in Tubes," *Proc. Royal Soc. London*, Ser. A200, 375 (1950).

Dhanuka, V. R., "Hydrodynamics and Mass Transfer Studies in Three Phase Fluidized Beds," Ph.D. Thesis, Univ. of Salford, England (1978).

Dhanuka, V. R., and J. B. Stepanek, "Gas and Liquid Hold-up and Pressure Drop Measurements in a Three-Phase Fluidized Bed," *Fluidization*, J. F. Davidson and D. L. Keairns, Eds., 179, Cambridge Univ. Press (1978).

Dhanuka, V. R., and J. B. Stepanek, "Gas-Liquid Mass Transfer in a Three-Phase Fluidized Bed," *Fluidization*, G. R. Grace and G. M. Matsen, Eds., 261, Plenum Press (1980a).

Dhanuka, V. R., and J. B. Stepanek, "Simultaneous Measurement of Interfacial Areas and Mass Transfer Coefficient in Three-Phase Fluidized Beds," *AIChE J.*, **26**, 1029 (1980b).

Douglas, H. R., I. W. A. Snider, and G. H. Tomlinson II, "The Turbulent Contact Absorber," *Chem. Eng. Prog.*, **59**, No. 12, 85 (1963).

Douglas, W. J. M., "Heat and Mass Transfer in a Turbulent Bed Contactor," *Chem. Eng. Prog.*, **60**, No. 7, 66 (1964).

Edwards, A. M., "Biological Phenol Degradation in Packed Bed, Semi-fluidized Bed and Batch Reactor Systems," M. S. Thesis, The Ohio State Univ. (1981).

Efremov, G. I., and I. A. Vakhrushev, "A Study of the Hydrodynamics of Three-Phase Fluidized Beds," *Int. Chem. Eng.*, **10**, 37 (1970).

Elenkov, D., and A. Kosev, "Mass Transfer in the Liquid Phase in Apparatus with Mobile Packing," *Theo. Found. Chem. Eng.*, **4**, 100 (1970).

El-Temtamy, S. A., and N. Epstein, "Bubble Wake Solid Content in Three-Phase Fluidized Beds," *Proc. 2nd PACHEC*, 1397, Denver (1977).

El-Temtamy, S. A., and N. Epstein, "Bubble Wake Solid Content in Three-Phase Fluidized Beds," *Int. J. Multiphase Flow*, **4**, 19 (1978).

El-Temtamy, S. A., and N. Epstein, "Contraction or Expansion of Three Phase Fluidized Beds Containing Fine/Light Solids," *Can. J. Chem. Eng.*, **57**, 520 (1979).

El-Temtamy, S. A., Y. D. El-Sharnoubi, and M. M. El-Halwagi, "Liquid Dispersion in Gas-Liquid Fluidized Beds: Part I," *Chem. Eng. J.*, **18**, 151 (1979a).

El-Temtamy, S. A., Y. D. El-Sharnoubi, and M. M. El-Halwagi, "Liquid Dispersion in Gas-Liquid Fluidized Beds: Part II," *Chem. Eng. J.*, **18**, 161 (1979b).

El-Temtamy, S. A., and N. Epstein, "Rise Velocities of Large Single Two-Dimensional and Three-Dimensional Gas Bubbles in Liquids and in Liquid Fluidized Beds," *Chem. Eng. J.*, **19**, 153 (1980a).

El-Temtamy, S. A., and N. Epstein, "Simultaneous Solids Entrainment and De-entrainment Above a Three-Phase Fluidized Bed," *Fluidization*, G. R. Grace and G. M. Matsen, Eds., 519, Plenum Press (1980b).

Epstein, N., et al., "Scrubbing Test Facility at the TVA Shawnee Power Plant," AIChE Mtg., Philadelphia (Nov., 1973).

Epstein, M. N., et al., "Incipient Stratification and Mixing in Aerated Liquid-Liquid or Liquid-Solid Mixtures," *Chem. Eng. Sci.*, **36**, 784 (1981).

Epstein, N., and D. Nicks, "Contraction or Expansion of Three-Phase Fluidized Beds," *Fluidization Technology*, **I**, D. L. Keairns, Ed., 389, Hemisphere (1976).

Epstein, N., "Criterion for Initial Contraction or Expansion of Three-Phase Fluidized Beds," *Can. J. Chem. Eng.*, **54**, 259 (1976).

Epstein, N., "Three-Phase Fluidization: Some Knowledge Gaps," *Can. J. Chem. Eng.*, **59**, 649 (1981).

Epstein, N., "Hydrodynamics of Three-Phase Fluidization," *Handbook of Fluids in Motion*, N. P. Cheremisinoff and R. Gupta, Eds., 1165, Ann Arbor Science (1983).

Ermakova, A., G. K. Ziganshin, and M. G. Slinko, "Hydrodynamics of a Gas-Liquid Reactor with a Fluidized Bed of Solid Matter," *Theor. Found. Chem. Eng.*, **4**, 84 (1970a).

Ermakova, A., and G. K. Ziganshin, "Effect of Mass Transfer on the Rate of a Heterogeneous Gas-Liquid Reaction at the Surface of a Solid Catalyst," *Theor. Found. Chem. Eng.*, **4**, 271 (1970b).

Ermakova, A., et al., "A Catalytic Reactor with a Three-Phase Gas-Liquid-Solid Catalyst Fluidized Bed," *Theor. Found. Chem. Eng.*, **7**, 29 (1973).

Ermakova, A., et al., "Mathematical Simulation of Three-Phase Catalytic Reactors (Gas/Liquid/Solid Catalyst)," *Theor. Found. Chem. Eng.*, **11**, 576 (1977).

Ermakova, A., et al., "Effect of Packing on the Rate of a Heterogeneous Catalytic Reaction in a Three-Phase Fluidized Bed," *Int. Chem. Eng.*, **19**, 174 (1979).

Evstropeva, I. P., I. N. Taganov, and P. G. Romankov, "Experimental Study of the Rates of Motion of the Phases in a Three-Phase Solid-Liquid-Gas System," *Theor. Found. Chem. Eng.*, **6**, 545 (1972).

Fan, L.-S., "Absorption of Sulfur Dioxide in Spray Columns and Turbulent Contact Absorbers," Ph.D. Thesis, West Virginia Univ. (1975).

Fan, L.-S., K. Muroyama, and S. H. Chern, "Hydrodynamics of Inverse Fluidization in Liquid-Solid and Gas-Liquid-Solid Systems," *Chem. Eng. J.*, **24**, 143 (1982a).

Fan, L.-S., K. Muroyama, and S. H. Chern, "Some Remarks on Hydrodynamics of Inverse Gas-Liquid-Solid Fluidization," *Chem. Eng. Sci.*, **37**, 1570 (1982b).

Fan, L.-S., S. H. Chern, and K. Muroyama, "Hydrodynamic Characteristics of a Gas-Liquid-Solid Fluidized Bed Containing a Binary Mixture of Particles," AIChE Mtg., Los Angeles (Nov. 14–19, 1982c).

Fan, L.-S., S.-J. Hwang, and A. Matsuura, "Hydrodynamic Behavior of A Draft Tube Gas-Liquid-Solid Spouted Bed," *Chem. Eng. Sci.* (1984a).

Fan, L.-S., T.-R. Long, and K. Fujie, "Gas-Liquid Mass Transfer and Biological Phenol Degradation in a Draft Tube Gas-Liquid-Solid Spouted Bed Bioreactor," AIChE Mtg., San Francisco (Nov. 25–30, 1984b).

Fan, L.-S., S. Satija, and K. Wisecarver, "Pressure Fluctuation in a Gas-Liquid-Solid Fluidized Bed," AIChE Mtg., San Francisco (Nov. 25–30, 1984c); AIChE J., (in review).

Fan, L-S., S.-J. Hwang, and A. Matsuura, "Some Remarks on Hydrodynamic Behavior of a Draft Tube Gas-Liquid-Solid Spouted Bed," *AIChE Symp. Ser.*, **80**(234), 91 (1984d).

Fan, L.-S., S. H. Chern, and K. Muroyama, "Qualitative Analysis of Solids Mixing in a Gas-Liquid-Solid Fluidized Bed Containing a Binary Mixture of Particles," *AIChE J.*, **30**(5), 858 (1984e).

Fan, L.-S., T. Yamashita, and R.-H. Jean, "Solids Mixing and Segregation in a Gas-Liquid-Solid Fluidized Bed," AIChE Mtg., San Francisco (Nov. 25–30, 1984f).

Fan, L. T., and C. Y. Wen, "Semifluidization: Mass Transfer in Semifluidized Beds," *AIChE J.*, **5**, 407 (1959).
Fukushima, S., "Gas-Liquid Mass Transfer in Three-Phase Fluidized Bed," *J. Chem. Eng. Japan*, **12**, 489 (1979).
Gal-Or, B., and S. Waslo, "Hydrodynamics of an Ensemble of Drops (or Bubbles) in the Presence or Absence of Surfactants," *Chem. Eng. Sci.*, **23**, 1431 (1968).
Garside, J., and M. R. Al-Dibouni, "Velocity-Voidage Relations for Fluidization and Sedimentation in Solid-Liquid Systems," *Ind. Eng. Chem. Process. Des. Dev.*, **16**, 206 (1977).
Gartsman, A. N., et al., "Mass Transfer with Chemical Reaction in the Three-Phase System Gas-Liquid-Solid Catalyst," *Int. Chem. Eng.*, **17**, 697 (1977).
Gel'perin, N. I., et al., "Investigation of the Operation of Absorption Apparatus with a Refluxed Ball Packing Type of Pseudoliquified Layer," (UDC 621.57.046; 55,096,5.001,5), Translated from *Khimicheskoe i Heftyanoe Mashinostroenie*, No. 1 (Jan. 22, 1966).
Gel'perin, N. I., Uy. M. Latysher, and L. I. Blyakman, "Rectification in a Column with Fluidized Beds of Spherical Packing," *Int. Chem. Eng.*, **8**, 691 (1968a).
Gel'perin, N. I., V. I. Savchenko, and V. Z. Grishko, "Some Hydrodynamic Laws of Absorption Apparatus Packed with Fluidized Spheres," *Theor. Found. Chem. Eng.*, **2**, 65 (1968b).
Gel'perin, N. I., and V. G. Einstein, "Heat Transfer in Fluidized Beds," *Fluidization*, J. F. Davidson and D. Harrison, Eds., Chap. 10, 471, Academic Press, New York (1972).
Gel'perin, N. I., V. Z. Grishko, and V. A. Mikhailov, "Determination of Phase Contact Surface in Mass-Transfer Equipment with Fluidized Spherical Packing," *Theor. Found. Chem. Eng.*, **6**, 534 (1972).
Grace, J. R., "Fluidized-Bed Heat Transfer," *Handbook of Multiphase Systems*, G. Hestroni, Ed., Chap. 8.2, 8, Hemisphere (1982).
Griswold, C. R., and R. P. Van Driesen, "Commercial Experience with H-Oil," *Hydroc. Processing*, **45**, No. 5, 153 (May, 1966).
Hanratty, T. J., G. Latinen, and R. H. Wilhelm, "Turbulent Diffusion in Particulately Fluidized Beds of Particles," *AIChE J.*, **2**, 372 (1956).
Happel, J., and H. Brenner, *Low Reynolds Number Hydrodynamics*, 115, Prentice-Hall, Englewood Cliffs, NJ (1965).
Henriksen, H. K., and K. Ostergaard, "Characteristics of Large Two-Dimensional Air Bubbles in Liquids and in Three-Phase Fluidized Beds," *Chem. Eng. J.*, **7**, 141 (1974a).
Henriksen, H. K., and K. Ostergaard, "On the Mechanism of Break-up of Large Bubbles in Liquids and Three-Phase Fluidized Beds," *Chem. Eng. Sci.*, **29**, 626 (1974b).
Hetzler, R., and M. C. Williams, "Fluidized Bed Viscosity and Expansions, Correlated with Glass-Forming Liquid Model," *Ind. Eng. Chem. Fund.*, **8**, 668 (1969).
Hirata, A., et al., "Biological Treatment of Phenolic Wastewater in a Three-Phase Fluidized Bed (No. 1): Control of Biofilms by Mechanical Stirring," *Water Purification and Liquid Waste Treatment*, Japan, **23**, 15 (1982).
Holladay, D. W., et al., "Biodegradation of Phenolic Waste Liquors in Stirred-Tank, Columnar and Fluidized-Bed Bioreactor," *AIChE Symp. Ser.*, **74**, No. 172, 241 (1978a).
Holladay, D. W., et al., "Biodegradation of Phenolic Waste Liquors in Stirred-Tank, Packed-Bed, and Fluidized Bed Bioreactors," *J. WPCF*, **50**, 2573 (1978b).
Ishida, M., and H. Tanaka, "An Optical Probe to Detect Both Bubbles and Suspended Particles in a Three-Phase Fluidized Bed," *J. Chem. Eng. Japan*, **15**, 389 (1982).
Joshi, J. B., "Axial Mixing in Multiphase Contactors—A Unified Correlation," *Trans. Inst. Chem. Eng.*, **58**, 155 (1980).
Kafarov, V. V., V. A. Klipinitser, and O. I. Saks, "Solid-Phase Distribution and Holdup in a Column-Type Reactor with a Gas-Liquid-Solid Three-Phase System," *Theor. Found. Chem. Eng.*, **1**, 742 (1973).
Kato, Y., "Gas-Liquid Contact in a Gas-Liquid-Solid Fluidized Bed," *Kagaku Kogaku*, **27**, 7 (1963); *Kagaku Kogaku* (Abr. English, Eds.), **1**, 3 (1963).
Kato, Y., T. Kago, and S. Morooka, "Heat Transfer from Wall to Packed and Fluidized Bed for Gas-Liquid Cocurrent Up-Flow," *Kagaku Kogaku Ronbunshu*, **4**, 328 (1978).
Kato, Y., et al., "Wall-Bed Heat Transfer Characteristics of Three-Phase Packed and Fluidized Bed," *Kagaku Kogaku Ronbunshu*, **6**, 579 (1980).
Kato, Y., et al., "Liquid Holdup and Heat Transfer Coefficient Between Bed and Wall in Liquid-Solid and Gas-Liquid-Solid Fluidized Beds," *Powder Technol.*, **28**, 173 (1981).
Kielback, A. W., "The Development of Floating-Bed Scrubbers," *Chem. Eng. Prog. Symp. Ser.*, **57**, No. 35, 51 (1959).
Kielback, A. W., "Apparatus and Procedure for Contact Between Fluids," U.S. Patent 3,122,594 (Feb. 25, 1964).
Kim, C. H., and S. D. Kim, "Liquid Phase Dispersion in Three Phase Fluidized Beds," Proc. of 2nd World Congress of Chem. Eng., **III**, 1, Montreal, Canada (Oct. 4–9, 1981).
Kim, S. D., C. G. J. Baker, and M. A. Bergougnou, "Hold-up and Axial Mixing Characteristics of Two and Three Phase Fluidized Beds," *Can. J. Chem. Eng.*, **50**, 695 (1972).
Kim, S. D., C. G. J. Baker, and M. A. Bergougnou, "Phase Hold-up Characteristics of Three Phase Fluidized Beds," *Can. J. Chem. Eng.*, **53**, 134 (1975).
Kim, S. D., C. G. J. Baker, and M. A. Bergougnou, "Bubble Characteristics of Three Phase Fluidized Beds," *Chem. Eng. Sci.*, **32**, 1299 (1977).
Kim, S. D., and C. H. Kim, "Three Phase Fluidized Beds: A Review," *Hwahak Konghak*, **18**, No. 5, 313 (1980).
Kim, S. D., and C. H. Kim, "Axial Dispersion Characteristics of Three-Phase Fluidized Beds," *J. Chem. Eng. Japan*, **16**, 172 (1983).
Kinno, B., and S. Nioh, "Scale Up of Granulation Process," *Proc. of PACHEC'83*, Seoul, Korea, **I**, 118 (May 8–11, 1983).
Kito, M., et al., "Performance of Turbulent Bed Contactor: Gas Holdup and Interfacial Area under Liquid Stagnant Flow," *Fluidization Technology*, D. L. Keairns, Ed., **I**, 411, Hemisphere (1976a).
Kito, M., et al., "Gas Holdup in Mobile Beds under Liquid Stagnant Flow," *Kagaku Kogaku Ronbunshu*, **2**, 12 (1976b).
Kito, M., et al., "Effective Interfacial Areas in Mobile Bed Contactors under Liquid Stagnant Flow," *Kagaku Kogaku Ronbunshu*, **2**, 16 (1976c).
Kito, M., et al., "Minimum Fluidization Velocity in a Mobile Bed," *Kagaku Kogaku Ronbunshu*, **2**, 21 (1976d).
Kito, M., et al., "Pressure Drop and Bed Expansion in a Mobile Bed," *Kagaku Kogaku Ronbunshu*, **2**, 476 (1976e).
Kito, M., K. Tabei, and K. Murata, "Gas and Liquid Holdups in Mobile Beds under the Countercurrent Flow of Air and Liquid," *Ind. Eng. Chem. Process Des. Dev.*, **17**, 568 (1978).
Kolbel, H., P. Langemann, and J. Platz, "Eigenshaften des Blasensauien-Reactors-Das Verweilzeitspektrum dergroformigen Phase," *Dechema Monograph*, **41**, 225 (1962).
Kono, H., "A New Concept for . . . Three Phase Fluidized Beds," *Hydroc. Processing*, 123 (Jan., 1980).
Kossev, A., C. Peev, and D. Elenkov, "On the Interfacial Area in Floating Bed Contactors," *Verfahrenstechnik*, **5**, 230 (1971).
Kossev, A., and E. Elenkov, "Mass Transfer in the Gas Phase in Apparatus with a Mobile Packing," *Theor. Found. Chem. Eng.*, **7**, 795 (1973).
Koval, Zh. A., A. V. Bespalov, and O. G. Kuleshov, "Axial Mixing of a Liquid in a Vessel with Mobile Spherical Packing," *Theor. Found. Chem. Eng.*, **9**, 289 (1975).
Kunii, D., and O. Levenspiel, *Fluidization Engineering*, Wiley, New York (1969).
Kuroda, M., and K. Tabei, "Theoretical Description of the Minimum Fluidizing Velocity," *Kagaku Kogaku Ronbunshu*, **5**, 449 (1979); *Int. Chem. Eng.*, **21**, 219 (1981).
Kurten, H., and P. Zehner, "Slurry Reactors," *Ger. Chem. Eng.*, **2**, 220 (1979).
Lapidus, L., and J. C. Elgin, "Mechanics of Vertical Moving Fluidized Systems," *AIChE J.*, **3**, 63 (1957).
Lee, J. C., Discussion in the Paper of Adlington and Thompson, *Proc. 3rd Europ. Symp. Chem. React. Eng.*, 211, Pergamon Press, Oxford (1965).
Lee, J. C., A. J. Sherrard, and P. S. Buckley, "Optimum Particle Size in Three Phase Fluidized Bed Reactors," *Fluidization and Its Applications*, H. Angelino et al., Eds., 407, Cepadues-Editions, Toulouse (1974).
Lee, J. C., and H. Worthington, "Gas-Liquid Mass Transfer in Three-Phase Fluidized Beds," *Int. Chem. E. Symp. Ser.*, No. 38, *Multi-Phase Flow Systems*, **I**, The Inst. Chem. Engrs., London (1974).
Lee, J. C., and A. Al-Kaisi, "Bubble-Particle Interaction in Three-Phase Fluidized Beds," Instn. Chem. Engrs. Research Mtg., Univ. of Salford (Mar., 1976).
Lee, J. C., and N. J. Al-Dabbagh, "Three Phase Fluidized Beds—Onset of Fluidization at High Gas Rates," *Fluidization*, J. F. Davidson and D. L. Keairns, Eds., 184, Cambridge Univ. Press (1978).
Lee, J. C., and P. S. Buckley, "Fluid Mechanics and Aeration Characteristics of Fluidized Beds," *Biological Fluidized Bed Treatment of Water and Wastewater*, P. F. Cooper and B. Atkinson, Eds., Chap. 4, 62, Ellis Horwood Publishers, Chichester, England (1981).
Letan, R., and E. Kehat, "The Mechanism of Heat Transfer in a Spray Column Heat Exchanger," *AIChE J.*, **14**, 398 (1968).
Levsh, I. P., N. I. Krainev, and M. I. Niyazov, "Calculation of the Pressure Drop and Heights of Three-Phase Fluidized Beds," *Int. Chem. Eng.*, **8**, 311 (1968a).
Levsh, I. P., et al., "Mass Transfer in Absorbers with Fluidized Packed Beds," *Int. Chem. Eng.*, **8**, 379 (1968b).
Levsh, I. P., N. I. Krainev, and M. I. Niyazov, "Hydrodynamic Calculation of Absorbers with Fluidized Beds," *Int. Chem. Eng.*, **8**, 619 (1968c).

Li, A., and D. Lin, "Scale-up Performance and Thermal Stability Analysis of H-Oil and H-Coal Ebulated-Bed Reactors," AIChE Mtg., New Orleans, LA (Nov. 8–11, 1981).
Mach, W., "Surpendierung fester korper im turbulenten Gas/Flussigkeitsstrom," *Chemie-Ing. Tech.*, **42**, 311 (1970).
Massimilla, L., N. Majuri, and P. Signorini, "Sull Assorbimento Di Gers in Sistema: Solido-Liquido-Fluidizzato," *La Ricerca Scientifica*, **29**, 1934 (1959).
Massimilla, L., A. Solimand, and E. Squillace, "Gas Dispersion in Solid-Liquid Fluidized Beds," *Brit. Chem. Eng.*, **6**, 232 (1961).
Matsuura, A., and L.-S. Fan, "Distribution of Bubble Properties in a Gas-Liquid-Solid Fluidized Bed," Colloquium, Tokai Branch, Soc. of Chem. Eng. of Japan (May 26, 1983); *AIChE J.*, **30**(6), 894 (1984).
Mayak, V. I., and V. I. Matrozov, "Hydraulic Resistance of Plate Columns with Fluidized Packing," *Theor. Found. Chem. Eng.*, **3**, 64 (1969).
McMichael, W. J., L.-S. Fan, and C. Y. Wen, "Analysis of Sulfur Dioxide Wet Limestone Scrubbing Data from Pilot Plant Spray and TCA Scrubbers," *Ind. Eng. Chem. Process Des. Dev.*, **15**, 459 (1976).
Michelsen, M. L., and K. Ostergaard, "Hold-Up and Fluid Mixing in Gas-Liquid Fluidized Beds," *Chem. Eng. J.*, **1**, 37 (1970).
Miconnet, M., P. Guigon, and J.-F. Large, "The Scrubbing of Acid Gases in Columns with Fixed or Mobile Packings," *Int. Chem. Eng.*, **22**, 133 (1982).
Moebus, O., and M. Teuber, "Production of Ethanol by Solid Particles of Saccharomyces Cerevisiae in a Fluidized Bed," *European J. Appl. Microbiol. Biotechnol.*, **15**, 194 (1982).
Morooka, S., K. Kusakabe, and Y. Kato, "Mass Transfer Coefficient at the Wall of a Rectangular Fluidized Bed for Liquid-Solid and Gas-Liquid-Solid Systems," *Kagaku Kogaku Ronbunshu*, **5**, 162 (1979); *Int. Chem. Eng.*, **20**, 433 (1980).
Morooka, S., K. Uchida, and Y. Kato, "Recirculating Turbulent Flow of Liquid in Gas-Liquid-Solid Fluidized Bed," *J. Chem. Eng. Japan*, **15**, 29 (1982).
Mrowiec, M., and A. Laszuk, "The Investigation of Mass Exchange Kinetics in the Apparatus with the Bed of Fluidized Packing Sprayed from Below," *Fluidization and Its Applications*, H. Angelino et al., Eds., 417, Cepadues-Editions, Toulouse (1974).
Mukherjee, R. N., P. Bhattacharya, and D. K. Taraphdar, "Studies on the Dynamics of Three Phase Fluidization," *Fluidization and Its Application*, H. Angelino et al., Eds., 372, Cepadues-Editions, Toulouse (1974).
Muroyama, K., "Studies of Gas-Liquid-Solid Packed and Fluidized Bed Reactors," Dr. of Engr. Thesis, Kyoto Univ., Japan (1976).
Muroyama, K., et al., "Axial Liquid Mixing in Three-Phase Fluidized Beds," *Kagaku Kogaku Ronbunshu*, **4**, No. u, 622 (1978).
Muroyama, K., M. Fukuma, and A. Yasunishi, "Heat Transfer in Three-Phase Fluidized Beds," *AIChE Symp. Ser.*, No. 308, **77**, 385 (1981).
Muroyama, K., and L.-S. Fan, "Classification of Three-Phase Operations and Reactors in Suspended and Fluidized Beds," *Kagaku Kogaku*, **46**, 220 (1982).
Nicklin, D. J., "Two Phase Bubble Flow," *Chem. Eng. Sci.*, **17**, 693 (1962).
Nishikawa, M., K. Inui, and S. Nagata, "Mass Transfer from Solid Particles in Spouted Vessel," *Kagaku Kogaku Ronbunshu*, **2**, 42 (1976); *Int. Chem. Eng.*, **16**, 714 (1976).
Nishikawa, M., K. Kosaka, and K. Hashimoto, "Gas Absorption in Gas-Liquid or Solid-Gas-Liquid Spouted Vessel," Pacific Chem. Eng. Cong., Denver, 1389 (Aug. 1977).
Ohshima, S., et al., "Liquid Mixing in Gas-Liquid Cocurrent Up-Flow Through Packed and Fluidized Particle Bed," *Kagaku Kogaku Ronbunshu*, **3**, 406 (1977).
O'Neill, B. K., et al., "The Hydrodynamics of Gas-Liquid Contacting in Towers with Fluidized Packing," *Can. J. Chem. Eng.*, **50**, 595 (1972).
Ostergaard, K., Discussion in the Paper of R. Turner, "Fluidization," 58, Soc. for the Chem. Ind., London (1964).
Ostergaard, K., "On Bed Porosity in Gas-Liquid Fluidization," *Chem. Eng. Sci.*, **20**, 165 (1965).
Ostergaard, K., "On the Growth of Air Bubbles Formed at a Single Orifice in a Water Fluidized Bed," *Chem. Eng. Sci.*, **21**, 470 (1966).
Ostergaard, K., and M. L. Michelsen, "Holdup and Axial Dispersion in Gas-Liquid Fluidized Bed: The Effect of Fluid Velocities and Particle Size," Joint AIChE–I.I.Q.P.R. Mtg., Tampa, FL (1968).
Ostergaard, K., "Gas-Liquid-Particle Operation in Chemical Reaction Engineering," *Adv. in Chem. Eng.*, T. B. Drew et al., Eds., **7**, 71, Academic Press (1968).
Ostergaard, K., and M. L. Michelsen, "On the Use of the Imperfect Tracer Pulse Method for Determination of Hold-up and Axial Mixing," *Can. J. Chem. Eng.*, **47**, 107 (1969).
Ostergaard, K., and W. Suchozebrski, "Gas-Liquid Mass Transfer in Gas-Liquid Fluidized Beds," *Proc. Eur. Symp. Chem. React. Eng.*, 21, Pergamon Press, Oxford (1969).
Ostergaard, K., *Studies of Gas-Liquid Fluidization*, Danish Technical Press, Copenhagen (1969).
Ostergaard, K., "Three-Phase Fluidization," *Fluidization*, J. F. Davidson and D. Harrison, Eds., Chap. 18, 751, Academic Press, New York (1971).
Ostergaard, K., and P. Fosbol, "Transfer of Oxygen Across the Gas-Liquid Interface in Gas-Liquid Fluidized Beds," *Chem. Eng. J.*, **3**, 105 (1972).
Ostergaard, K., "Fluid Mechanics of Three Phase Fluidization," Can. Chem. Eng. Conf., Calgary, Alberta (1977).
Ostergaard, K., "Holdup, Mass Transfer and Mixing in Three-Phase Fluidization," *AIChE Symp. Ser.*, **74**, 82 (1978).
Page, R. E., and D. Harrison, "The Size Distribution of Gas Bubbles Leaving a Three-Phase Fluidized Bed," *Powder Technol.*, **6**, 205 (1972).
Page, R. E., and D. Harrison, "Particle Entrainment from a Three-Phase Fluidized Bed," *Fluidization and Its Applications*, H. Angelino et al., Eds., 393, Cepadues-Editions, Toulouse (1974).
Parulekar, S. J., and Y. T. Shah, "Steady-State Behavior of Gas-Liquid-Solid Fluidized Bed Reactors," *Chem. Eng. J.*, **20**, 21 (1980).
Patel, R. D., and J. M. Simpson, "Heat Transfer in Aggregative and Particulate Liquid-Fluidized Beds," *Chem. Eng. Sci.*, **32**, 67 (1977).
Pitt, Jr., W. W., C. W. Hancker, and H. W. Hsu, "The Tapered Fluidized Bed Bioreactor: An Improved Device for Continuous Cultivation," *AIChE Symp. Ser.*, **74**(181), 119 (1978).
Razumov, I. M., V. V. Manshilin, and L. L. Nemets, "The Structure of Three-Phase Fluidized Beds," *Int. Chem. Eng.*, **13**, 57 (1973).
Richardson, J. F., and W. N. Zaki, "Sedimentation and Fluidization: Part I," *Trans. Instn. Chem. Engrs.*, **32**, 35 (1954).
Richardson, J. F., "Transient Fluidization and Particulate Systems," *Fluidization*, J. F. Davidson and D. Harrison, Eds., Chap. 2, 39, Academic Press, New York (1971).
Rigby, G. R., et al., "Properties of Bubbles in Three-Phase Fluidized Bed as Measured by an Electroresistivity Probe," *Chem. Eng. Sci.*, **25**, 1729 (1970a).
Rigby, G. R., and C. E. Capes, "Bed Expansion and Bubble Wakes in Three-Phase Fluidization," *Can. J. Chem. Eng.*, **48**, 343 (1970b).
Robinson, C. W., and C. R. Wilke, "Simultaneous Measurement of Interfacial Area and Mass Transfer Coefficient for a Well-Mixed Gas Dispersion in Aqueous Electrolyte Solutions," *AIChE J.*, **20**, 285 (1974).
Roszak, J., and R. Gawronski, "Cocurrent Liquid-Liquid Extraction in Fluidized Bed," *Chem. Eng. J.*, **17**, 101 (1979).
Rundell, D. N., et al., "Application of Bhatia-Epstein Model to the H-Coal Fluidized Bed Reactor," AIChE Mtg., Chicago (Nov. 16–20, 1980).
Satterfield, C. N., A. A. Pelossof, and T. K. Sherwood, "Mass Transfer Limitations in a Trickle-Bed Reactor," *AIChE J.*, **15**, 226 (1969).
Schaefer, R. J., D. N. Rundell, and J. K. Shou, "Study of Ebulated Bed Fluid Dynamics," Final Progress Report to U.S. Dept. of Energy, Contract DE-AC22-80PC30026 (1983).
Schmidt, M., "Fluiddynamische Untersuchungen einer Mehrstufigen Dreiphasigen Wirbelschicht," *VDI-Forsch.*, **48**, 1 (1976).
Schuman, S. C., R. H. Wolk, and M. C. Chervenak, "Hydrogenation of Oils," U.S. Patent 3,183,180 (1965).
Schuman, S. C., R. H. Wolk, and M. C. Chervenak, "Hydrogenation of Coal," U.S. Patent 3,301,393 (1967).
Scott, C. D., et al., "A Tapered Fluidized Bed Bioreactor for Treatment of Aqueous Effluents from Coal Conversion Processes," *Proc. of Symp. on Evn. Asp. of Fuel Conv. Tech.*, Hollywood, FL (Dec. 15–18, 1975).
Scott, C. D., and C. W. Hancher, "Use of a Tapered Fluidized Bed as Continuous Bioreactor," *Biotech. and Bioeng.*, **18**, 1393 (1976).
Shah, Y. T., G. J. Stiegel, and M. M. Sharma, "Backmixing in Gas-Liquid Reactors," *AIChE J.*, **24**, 369 (1978).
Shah, Y. T., *Gas-Liquid-Solid Reactor Design*, McGraw-Hill (1979).
Shah, Y. T., S. J. Parulekar, and N. L. Carv, "Design of Coal Liquefaction Reactors," *Reaction Engineering in Direct Coal Liquefaction, Energy Science and Technology*, No. 3, Chap. 5, 213, Addison-Wesley (1981).
Shah, Y. T., and S. J. Parulekar, "Steady State Thermal Behavior of an Adiabatic Three Phase Slurry Reactor: Coal Liquefaction under Slow Hydrogen Consumption Reaction Regime," *Chem. Eng. J.*, **23**, 15 (1982).
Shimodaira, C., et al., "Process for Biological Treatment of Waste Water in Downflow Operation," U.S. Patent 4,256,573 (Mar. 17, 1981).
Soung, W. Y., "Bed Expansion in Three-Phase Fluidization," *Ind. Eng. Chem. Process Des. Dev.*, **17**, 33 (1978).
Stewart, P. S. B., and J. F. Davidson, "Three-Phase Fluidization: Water, Particles and Air," *Chem. Eng. Sci.*, **19**, 319 (1964).
Stretton, P. J., and P. D. Stuckey, "Tripos Project Reports," Univ. of

Cambridge, Cambridge (1971).
Strumillo, C., J. Adamiec, and T. Kudra, "Packed Columns with Expanding Beds," *Int. Chem. Eng.*, **14**, 652 (1974).
Strumillo, C., and T. Kudra, "Interfacial Area in Three-Phase Fluidized Beds," *Chem. Eng. Sci.*, **32**, 229 (1977).
Tichy, J., A. Wong, and W. J. M. Douglas, "Pressure Drop in a Mobile-Bed Contactor," *Can. J. Chem. Eng.*, **50**, 215 (1972).
Tichy, J., and W. J. M. Douglas, "Bed Expansion in a Mobile-Bed Contactor," *Can. J. Chem. Eng.*, **50**, 702 (1972).
Tichy, J., and W. J. M. Douglas, "Certain Hydrodynamic Characteristics of Mobile-Bed Contactors," *Can. J. Chem. Eng.*, **51**, 618 (1973).
Towell, G. D., and G. H. Ackerman, "Axial Mixing of Liquid and Gas in Large Bubble Reactors," *Proc. of Int. Symp. on Chem. Reaction Eng.*, B3-1, Elsevier, Amsterdam (1972).
Turner, R., "Fluidization in the Petroleum Industry," *Fluidization*, 47, Soc. Chem. Ind., London (1964).
Turpin, J. C., and R. L. Huntington, "Prediction of Pressure Drop for Two-Phase, Two-Component Concurrent Flow in Packed Beds," *AIChE J.*, **13**, 1196 (1967).
Ubaidullaev, A. K., et al., "Investigation of Optimal Regimes of Absorber and Scrubber Trays with Mobile (Fluidized) Packing, on the Basis of Energy Parameters," *Theor. Found. Chem. Eng.*, **15**, 118 (1981).
Uchida, S., C. S. Chang, and C. Y. Wen, "Mechanism of a Turbulent Contact Absorber," *Can. J. Chem. Eng.*, **55**, 392 (1977).
Uchida, S., T. Suzuki, and H. Maejima, "The Flooding Condition of a Turbulent Contact Absorber," *Can. J. Chem. Eng.*, **58**, 406 (1980).
Ueyama, K., and T. Miyauchi, "Properties of Recirculating Turbulent Two Phase Flow in Gas Bubble Columns," *AIChE J.*, **25**, 258 (1979).
Uysal, B. Z., "Hydrodynamic and Particulate Recovery Studies in Mobile-Bed Contacting," Ph.D. Thesis, McGill Univ. (1978).
Vail, Yu. K., N. Kh. Manokov, and V. V. Manshilin, "Turbulent Mixing in a Three-Phase Fluidized Bed," *Int. Chem. Eng.*, **8**, 293 (1968).
Vail, Yu. K., N. Kh. Manokov, and V. V. Manshilin, "The Gas Contents of Three-Phase Fluidized Beds," *Int. Chem. Eng.*, **10**, 244 (1970).
Van Driesen, R. P., and N. C. Stewart, "How Cities Service's H-Oil Unit is Performing," *Oil and Gas J.*, 100 (May 18, 1964).
Vanderschuren, J., J. P. Schrayen, and S. Roland, "Etude du Transfert de Matiere Pendant Lascension D'une Grosse Bulle Gazeuse Dans Un Lit Fluidise Liquide," *Fluidization and Its Applications*, H. Angelino et al., Eds., 351, Cepadues-Editions, Toulouse (1974).
Vasalos, I. A., E. M. Bild, and D. N. Rundell, "Experimental Techniques for Studying the Fluid Dynamics of the H-Coal Reactor," AIChE Mtg., San Francisco (Nov. 25–29, 1977).
Vasalos, I. A., et al., "Study of Ebullated Bed Fluid Dynamics for H-Coal," *Quarterly Progress Report No. 6* to U.S. Dept. of Energy, Contract No. EF-77-C-01-2588 (June 1979).
Vasalos, I. A., et al., "Study of Ebullated Bed Fluid Dynamics for H-Coal," *Final Report*, U.S. Dept. of Energy under Contract DE-AC05-10149 (Feb., 1980).
Vasalos, I. A., et al., "Holdup Correlations in Slurry-Solid Fluidized Beds," *AIChE J.*, **28**, 346 (1982).
Visvanathan, C., and L. S. Leung, "On the Design of a Fluidized Bed Scrubber," *Ind. Eng. Chem. Proc. Des. Dev.*, (1984, in review).
Viswanathan, S., A. S. Kakar, and P. S. Murti, "Effect of Dispersing Bubbles into Liquid Fluidized Beds on Heat Transfer Hold-up at Constant Bed Expansion," *Chem. Eng. Sci.*, **20**, 903 (1964).
Volpicelli, G., and L. Massimilla, "Three-Phase Fluidized Bed Reactors, An Application of the Production of Calcium Bisulphite Acid Solutions," *Chem. Eng. Sci.*, **25**, 1361 (1970).
Vukovic, D. V., et al., "Pressure Drop, Bed Expansion and Liquid Holdup in a Three Phase Spouted Bed Contactor," *Can. J. Chem. Eng.*, **52**, 180 (1974).
Vunjak-Novakovic, G. V., and D. V. Vukovic, "Hydrodynamics and Mass Transfer Performance of Turbulent Contact Absorbers," *Fluidization*, G. R. Grace and G. M. Matsen, Eds., 253, Plenum Press, New York (1980).
Wallis, G. B., *One Dimensional Two-Phase Flow*, McGraw-Hill (1969).
Wasmund, B., and J. W. Smith, "Wall to Fluid Heat Transfer in Liquid Fluidized Beds, Part 2," *Can. J. Chem. Eng.*, **45**, 156 (1967).
Werner, G., and K. Schugerl, "Three-Phase Counter-Current Fluidized Beds with Large Gas-Phase Volume Fractions," *Proc. of Int. Symp. on Chem. Reaction Eng., B9-1*, Elsevier, Amsterdam (May 2–4, 1972).
Wild, G., et al., "Les réacteurs à lits fluidisés gaz-liquide-solide. Etat de l'art et perspectives industrielles," Entropie N°, 106, 3 (1982).
Wozniak, M., and K. Ostergaard, "An Investigation of Mass Transfer in a Countercurrent Three-Phase Fluidized Bed," *Chem. Eng. Sci.*, **28**, 167 (1973).
Wozniak, M., "Pressure Drop and Effective Interfacial Area in a Column with a Mobile Bed," *Int. Chem. Eng.*, **17**, 553 (1977).
Yushina, Y., and H. Sata, "Overall Oxygen Transfer Coefficient in Downward Three Phase Fluidized Bed," Preprint for the Muroran Mtg. of the Soc. of the Chem. Eng., Japan, 131 (1983).
Ziganshin, G. K., and A. Ermakova, "Gas Content with the Ascending Direct Flow of a Gas-Liquid Stream in the Presence of Fixed and Fluidized Beds of Granular Material," *Theor. Found. Chem. Eng.*, **4**, 576 (1970).
Zhukov, A. P., et al., "Investigation of Mass Transfer in the Gas Phase in an Apparatus with Mobile Bead Packing with Allowance for Lengthwise Liquid Mixing," *Theor. Found. Chem. Eng.*, **11**, 371 (1977).
——, "New Floating-Bed Scrubber Won't Plug," *Chem. Eng.*, **66**, 106 (Dec. 14, 1959).

Manuscript received April 27, 1983; revision received June 14, and accepted July 2, 1984.